The Regulation of Keratin 8 by Aurora B During The Cell Cycle

by

Büşra Harmanda

A Dissertation Submitted to the Graduate School of Sciences and Engineering in Partial Fulfillment of the Requirements for the Degree of Doctor of Philosophy in

Molecular Biology and Genetics

KOÇ ÜNİVERSİTESİ

April 2022

The Regulation of Keratin 8 by

Aurora B During The Cell Cycle

Koç University

Graduate School of Sciences and Engineering

This is to certify that I have examined this copy of a doctoral dissertation by

Büşra Harmanda

and have found that it is complete and satisfactory in all respects,
and that any and all revisions required by the final
examining committee have been made.

Committee Members:

_____

Assc. Prof. Dr. Nurhan Özlü (Advisor, Koç University)

_____

Asst. Prof. Dr. Ayşe Koca Çaydaşı (Koç University)

_____

Asst. Prof. Dr. Elif Nur Fırat Karalar (Koç University)

_____

Prof. Dr. Arzu Karabay Korkmaz (Istanbul Technical University)

_____

Assist. Prof. Güneş Özhan (Dokuz Eylül University)

Date: _____

This thesis is dedicated to my dearest father; Recep,

The person I will always love and admire the most,

Who is always there to support me morally and physically.

ABSTRACT

The Regulation of Keratin 8 by Aurora B During The Cell Cycle

Büşra Harmanda

Doctor of Philosophy in Molecular Biology and Genetics

April 2022

Cell division is required for living organisms to carry out their most basic functions, such as transmitting genetic information to the future generation. The morphology and biochemistry of a cell changes dramatically during cell division. Dynamic changes occur in multiple components of the cell including chromosomes, membranous organelles and cytoskeletal elements during mitosis and cytokinesis. Various cell cycle-dependent kinases strictly regulate these intricate activities. The molecular details of regulatory mechanisms during cell division and master regulators and their dynamic targets are active research questions in cell division. Microtubule and actin filaments are two main elements of the cytoskeleton that play critical roles in mitosis and cytokinesis and have relatively well-understood in terms of their functions and regulatory mechanisms. In contrast, intermediate filaments, a type of cytoskeletal element, are a less well-studied component of cell division. Keratins are the most diverse family of intermediate filaments. They are expressed in tissue-specific manner. Additionally, they are used as a biomarker in cancer diagnosis because of their differential expression in malignant tissues. The primary function of keratins is to provide mechanical strength to the cell. However, how the Keratins are re-organized during cell division and their regulatory mechanisms are not well studied. I aimed to investigate how the master mitotic kinases regulate keratins during mitosis and cytokinesis by using both proteomic and cell biology-based approaches. Our mass spectrometry analysis revealed six Aurora B kinase-dependent phosphorylation sites of Keratin 8. By creating phospho-mutant versions, I analyzed and characterized the roles of the phosphorylation site of Keratin 8 during mitosis and cytokinesis. Our study provides insight into the function and regulation of Keratin 8 during cell division. We showed that cytokinesis-specific phosphorylation of Keratin 8 is required for successful cytokinesis by reorganizing Keratin 8 fibers by Aurora B kinase.

ÖZETÇE

Keratin 8 Proteininin Aurora B Tarafından

Hücre Bölünmesi Sırasında Regulasyonu

Büşra Harmanda

Moleküler Biyoloji ve Genetik, Doktora

Nisan 2022

Canlı organizmaların genetic bilgiyi gelecek nesillera katarma gibi en temel işlevlerini yerine getirebilmesi için hücre bölünmesi gereklidir. Hücre döngüsüne bağlı kinazlarla kontrollü bir şekilde düzenlenen hücre bölünmesi sırasında bir hücrenin morfolojisinde büyük değişiklikler gerçekleşir. Kromozomlar, hücre zarı ve sitoskeletal elementler, dinamik ve geniş kapsamlı bir şekilde değişiklikler gösteren hücre elementlerinin en başlıcalarıdır. Hücre bölünmesindeki master düzenleyiciler olan kinazlar ve onların hedef proteinleri bir çok açıdan araştırılmış olsa da moleküler düzeyde henüz keşfedilmemiş birçok mekanizma bulunmaktadır. Örneğin, hücre iskeletinin başlıca iki elementinden olan ve hücre bölünmesinde kritik rol oynayan aktin ve mikrotübül filamentlerinin roller ve düzenlenme mekanizmaları literatürde iyi tanımlanmış olmasına ragmen hücre iskeletinin diğer bir üyesi olan ara filamentlerin hücre bölünmesindeki roller ve regulasyonları hakkında daha çalışma bulunmaktadır. Keratinler Ara filamentlerin en çeşitli ailesindendir ve dokuya özgü bir şekilde ifade edilirler. Ek olarak, malignant dokudaki farklı ifadeleri nedeniyle kanser tanısında biyobelirteç olarak sıklıkla kullanılırlar. Keratinlerin temel işlevi hücreye mekanik güç sağlamaktır. Diğer hücre iskeleti elementleri olan aktin ve mikrotübül filamentlere kıyasla hücre bölünmesi sırasındaki regulasyonları iyi karakterize edilmemiştir. Bu nedenle, ana mitotic kinazların mitoz ve sitokinez sırasında ara filamentlerin önemli bir üyesi olan keratinlerin düzenlenme mekanizmalarını araştırmayı hedefledik. Burada, kütle spektrometrisi yaklaşımımız sayesinde Keratin 8'in Aurora B kinaz aktivitesine bağlı 11 fosforilason bölgesini ortaya çıkardı. Ayrıca, biyokimyasal yaklaşımlar kullarak Keratin 8'in mitoz ve sitokinez fosforilasyon bölgelerini analiz ve karakterize ettik. Çalışmamız, hücre bölünmesi sırasında Keratin 8'in işlevi ve düzenlenmesi konusunda hücresel mekanizmasını ortaya koymuştur.

ACKNOWLEDGEMENTS

First and foremost, I want to express my sincere thanks to my advisor Assc. Prof. Dr. Nurhan Özlü for giving me this opportunity to complete my Ph.D. studies in her laboratory and under her guidance and patience. She was there for not just me but anybody who asked for her help. Working on my Ph.D. under her guidance has been a life-changing experience. Her mentorship added numerous qualities that I am most certain would help me in the days to come. I feel incredibly privileged and lucky to be a part of Nurhan Özlü's team and have her as a mentor.

I would like to thank my thesis monitoring committee members, Prof. Dr. Arzu Karabay Korkmaz and Dr. Ayşe Koca Çaydaşı, for their precious guidance, comments and discussions throughout my Ph.D. I would like to thank Dr. Elif Nur Fırat Karalar and Dr. Güneş Özhan for their participation in my Ph.D. thesis defense jury. I would like to thank all my jury committee for giving their valuable time and critical reading.

I want to acknowledge the financial support of Scientific and Technological Research Council of Turkey (TUBITAK) and Koç University during my doctoral education and research.

I would like to acknowledge the Proteomics Facility of Koç University and Molecular Imaging Core Facility of Koç University Research Center for Translational Medicine (KUTTAM-CMIC) funded by the Republic of Turkey Ministry of Development. I want to thank Dr. Berna Morova for her assistance with KUTTAM-CMIC equipment. I want to thank MSc. Büşra Aytül Kırım Akarlar for her help with proteomic experiments and her precious support as friend.

I would like to thank all former and present members of Nurhan Ozlu Lab. I want to thank our postdocs Dr. Nazan Saner and Dr. Nazlı Ezgi Özkan Küçük for their support. I know all former and current lab members were always supportive and helpful for any situation that I encountered. They helped me a lot to benefit from their experience and knowledge. I especially thank Tuğçe, Beste, Ceyda and Berfu for all their support during my doctoral study as a friend and colleagues. They have always encouraged me to cope with my difficulties,

especially in the last years. We had shared so many fun and emotional moments that I cannot forget.

I want to thank my dearest friend Mohammad Haroon Qureshi. I am grateful for his guidance and support in scientific and non-scientific matters. Whenever my morale was down, he found a way to cheer me up.

I need to express my gratitude to my dearest friends Selen Manioğlu and Artür Manukyan. I would like to specially thank to Mehmet for always being helpful whenever I need it. He was one of the most intelligent persons whom I've met. He has always been loving, patient and understanding toward me. I could not mention all the rest here for being my friend and my family, making my life colorful and enjoyable.

I am also grateful to Gizem Bener and Fulya Bozoklu for their precious friendships. Being an aunt during these challenging times was an endless source of hope and happiness for me. I cannot wait to hold them in my arms.

I want to thank all KU Krav Maga club members for being my friend and family. Especially, Matt Howel and Samet Kuru had a considerable impact on me for my love for martial arts. They were very affectionate and helpful toward me. Ali Özgür Güven, whom I respect very much as a person, contributed a lot to me in martial arts and my perspective on life. We shared many wonderful moments. Each member of Krav Maga helped me become a stronger person physically and mentally. I feel fortunate to be part of this prestigious family.

Lastly, I feel the greatest gratitude towards my family: Recep, Mümine and Sinan. I would not be the person I am today without the support of my beloved family. They always gave me all their support and encouragement to achieve my dreams throughout my life, not only in my graduate life.

TABLE OF CONTENTS

LIST OF TABLES

LIST OF FIGURES

NOMENCLATURE

ALIX	ALG-2-interacting protein X
APC	Anaphase-Promoting Complex
APC/C	Anaphase-Promoting Complex/Cyclosome
ATP	Adenosine 5’-Triphosphate
BSA	Bovine Serum Albumin
CDK	Cyclin-Dependent Kinase
CEP55	Centrosomal protein of 55 kDa
CPC	Chromosomal Passanger Complex
DAPI	4',6-diamidino-2-phenylindole
DMEM	Dulbecco's Modified Eagle Medium
DTT	Dithiothreitol
ECL	Enhanced chemiluminescence
ECT2	Epithelial Cell Transforming 2
EDTA	Ethylenediaminetetraacetic acid
EMT	Epithelial-to-mesenchymal transition
ESCRT	Endosomal Sorting Complex Required For Transport
FBS	Fetal Bovine Serum
G0	Gap Zero
G1	Gap One
G2	Gap Two
GFP	Green Fluorescent protein
GST	Glutathione S-transferase
GTPase	Guanosine Triphsphophatase
HeLa	Human cervical cancer cell line
HRP	Horseradish peroxidase
IAA	Iodoacetamide
IF	Intermediate Filaments
INCENP	Inner Centromere Protein
IPTG	Isopropyl β-D-1-thiogalactopyranoside

kDa	Kilodalton
K18	Keratin18
K8	Keratin 8
M	Mitosis
MPF	Mitosis Promoting Factor
PBS	Phosphate buffered saline
P/S	Penicillin-Streptomycin
PLK1	Polo-like Kinase 1
PRC1	Protein Regulator of Cytokinesis 1
RhoA	Ras Homolog Family Member A
ROCK	Rho-associated protein kinase
S	Synthesis
Ser/S	Serine
SDS-PAGE	Sodium dodecyl sulfate polyacrylamide gel electrophoresis
STC	S-Trityl-L-cysteine
TBS	Tris buffered saline
TEMED	Tetramethylethylenediamine
WCL	Whole cell lysate
WT	Wild Type

Chapter 1

INTRODUCTION

In the process of cell division, a parent cell divides into two daughter cells which are genetically identical. It is a fundamental process for the reproduction of a cell and an organism. The cell undergoes a series of processes, known as 'the cell cycle, to divide into two daughter cells. In this process, DNA replication of the cell is followed by partitioning its cytoplasm and other components into two cells. At the end of the cell cycle, a genetically identical new organism is replicated from a parental cell. The cell cycle consists of different stages called G1, S, G2 and M phases. The cell prepares to divide in the G1 phase, then it replicates its chromosomes in the S phase, S represents for DNA Synthesis. Copied genetical material is organized and started to condense in the G2 phase. In the M phase, M represents for Mitosis, chromosome segregation and cytoplasmic division take place. The cell cycle is coordinated spatiotemporal and tightly controlled at specific time points. At particular time points, the specific control mechanisms are known as cell cycle checkpoints. The cell ends up with abnormalities or even a death if any error takes place during the cell cycle checkpoints.

The cell cycle generally takes approximately 24 hours in a typical mammalian cell. The longest phase is the G1 which takes 10-12 hours. The S phase is about 8-10 hours whereas the G2 phase is 4 hours. The shortest phase is the M phase which occurs in 1 hours. Contrarily, the cytoplasmic division occupies only a few minutes. Although the M phase lasts for a short time period, the most drastic changes in the cell morphology and biochemistry, which targets chromosome, membrane and cytoskeleton components, appears in the M phase. These components are tightly organized with the cell cycle regulators which are cyclins, cyclin-dependent kinases (CDKs), CDK inhibitors, transcription factors, kinases and phosphatases. These regulators provide the proper spatial organization of the cell component during the cell cycle. Aurora kinases are one of these master regulators in the cell

cycle. Aurora kinases consist of three proteins Aurora A, Aurora B and Aurora C. Aurora A and Aurora B take an essential role in mitotic entry, spindle assembly and cytokinesis in the M phase [1, 2, 3, 4]. Aurora B regulates various processes, starting from chromosomal condensation through cytoplasmic division of two daughter cells [5]. Aurora kinases are required for error-free cell division. When Aurora kinases are overexpressed in the cell, tumorigenesis, aneuploidy, chromosomal instability and centrosome amplification is associated within these cells [6, 7]. On the other hand, catalytically inactive Aurora B results in incomplete cytokinesis [8].

While CDKs are active in only mitosis or cytokinesis, Aurora B activity is interestingly high in both mitosis and cytokinesis. Although Aurora B activity lasts from mitosis until cytokinesis, its target proteins change throughout the process. It regulates a wide range of proteins by phosphorylating them. Histones are one of the major targets of Aurora B. Cytoskeleton proteins are another well-known target of it. For example, Aurora B regulates microtubules during mitosis and cytokinesis. Aurora B phosphorylates vimentin, which is one of the intermediate filament protein subtype [9]. However, there are many unknown mechanisms for the regulation of other intermediate filament proteins, especially keratins.

It is well known that keratin, which composes a wide range of Type I and Type II intermediate filaments, mainly functions in providing mechanical strength to the cell. The strongest parts of the organism, such as animal horns, nails and hair, are composed of highly enriched keratin. Additionally, they have expressed in mammalian epithelial cells in a tissue-specific manner. They form a solid and robust structure in the cell. However, for the sake of the cell, keratin should not maintain its rigid form during cytokinesis in the cleavage furrow. Keratin should be cleared from cleavage furrow, which is an entirely dynamic process maintained in minutes. Otherwise, cytoplasmic division ends up in failure. Therefore, there should be a valid mechanism to reorganize keratin proteins during cell division. However, it has not been studied as well as other cytoskeleton components. It is highly possible that keratin proteins are regulated through phosphorylation during mitosis and cytokinesis by the major kinases like CDK1, Rho kinase, Aurora kinases, and Polo kinases. Since Aurora B interestingly maintains its activity in both mitosis and cytokinesis, keratins may be regulated

by depending on Aurora B. In this thesis, I aimed to investigate the role of Keratin 8 in cell division and its regulation by Aurora B by taking biochemical and proteomic approaches.

A complete literature review relating to the subject in this thesis is included in Chapter 2. It starts with a brief overview of the cell cycle before moving on to the role of Aurora B and the significance of keratin proteins. It concludes with recent research on the Aurora B-Keratin 8 connection. The materials that were used and the methods that were used are described in Chapter 3. The experiments' outcomes are discussed in Chapter 4. In chapter 5, the results are interpreted and discussed in detail, as well as the study's future directions.

Chapter 2

LITERATURE REVIEW

2.1 The Cell Cycle

The cell cycle is a series of processes that occur in order to develop and divide the cell into two identical cells. The cell cycle is required for cells to reproduce by completing their most basic purpose of passing on their genetic information to the next generation. A more complex organism requires the development of the organism by constant repair and renewal of the tissues. This process is maintained with a successful cell division. In this way, the existence of a more complex organism is ensured. The cell cycle in eukaryotic cells has four stages: The G1, S, G2 and M phases. **Figure 2.1** shows a schema of the cell cycle.

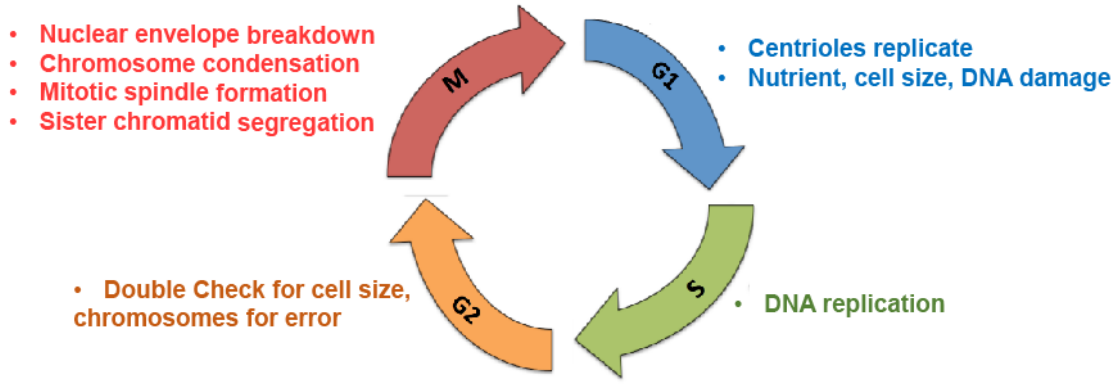

Figure 2.1. The Cell Cycle Stages in Eukaryotic Cell. Four major steps for the cell division.

The cell cycle begins with the interphase, consisting of the G1, S and G2 phases. The G1 is the first phase of cell division. It is known as the growth phase. The cell prepares itself by synthesizing required proteins, mRNA and organelles. Thus, the growth of the cell in size is provided. At the end of the G1, the cell has three fates: to continue the cell cycle with the S

phase, become arrested in the G1 and stop the cell cycle by entering the G0 stage, which is a resting phase in an unfavorable environment in the early stage of the cell cycle. After the G1, the cell progresses further through the S phase, where DNA is synthesized and duplicated. Although the rate of transcription and protein synthesis decreases, histone proteins are heavily synthesized in the S phase. Because precise genome duplication is essential for effective cell division, the mechanisms that take place during S-phase are highly regulated and conserved. The G2 is characterized by rapid cell growth and protein synthesis as the cell prepares itself for mitosis. The M phase is the last stage of the cell cycle. It takes place in a relatively short time compared to other phases. In the M phase, nuclear and cytoplasmic divisions take place. Sequential serial events are responsible for the successful generating of two daughter cells. The M phase consists of prophase, prometaphase, metaphase, anaphase and telophase.

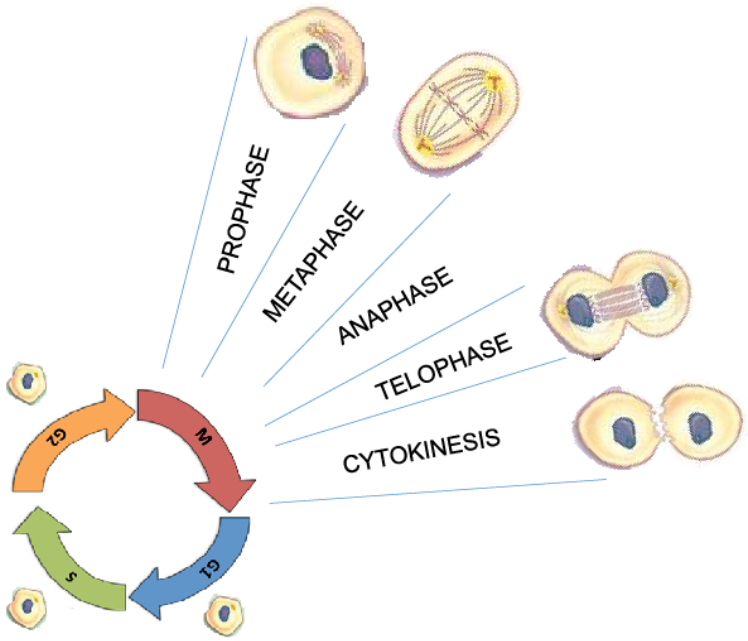

Figure 2.2. The Major Steps in the M-Phase.

2.2. Cell Cycle Control

The cell cycle is the highly complex cellular process that proceeds in order. Sequential events are tightly controlled by the cell in a time-dependent manner. Both internal and external events regulate the timing of events. External events may trigger or inhibit the initiation of cell division. The cell cycle control system works similarly to a timer, activating the events in a predetermined order. If any mistakes in the chromosome duplication or distribution arise during the cell division, it may lead production of an abnormal cell. The cell cycle is regulated at specific checkpoints to maintain successful cell division. Three major cell cycle checkpoints control the sequence of events: The G1, the G2, and spindle checkpoints. The G1 checkpoint is necessary to determine whether external and internal conditions are favorable for the cell to proceed with the cell division. Growth factors are important to progress into the S phase. The G1 checkpoint checks for genomic DNA damage in addition to appropriate reserves and cell size. The cell can halt the cell cycle until the problem is fixed or it can enter the G0 phase. The G2 checkpoint ensures chromosome replication and replicated DNA damage. The spindle checkpoint determines whether all chromosomes are attached to the microtubules correctly.

Cell cycle checkpoints are controlled by a reliable and well-organized process. The expression of cyclins is stage-dependent and oscillates in the cell cycle. G1-cyclins, G1/S-cyclins, S-cyclins, and M-cyclins are the four main classes of cyclins which are called after their active phases. G1-cyclins regulate cell growth. G1/S-cyclins trigger entering a new cell cycle. S-cyclins initiates chromosome duplication. M-cyclins activate initiation of M phase. **Figure 2.3** shows Cyclin oscillation during the cell cycle.

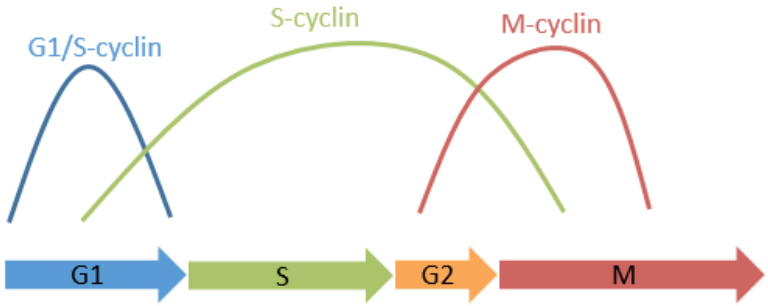

Figure 2.3. Cyclins Oscillation During The Cell Cycle. The overview of cyclin activities during the cell cycle. Adapted from [10]

Cyclins and CDKs assemble to partially active cyclin-CDK complexes. Each cyclin interacts with specific CDKs. **Figure 2.4** represents cyclins and CDK interactions. Fully active cyclin-CDK complexes are achieved through phosphorylation on their activation sites. Vice versa, the Inhibition of cyclin-CDK complexes is accomplished by phosphorylation on their inhibitory sites. When a cell decides that internal and external circumstances are favorable for progressing to the next cell cycle stage, relevant cyclin proteins are ubiquitylated, allowing proteases to destroy them. An error-correction method is provided by positive and negative control mechanisms. Arresting the cell cycle gives this process the time it needs to correct the situation.

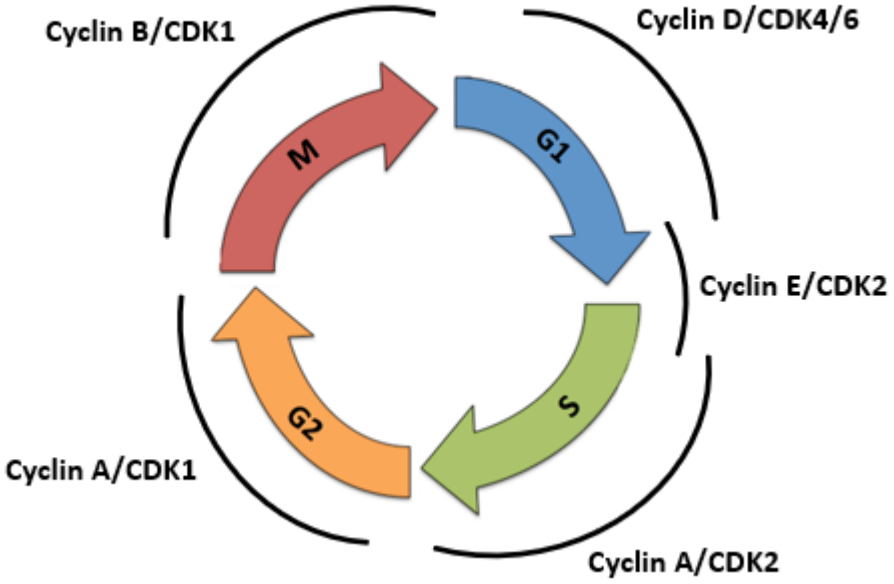

Figure 2.4. Cyclins and Their CDK Partners During The Cell Cycle.

Phosphorylation and dephosphorylation events occur during the cell cycle, resulting in the activation of downstream pathways. For example, the phosphorylation of CDK1 on nuclear envelope proteins causes their breakdown and chromosomal accession [11, 12, 13]. CDK1 phosphorylation on its targets also facilitates spindle formation and sister chromatin alignment. In the case of appropriate chromosome alignment and kinetochore attachment, phosphorylation of the anaphase-promoting complex (APC), a member of the ubiquitin ligase family of enzymes, is activated by CDK1 to initiate the metaphase to anaphase transition [14]. APC targets proteins like Securin, S- and M-cyclins. Chromosome segregation is initiated by the degradation of Securin protein.

2.3. Cytokinesis

Cytokinesis is the final step of cell division, in which two daughter cells are separated by cytoplasmic division. Cytokinetic entrance, early cytokinesis, late cytokinesis, and abscission are the four stages of cytokinesis [15] (**Figure 2.5)**. The formation of a contractile ring and the presence of anti-parallel midzone microtubules between separated chromosomes

signal cytokinetic entrance. Actin filaments, myosin II filaments, and other regulatory and structural proteins are components of the contractile ring [16]. During early cytokinesis, the contractile ring gradually contracts, causing the formation of a cleavage furrow and narrowing it. In late cytokinesis, compacted microtubules and another electron-dense material form an intercellular bridge called the midbody between two daughter cells. By recruiting and regulating abscission proteins in the final stage of cytokinesis, the midbody formation provides a favorable environment for abscission.

RhoA, a Ras family small GTPase, is one of the primary regulators of cytokinesis in mammalian cells [17]. RhoA plays a role in forming the contractile ring at the cell cortex. In this way, it orchestrates the ring contraction. It has two major targets: formins and ROCK kinase. Formin activation allows the formation of unbranched action filaments. ROCK kinase stimulation by RhoA initiates downstream processes. ROCK kinase phosphorylates myosin II at the regulatory light chain [18].

RhoA kinase is not the only significant player in orchestrating of cytoplasmic division, which is a complex mechanism. It involves the coordination of different pathways, such as removal of cytoskeleton components from the cytokinetic bridge, constriction of the cell cortex or plasma membrane fission. Despite the lack of the cell cycle checkpoint in cytokinesis, Many proteins, including PRC1, PLK1, CEP55, ECT2, ESCRT-III, ALIX, ANILIN and Aurora B, regulate the harmony for separation of the plasma membrane.

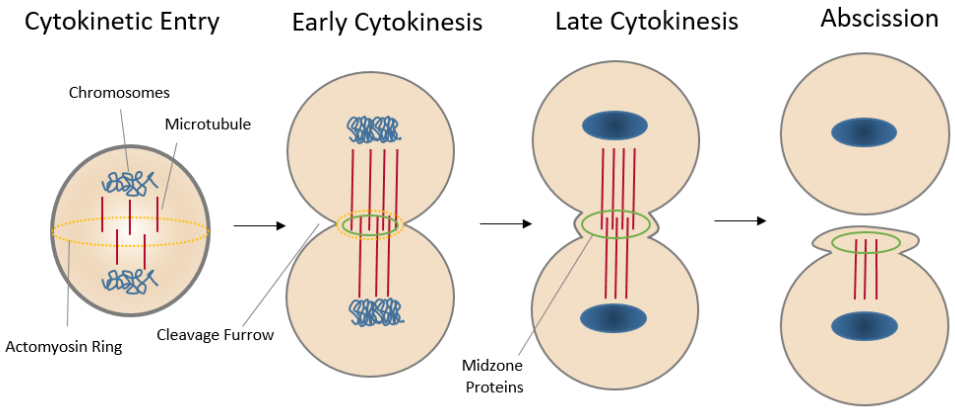

Figure 2.5. Four Stages of Cytokinesis. Cytokinetic entry, early cytokinesis, late cytokinesis and abscission. Adapted from [15]

2.4. Aurora Kinases

Aurora family consists of three groups of kinases: Aurora A, Aurora B and Aurora C. They are serine/threonine kinases. Aurora kinases are essential for cell division and play a critical role in the cell cycle. Aurora kinases are overexpressed in different cancer types [19]. They become potential targets for cancer therapies because of their differential expression in tumor cells [20].

Kinase domains of Aurora kinases share common homologies, but their functions and cellular localizations in the cell cycle differ [21]. Aurora A is required for mitosis and its activity reaches the highest in G2/M transition. It localizes at microtubule spindles and centrosomes. It mainly functions in the regulation of centrosome maturation, spindle stability and assembly. On the other hand, Aurora B is essential for both mitosis and cytokinesis. Aurora B localizes at chromosomes in mitosis and at the cleavage furrow and midbody during cytokinesis. It is a component of the Chromosomal Passenger Complex (CPC) which is one of the most important mitotic regulators. Aurora C also is a component of the CPC [22]. It localizes to the centrosome in mitosis and then to the cleavage furrow in cytokinesis. When Aurora A and B expression is higher in mitotic somatic cells, Aurora C expression is more frequent during meiosis [23].

2.4.1. Aurora B Kinase

In contrast to other Aurora kinase families, Aurora B activity interestingly prolongs starting from mitosis to the end of cytokinesis. Aurora B level reaches the peak in the G2/M phase. Aurora B has well-known interaction partners, including Survivin, Borealin and the Inner Centromere Protein (INCENP). Aurora B, INCENP, Borealin and Survivin assembly to form the CPC. The whole complex coordinates different processes like histone modification and chromosome alignment. Microtubule attachment between chromosomes and mitotic spindles is secured by CPC [24]. Aurora B is the enzymatic core of the CPC. INCENP, Survivin and Borealin function as localization modules by providing scaffolding. INCENP has the highly conserved IN-box domain in the C-terminal region where Aurora B interacts, whereas Borealin and Survivin interact with CEN-box in the N terminus to form a triple-helix bundle [25]. All subunits of the CPC are essential for proper localization. The complex starts accumulating at the inner centromeres with entry into mitosis. The CPC provides chromosome congression to the metaphase plate by ensuring a functional microtubule attachment to the chromosomes. If there is erroneous kinetochore-microtubule attachment, the CPC destabilizes it and activates the mitotic spindle assembly checkpoint (SAC) [26]. The complex changes its localization upon the metaphase-to-anaphase transition. It improves the initiation of cytokinesis by localizing to the cleavage furrow. Merotelic and syntelic attachments were increased upon Borealin depletion and Aurora B inhibition [27, 28, 29]. Nonfunctional CPC causes increase in chromosome congression and segregation defects that may end up with cell death, multinucleation, abnormal cell or tumorigenesis. Aurora B is the catalytic domain that plays a critical role in both CPC localization and phosphorylation of substrates. Therefore, it suppresses cell cycle progression when it is inactive. As a result, Aurora B, rather than the other Aurora kinases, has become a more favored target for cancer therapy.

Aurora B is found in the cytoplasm during interphase and then in the nucleus during prophase and metaphase, specifically in chromosome arms and centromeres. After drifting apart from the centromere, it accumulates at the central spindle as the metaphase to anaphase transition begins. It first appears near the cleavage furrow in the telophase to stimulate cytokinesis,

then moves to the midbody until cytokinesis is complete. Aurora B phosphorylates a wide range of substrates thanks to its various localization through cell division. In mitosis, Histone H3 protein is one of the major substrates of Aurora B. Histone H3 is phosphorylated at Ser10 [30]. Phosphorylation Histone H3 S10 is a well-known mitotic marker because it is specifically phosphorylated in mitosis. In cytokinesis, Aurora B phosphorylates MKLP and ZEN4, the kinesin-like proteins, for cleavage furrow formation [31]. Vimentin, a cytoskeleton protein, is another target of Aurora during cytokinesis. Vimentin at S72 are phosphorylated at cleavage furrow specific manner [32].

As described above, Aurora B orchestrates the harmony of cell cycle by targeting multiple substrates at different stages of it. It has a wide range of substrate types which could be kinases, histones, kinesins, cytoskeletal and membrane components. However, it is possible that there is more Aurora B substrates which are not discovered yet.

2.5. Cytoskeleton

Cytoskeleton proteins are vital participants in providing mechanical strength and maintaining the spatial organization of the cell. Actin filaments (microfilaments), microtubules, and intermediate filaments (IFs) are three cytoskeleton filament families that contribute to these processes, each with a different role in cellular functions. Cytoskeleton components have distinct types in terms of their protein subunits, intracellular distributions and structures. Actin polymers have the smallest diameter at 7 nm among cytoskeleton components. Microtubule polymers have the largest diameter at 25 nm. The diameter of intermediate filaments ranges from 8 to 12 nm. They are named intermediate filaments because their size is between actin and microtubule polymers. Basically, actin filament is important for the cell motility and functionality of the contractile ring. Microtubule enables the intracellular structure of organelles and the separation of two sister chromatids in mitosis. Microtubules and actins are well characterized in terms of their distinct role and association in different cellular processes. However, intermediate filaments are fewer studies subjects compared to two other cytoskeleton families.

2.5.1. Intermediate filaments

Actin and microtubule filaments are composed of a single type of polymer, whereas IF is composed of a variety of proteins. As a result, they can form homodimers as well as heterodimers. IF subtypes are expressed by more than 60 genes. Six subtypes of IF have been identified based on amino acid sequence similarity. They possess secondary structures that are similar in that they have three domains: the head, the alpha-helical rod, and the tail domains (**Figure 2.6**). Type I (acidic) and Type II (basic/neutral) keratin classes have the most various of IF subtypes. Type III consists of Vimentin, Peripherin, Desmin and GFAP, whereas type IV consists of neurofilaments, synemin, α-internexin and syncoilin. Lamins are Type V that contributes to the nuclear structure. Nestins are Type VI, which are found mostly in the nerve cells.

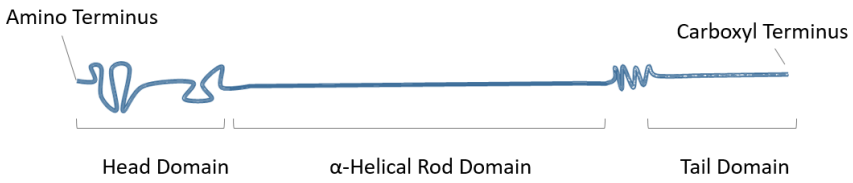

Figure 2.6. Similarity in Secondary Structure of Intermediate Filaments. Adapted from [33]

Vimentin from Type III subtype is a well-characterized intermediate filament component with regards to its cellular function, association partners and regulation mechanisms. Vimentin is a marker for epithelial-to-mesenchymal transition or mesenchymal derived cells because of its differential expression [34]. Additionally, vimentin protein is widely used as biomarker for colon cancer [35]. The mitosis-promoting factor (MPF) and Aurora B regulates vimentin through phosphorylation throughout the cell division. Aurora B mediates phosphorylation of vimentin Serine 34 and Ser 72, specifically in cytokinesis [9, 32]. Besides of vimentin, lamin protein regulation is a well-known concept in the literature. CDK1 regulates lamins in a cell cycle-dependent manner. Nuclear envelope breakdown is initiated by CDK1 phosphorylation on lamin proteins. Despite the fact that many significant members

of IF has been discovered in terms of their cell cycle-dependent regulation, there is more to reveal about the regulation of keratin proteins in the cell cycle.

Class	Protein	Distribution	Function	
I	Acidic Keratins	Epithelial Cells	Tissue Strength	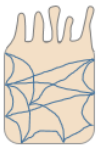 Epithelial cell
II	Basic Keratins	Epithelial Cells	Tissue Strength	
III	Desmin, Vimentin, GFAP	Muscle, Mesenchymal cells, Glial cells	Sarcomere Organization	 Smooth muscle
IV	Neurofilaments	Neurons	Axon Organization	 Axon
V	Lamins	Nucleus	Nuclear Organization	 Nuclei

Figure 2.7. Classes of Intermediate Filaments. Expression profile of intermediate filaments in different cell types. Adapted from [36]

2.5.2. Keratin Proteins

Keratin proteins are a huge class of intermediate filaments. They are fibrous proteins distinguished by their low solubility. Keratins are one of the major structural materials of strong organism components such as horns, hair, nail, claw, feather and hooves. Keratins are insoluble in both water and organic solvents.

There are two classes of Keratins: Type I and Type II. Acidic keratins constitute Type I class which are K9, K10, K11, K12, K13, K14, K15, K16, K17, K18, K19 and K20. Basic and neutral keratins constitute Type II classes which are K1, K2, K3, K4, K5, K6, K7 and K8. Keratin molecular weight ranges from 40 to 67 kDa. Fifty-four functional genes in the human genome contribute to keratin expression. Chromosome 12q and 17q encode different keratin proteins. A huge variety in keratin proteins enables the tissue-specific expression of keratins in epithelial cells (**Figure 2.8**).

The main function of keratins is to provide the cell stiffness, stability and integrity. Although their primary cellular function is increasing mechanical strength, some keratins play critical roles in distinct cellular functions like protecting the cell from stress, maintaining intracellular signaling, promoting wound healing, initiating differentiation and regulating apoptosis [37].

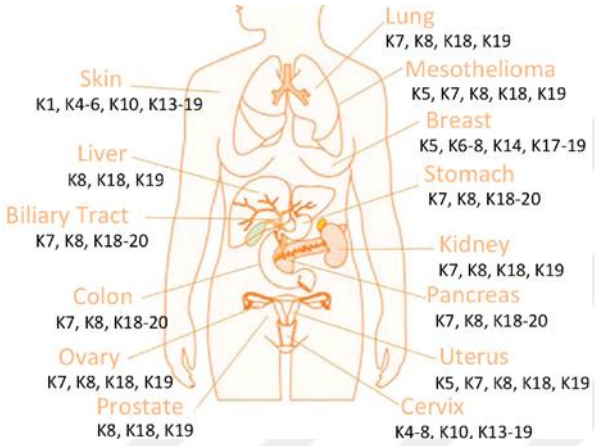

Figure 2.8. Tissue-Specific Manner Expression of Keratin Proteins. [38]

Generally, one acidic (Type I) and one basic (Type II) keratin are found together as a heterodimer. Most of the keratins are seen as a heterodimer and they are expressed in a tissue/organ-specific manner. K5 pairs with K14 and they are expressed in the stratified epithelium. K8 pairs with K18 and they are expressed in simple epithelial cells. Any mutation, resulting in disruptions in heterodimer pairing, could cause severe diseases in the organism. Inherited mutations in genes coding Keratin 5 or Keratin 14 are associated with epidermolysis bullosa simplex (EBS), is a severe condition in weakness in mechanical stress and fragility [39, 40].

Interestingly, keratins are important for other research fields like cancer biology rather than cell stress. Keratin proteins are widely used as a biomarker in tumor diagnosis. They are associated with many other diseases. It has been revealed that Keratin 5, Keratin 14 and Keratin 17 upregulation is associated with squamous cell carcinoma (SCC) and K18 with

adenocarcinoma [41]. Even more, it has been shown that collective invader cells become K14+ during an invasion in major breast cancer subtypes [42].

Keratin reorganization is significant for cellular functionality as well as how they are expressed in the cell. Intermediate filament reorganization and regulation are mainly coordinated through post-translational modifications (PTMs) (**Figure 2.9**). Phosphorylation, O-linked glycosylation, ubiquitination and sumoylation are among the major post-translational modifications. These modifications may result in drastic changes in keratin morphology or function in the cell. Therefore, Different cellular functions are correlated with different modifications. Even more, distinct modifications may be related to a disease. Dephosphorylated K8 Ser73/Ser431 was associated with increased tumor progression in oral squamous cell carcinoma (OSCC) [43]. Hyperphosphorylated K8/K18 takes a role in chronic liver disease progression [44,45].

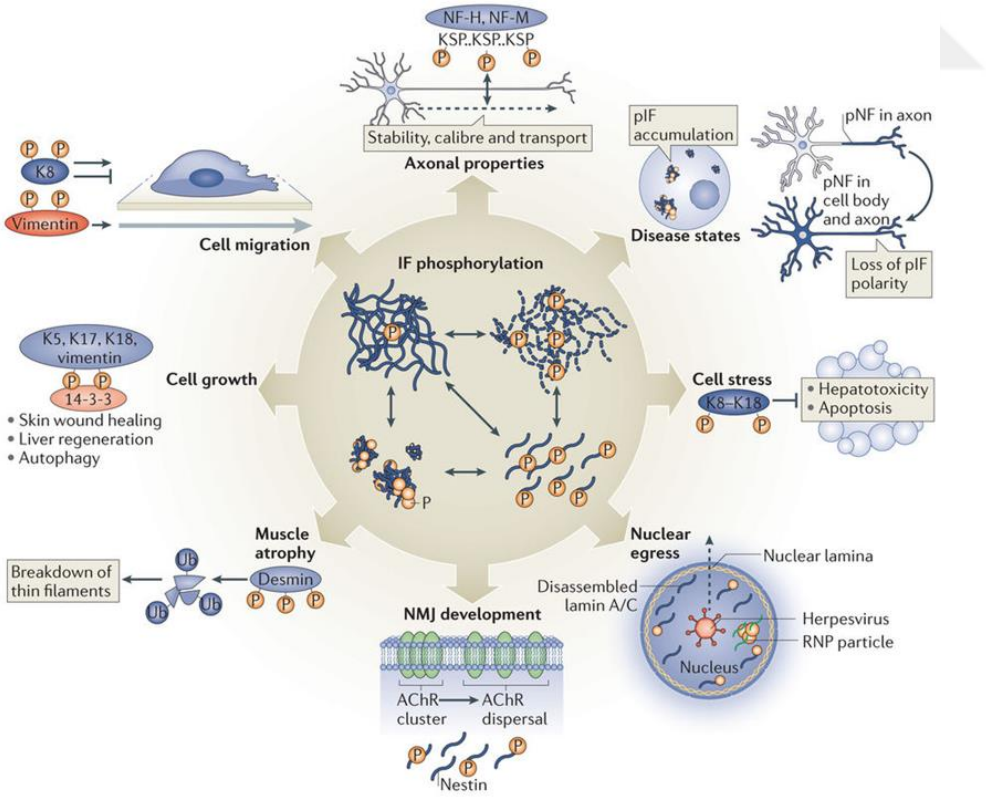

Figure 2.9. Intermediate Filament Regulation Through Post Translational Modification. [46]

The regulation of keratins is well established in some fields. They have heavily studied in cell stress, cell migration and apoptosis in terms of their associated partners and the underlying mechanism of their regulations. The role of keratins in the cell cycle has been ignored for a long time. It is tickling question how these robust structures are specifically reorganized at the curtain time point in the cell cycle, which is a very dynamic process. When the insoluble property of keratin is considered, it is interesting to understand how keratins are cleared up between two daughter cells. Therefore, there should be an efficient mechanism in the cell to provide disassembly of keratins from cleavage furrow. Otherwise, the cell could be halted in the cytokinesis stage because of failure in daughter cell separation. In this study, we tried to address these questions.

The first study on the regulation of keratins in cell division was revealed in the early 1980s. It has been shown that Keratin 8 appeared as speckles formation starting from prophase to telophase [47]. They suggested that CDK1 phosphorylation provoked speckle formation during mitosis (**Figure 2.10)**. However, they stated that the phenotype was not seen in all the cells in the population, but it was common in different cell types. Varieties in the rate of phenotype raise the possibility of the presence of multiple regulation mechanisms for keratin reorganization. Consequently, there could be other regulators which take a significant role in cell division, such as RhoA, Plk1, Aurora B, PRC1 and ESCRTIII.

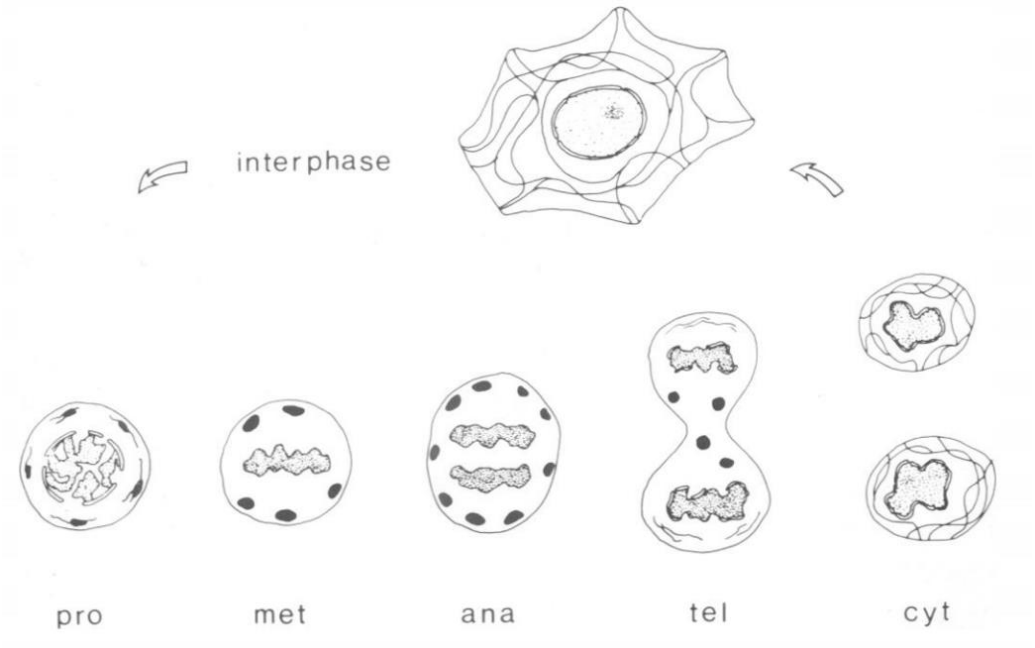

Figure 2.10. Proposed Model of Keratin Filament Reorganization During the Cell Cycle. Keratin 8 formation as a speckle is suggested for Keratin 8 regulation during the cell cycle. [47]

2.6. Aurora B and Keratin 8

Recent study reported that Keratin 5 protein is phosphorylated by CDK1, Aurora B and Rho-kinase for mitotic reorganization of K5/K14 network [48]. K5 T23 and K5 S30 phosphorylation were detected during early mitois and late mitosis respectively in HaCat cell **(Figure 2.11)**. This finding shows that cell cycle dependent phosphorylation of keratin filament may required.

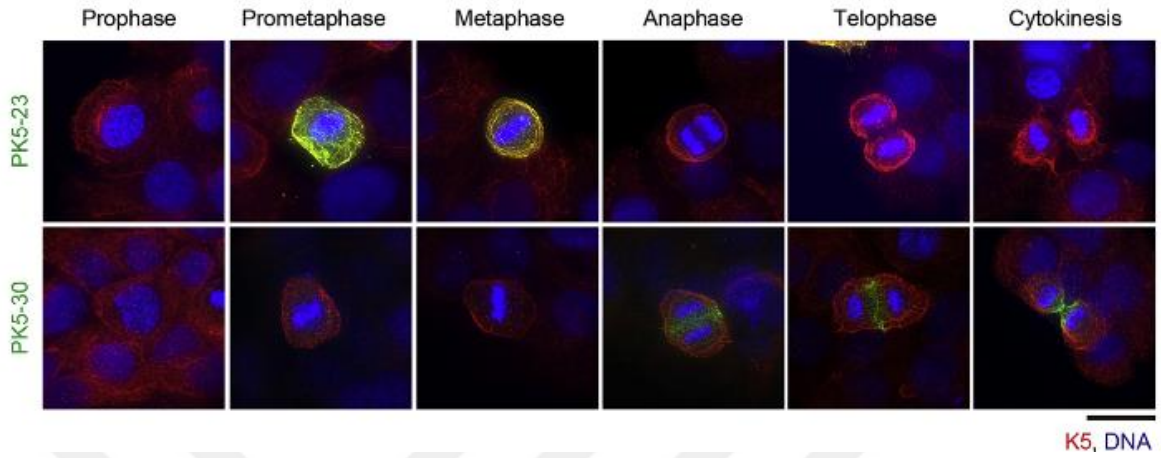

Figure 2.11. Localization of Keratin 5 T23 and S30 phosphorylation through cell cycle in HaCat cell [48].

In another study, it has been published keratin filaments are disassembled at the midplane of Xenopus laevis eggs by Aurora B phosphorylation [49]. In this study, they showed that Keratin 8 filaments were cleared up from cleavage furrow ingression region where CPC is enriched in Xenopus zygote **(Figure 2.12).** Aurora B kinase acts in cell division as part of the Chromosomal Passenger Complex (CPC). During metaphase and anaphase CPC localizes to centromeres and the surface of chromosomes where it regulates chromosome condensation and helps correct errors in kinetochore-microtubule attachments [50]. At the onset of cytokinesis, it translocates to the spindle midzone where is promotes assembly and ingression of the cleavage furrow. Midzone-localized Aurora B also generates a phosphorylation gradient that helps to resolve segregation errors in between segregating chromosomes [51].

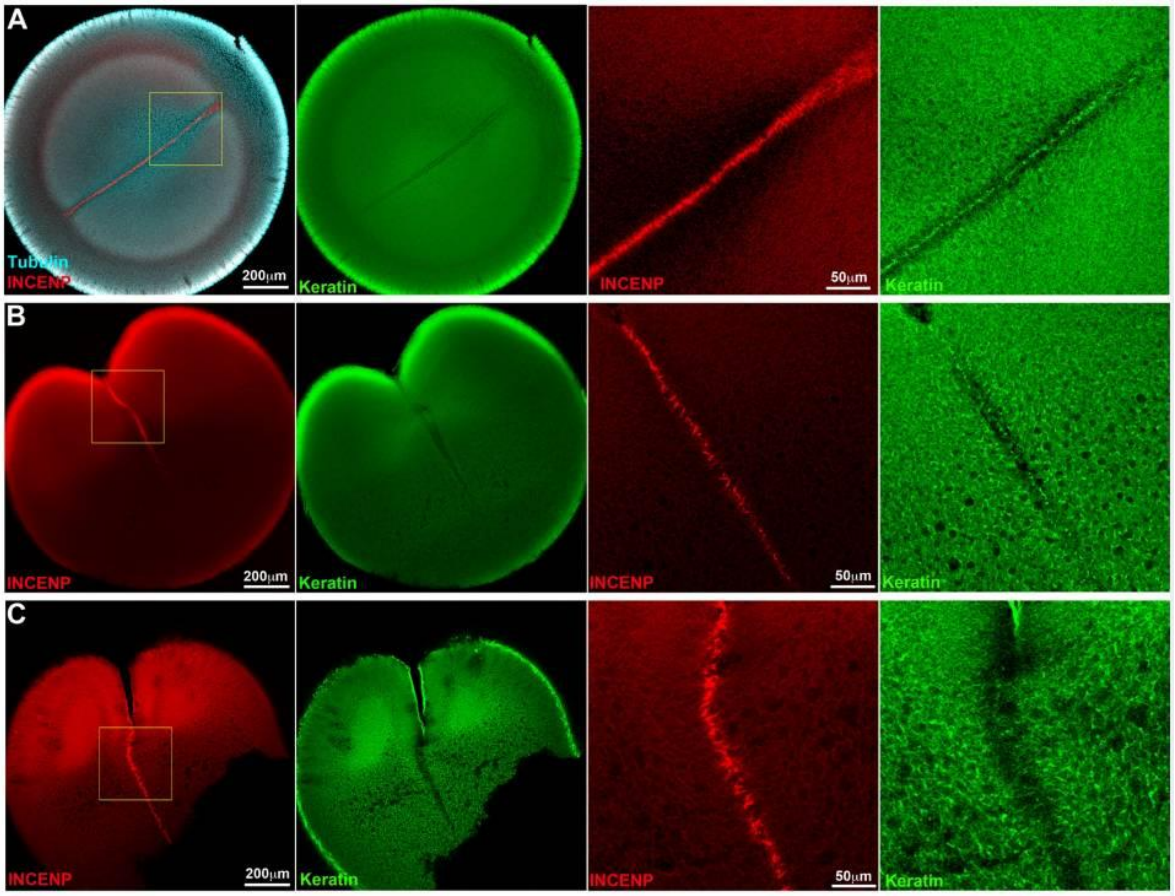

Figure 2.12. Keratin 8 filament clearance from cleavage furrow ingression in fixed Xenopus zygotes. A. 70 min post fertilization B. 90 min post fertilization C. 100 min post fertilization

In a previous genome-wide phosphoproteome study, Aurora B specific phosphosites were discovered in mitosis and cytokinesis. The study identified the specific phosphosites which are decrease upon Aurora B inhibition in cytokinesis. In this study, some specific Keratin 8 phosphopeptides were indicated as Aurora B dependent during mitosis and cytokinesis [52] (**Figure 2.13)**.

Protein Name	Sequence	Phos. Site	Mock/VX680	Mit/Cyt
Keratin-8	SYKV**S**TSGPR	S5	10.49	0.24
	SYTSGPGSRI**S**SS**S**FSR	S11, S14	8.45	0.38

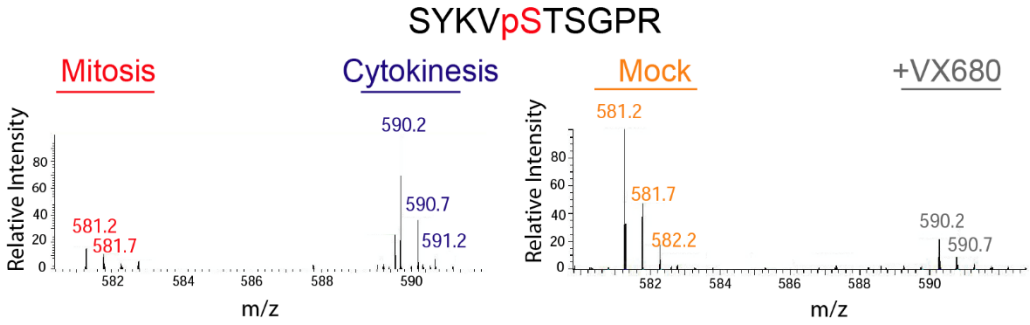

Figure 2.13. Aurora B dependent Cytokinesis Specific Phospho Keratin 8 peptides. Keratin 8 Ser13 and Ser34 were identified as cytokinesis-specific Aurora B phosphorylation residues [52].

The most current study revealed that Aurora B targets intermediate filaments as well as actin and microtubules [9] (**Figure 2.14)**. In this phosphoproteome analysis, up and down-regulated unique phosphopeptides were identified upon small molecule mediated Aurora B inhibition. Cytoskeleton proteins composed the majority of targets. In the light of the previous findings, we want to focus on the regulation of Keratin 8 depending on Aurora B phosphorylation.

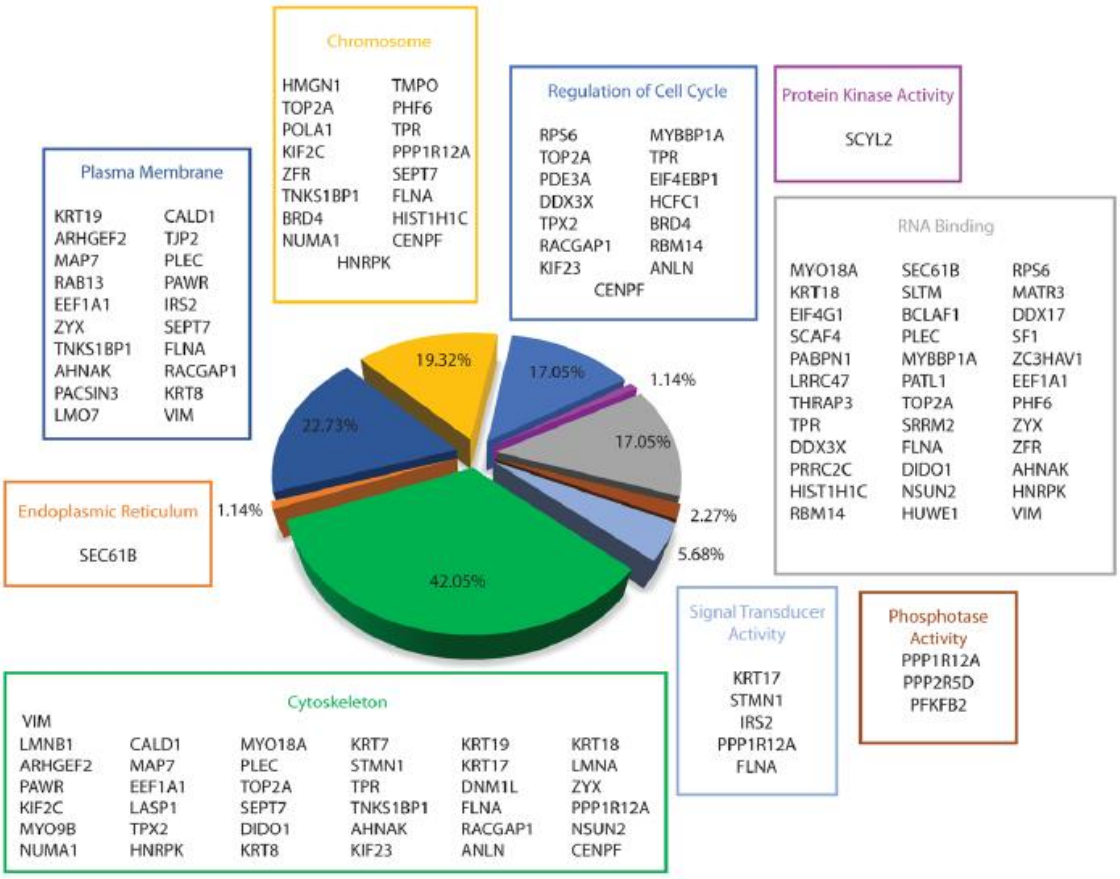

Figure 2.14. Targets of Aurora B During Cytokinesis. [9]

Chapter 3

MATERIALS AND METHODS

3.1. Cell Culture

HeLa cells were maintained in Dulbecco's modified Eagle's medium (DMEM) (Lonza, BE12-741F) at 5% CO2 and 37°C incubator. DMEM includes 10% Fetal Bovine Serum (FBS), 100 unit/ml Penicillin and 100 µg/ml Streptomycin (Lonza, DE17-602E). The cells were routinely passaged when they reached 90% confluency in the cell culture dish. 1X Phosphate Saline Buffer (PBS) was used to wash cells once. Then, the cells were treated with 0.25% Trypsin/EDTA (Sigma Aldrich, T4049) for 5 minutes at 5% CO2 and 37°C incubator to detach them from the dish. After 5 minutes of incubation, DMEM, that is at least 3X volume of trypsin, was added to the dish to deactivate trypsin activity. The required number of cells were seeded on a new cell culture plate.

To harvest cells, the cells were detached from the plate by trypsinization. Trypsin deactivated suspension pelleted at 1,200 rpm for 5 minutes at 4°C by centrifugation. The supernatant was discarded and the cells were washed with 1X PBS. Then pelleted cells were quickly frozen by deeping them into liquid nitrogen. Cell pellets were kept at -80°C for long-term storage. On the parallel, to freeze cells for storage in nitrogen, a freezing medium (70 % DMEM, 20% FBS and 10 % dimethyl sulfoxide (DMSO) was used.

HeLa Kyoto cells stably expressing Aurora B-LAP-tagged BAC transgenes were maintained in DMEM, including 10 % FBS, 100 unit/ml Penicillin, 100 µg/ml Streptomycin and 400 µg/ml Geneticin at 5% CO2 and 37°C incubator. The passing, harvesting and freezing procedure was the same as described above.

3.2. Cell Synchronization

Synchronization experiments was proceeded with the cells whose occupancy reached 30%. Cell synchronization aims to arrest cells at interphase or mitosis. Double thymidine block was applied to arrest cells at interphase. Briefly, 2 mM Thymidine (Santa Cruz, 296542A) was given in DMEM to the cells along 20 hours for the first thymidine block. The cells are synchronized at G1/S phase because G1/S cell cycle checkpoint was not satisfied under unsuitable environmental conditions. Thymidine arrest is reversible. When thymidine is removed from the environment, the cell proceeds with the cell cycle. 1X PBS was used to remove excess thymidine. PBS wash was repeated three times to complete the removal of thymidine. After PBS wash, the cells were released from G1/S arrest to the next cell cycle stage for 7-8 hours. To increase synchronization efficiency, thymidine arrest was repeated by incubating cells in 2 mM Thymine for 17 hours. If Interphase cell arrest was required, the cells were harvested or fixed at the end of second thymidine block. To arrest cells at mitosis specifically in prometaphase, the cells were washed with PBS and released from thymidine for 7 hours. At the end of the second thymidine release, the cells were incubated with 30 nM Nocodazole (Calbiochem, 487928) for 5 hours. Nocodazole is an inhibitor for microtubule polymerization and its effect is reversible. In the presence of Nocodazole, the cells cannot satisfy the spindle assembly checkpoint (SAC) and are arrested at prometaphase. If mitosis cell arrest was required, the cells were harvested or fixed at the end of Nocodazole treatment. To synchronize the cells at cytokinesis, Nocodazole was removed by 1XPBS wash three times. After one hour's release from Nocodazole, the cells were harvested or fixed at bipolar cytokinesis.

As alternative to nocodazole arrest, 10 µM Kinesin 5 inhibitor S-Trityl-L-cycsteine (STC) (Sigma, 164739) was incubated for 12-16 hours after double thymidine block. At the end of STC incubation, cells were harvested for mitosis.

If Aurora B inhibition was required for the experiment, 1 µM AZD1152 or 0.5 µM VX680 were incubated for 30 minutes in the 30th minute of nocodazole release.

3.3. CRISPR/Cas9 mediated Keratin 8 Knockout

Targeting guide with sequence 5' CGAGGAGCTGATGCGGGAA 3' and non-targeting guide with sequence 5'-ACGGAGGCTAAGCGTCGCAA-3' were cloned into pLenti CRISPRv2 using BsmBI restriction digestion of backbone using protocol from Zhang lab. HeLa S3 cells were transiently transfected with plentiCRISPRv2 plasmid containing Keratin 8 guide and non-targeting control by using Lipofectamine. Transfected cells were selected with puromycin. Serial dilution was used to prepare monoclonal cells. Loss of Keratin 8 expression in HeLa cells was detected by using immunoblotting.

3.4. Cloning and Transfection

3.4.1. Side Directed Mutagenesis of 5XA Keratin8-GFP vector

We took wild type Keratin 8 in pEGFP-N3 (Addgene) (WT-K8-GFP) vector as a gift from Dr. Milind Vaidya (ACTREC). GFP protein was fused to Keratin 8 at the N terminus in the vector. Our former master student Gurkan Mullaoglu (M.Sc. Molecular Biology and Genetic Department, Koc University) and Goksu Ozlu (former intern student) mutated S13, S34 and S35 residues to Alanine on wild type K8-GFP construct by the side directed mutagenesis procedure. To obtain S13A, S34A, S35A, S36A, and S37A residue mutations on the same construct, we performed further side-directed mutagenesis procedures to introduce additional S36A and S37A mutations. Since the final construct had five serine to alanine mutations, we named the construct as 5XA K8-GFP. In brief, target templates including mutations were exponentially amplified by polymerase chain reaction (PCR). To set up 25 µl PCR reaction mix, we used 50 ng/µl Keratin 8 S13A, S34-35A in pEGFP-N3 vector supplemented with 200 nM forward primer (5' GGTTCCCGCATCGCCGCCGCCGCCTTCTCCCGAGTGGGC 3'), 200 nM reverse primer (5' GCCCACTCGGGAGAAGGCGGCGGCGGCGATGCGGGAACC 3'), 280 µM dNTP mix (NEB, N0447S), 1X Pfu DNA polymerase reaction buffer, 1.25 unit Pfu Turbo DNA polymerase (Stratagene, 600252) and distilled water (dH_2O). PCR conditions were determined as follows: Initial denaturation at 98°C for 30 seconds, 19 cycles of; denaturation

at 95°C for 40 seconds, annealing at 58°C for 3.5 minutes, extension at 68°C for 15 minutes and final extension at 68°C for 5 minutes. 1% agarose gel was used to confirm the PCR product by running in gel electrophoresis. Band intensity of PCR product was compared to control without primers. Further, 5 Unit DpnI was used to remove the parental template from the PCR product by digesting methylated DNA at 37°C for 1 hour. DpnI treatment was followed by template transformation into Escherichia coli (E. coli) DH5α competent cells. Briefly, 100 ul E.coli DH5α competent cells were used for all digested PCR products. E.coli and PCR template mix was incubated on the ice for 30 minutes. Then, the mixture was exposed to 42°C for 45 seconds to induce heat shock and the formation of a pore. The cells were immediately placed on ice for a few minutes. 1 ml of Lysogeny broth (LB) without any selective antibiotic was added to the mixture. Bacteria were grown in LB for 1 hour and 30 minutes. Bacteria were concentrated by benchtop centrifuge for a few minutes. Concentrated bacteria were sed into 50 µg/ml Kanamycin agar plates. Inoculated bacteria were incubated at 37 °C for 17 hours to let a single colony grow. Single colonies were picked and inoculated into liquid 50 µg/ml Kanamycin LB for 17 hours of incubation at 37 °C. Plasmid DNA was purified from growth bacteria with Macherey-Nagel Nucleospin Plasmid mini-prep kit by following the manufacturer's instructions. Sequence confirmation of purified plasmids was done by Macrogen (Europe) with a universal CMV forward primer. Confirmed plasmids were selected to use in further experiments.

3.4.2. Cloning Wild Type Keratin pGEX-6P-1 vector

In this part, we aimed to generate Keratin 8 pGEX-6P-1 vector (K8-GST) to use in Keratin 8 purification experiments with glutathione beads. Empty pGEX-6P-1 (Addgene) was used to clone wild-type Keratin 8. Basically, Keratin 8 is copied from Keratin 8-GFP-pEGFP-N3 with PCR and cut into the pGEX-6P-1 vector. Keratin 8 amplification reaction was determined for 20 µl reaction as follows: 20 ng/µl WT Keratin 8 pEGFP-N3 vector, 1X Phusion High Fidelity (HF) DNA polymerase reaction buffer, 200 nM forward primer including EcoRI restriction site (5' *GCGCGCGAATTCATGTCCATCAGGGTGACCCAG* 3'), 200 nM reverse primer including SalI restriction site (5' *GCGCGCGTCGACCTTGGGCAGGACGTCAGAGGAC* 3'), 200 µM dNTP mix (NEB,

N0447S), 0.6 Unit Phusion High Fidelity DNA polymerase (NEB, M0530S) and dH_2O. PCR conditions were determined as follows: Initial denaturation at 98°C for 1 minute, 35 cycles of denaturation at 95°C for 10 seconds, annealing at 70°C for 30 seconds, extension at 72°C for 3 minutes and final extension at 72°C for 5 minutes. 1% agarose gel was used to confirm the PCR product by running in gel electrophoresis. Correct PCR product was determined by comparing the DNA ladder. Macherey-Nagel Nucleospin Gel and PCR Clean-up Kit was used to purify PCR product by following manufacturer's instructions.

pGEX-6P-1 (acceptor vector) and cleared up PCR fragment (insert) were treated with EcoRI-HF and SalI-HF restriction enzymes. Digestion reaction was performed in 50 µl reaction mixture as follows: 1X Cut Smart buffer, one unit of each restriction enzyme (EcoRI-HF and SalI-HF), 1 µg of PCR fragment or acceptor vector and dH_2O at 37°C for 2 hours. Then, only digested acceptor vector was treated with Antarctic phosphatase in the reaction mixture as follows: 1 unit Antarctic Phosphatase (NEB, M0289S) and 1X Antarctic phosphatase reaction buffer (final concentration). To heat inactivate reaction enzymes, the digested insert was inactivated at incubated at 65°C for 10 minutes. Restriction enzymes and Antarctic phosphatase in digested acceptor vectors were inactivated at 70°C for 10 minutes. Heat-inactivated products were purified with Macherey-Nagel Nucleospin Gel and PCR Clean-up Kit by following the manufacturer's instructions.

Further, ligation reaction was performed in 20 µl reaction buffer as follows: 1X T4 DNA ligase buffer, 50 ng acceptor vector (digested p-GEX-6p-1), 45 ng digested PCR fragment (K8 insert), 1 µl T4 DNA ligase (NEB, M0202S) and dH_2O at 16 °C for overnight. Ligated vector was transformed into Escherichia coli (E. coli) Stbl3 competent cells. For the transformation process, the previously described protocol was followed. Concentrated bacteria were seeded into 100 µg/ml Ampicillin agar plate. The Agar plate was incubated at 37 °C for 17 hours. Chosen single colonies were inoculated into liquid 100 µg/ml Ampicillin LB and incubated at 37 °C for 17 hours. Plasmids were purified with Macherey-Nagel Nucleospin Plasmid mini-prep kit by following the manufacturer's instructions. Sequence confirmation of purified plasmids was done by Macrogen (Europe) with universal M13-pUC reverse primer. Confirmed plasmids were selected to use in further experiments.

3.5 Transfection

For plasmid transfection to HeLa cells, Lipofectamine 2000 was used by following manufacturer's instructions. Transfected cells were used in immunostaining, live cell imaging or western blot experiments. Transfection was performed as followed procedure. First, DMEM containing 10% FBS was changed to DMEM containing 1% FBS to increase transfection efficiency. Then, the transfection mixture was prepared. 300-1500 ng DNA was diluted in 100 µl Optimem (Thermo Fisher, 31985047) and incubated at room temperature for 5 minutes. On the parallel, 1-5 µl Lipofectamine 2000 (~3X volume of DNA amount) was diluted in 100 µl Optimem and incubated at room temperature for 5 minutes. Then DNA and Lipofectamine were combined 1:1 ratio and incubated at room temperature for 15 minutes. DNA/Lipofectamine mixture was added to one well of 12-well plated cells drop by drop. DNA and Lipofectamine amounts are fixed for 12-well plate transfection. However, amounts are arranged regarding bigger or smaller plates. After 6-10 hours of transfection, DMEM including Lipofectamine was changed to prevent toxicity.

3.6 Keratin 8 Purification from Bacteria

3.6.1. Keratin 8-GST Isolation from Inclusion Body of Bacteria

Proteins are routinely produced in bacteria for a large amount of purification. However, some proteins are failed to proper folding and form aggregates named as inclusion body. In this part, we aimed to isolate Keratin8-GST from the inclusion body in bacteria. To achieve that, we transformed WT K8-GST (in pGEX-6P-1 vector) into E. coli BL21 competent cells by following the previously described transformation protocol. A single colony was inoculated in 100 µg/ml Ampicillin LB 50 ml starter culture and incubated at 37 °C for 17 hours. The next day, 10 ml of starter culture was added into fresh 250 ml 100 µg/ml Ampicillin LB. It was incubated at 37 °C until its OD600 reached 0.5. Protein production was increased by induction with 1 mM Isopropyl β-D-1-thiogalactopyranoside (IPTG) at OD600≈0.5 for overnight at 37°C. On the third day, bacteria were harvested by centrifuging at 5000rpm for 10 min at 4 °C. Pelleted bacteria was weighted. 4-fold volume (ml) lysis buffer of bacteria

weight (g) was added to lyse bacteria. Lysis buffer included 100 mM TrisCl pH 8, 5mM EDTA, 5mM DTT and 1X Protease Inhibitor (Roche, **11**836170001). Tissue grid homogenizer was used to re-suspend pellet in lysis buffer on ice. Next, the suspension was sonicated with sonicator at power 45, 8 % for 10 seconds for 4 cycles by 30 seconds break on ice between cycles. Then, the sonicated suspension was pelleted by centrifuging at 13,500 rpm at 4°C for 30 minutes. The pellet was washed with lysis buffer with a centrifuge step by skipping the sonication procedure. Excess NaCl was removed with washing steps. After washing, the pellet was suspended in extraction buffer including 8 M Urea, 5 mM DTT, 2 mM EDTA, 10 mM TrisCl pH 8. The suspension was homogenized with a tissue grid homogenizer. The suspension was tumbled for 3 hours at room temperature. Lastly, the suspension was pelleted by centrifuging at 100,000 xg for 1 hour at 4°C. The supernatant was stored as isolated recombinant protein from inclusion body in bacteria.

3.6.2. Refolding of WT K8-GST by Dialysis

To obtain Keratin 8 in its native folding, we performed dialysis. In the previous part, isolated recombinant protein was obtained in extract buffer including 8M Urea. Since urea breaks hydrogen and hydrophobic bonds, Keratin 8 cannot fold properly in extract buffer. Therefore, we changed the buffer of isolated recombinant protein by dialysis. We used dialysis buffer including 25 mM Hepes pH 7.4, 100 mM KCl, 5mM $MgCl_2$, 0.5 mM EGTA. Isolated recombinant protein product was incubated in a dialysis bag including dialysis buffer at 4°C for overnight by stirring.

3.6.3. Batch Purification of K8-GST

In this part, we aimed further purify isolated recombinant protein because it includes unwanted proteins. To do that, we started with the preparation of glutathione beads. 10-fold volume 1X PBS of glutathione beads was used to wash 75 µl beads by centrifuging at 500 xg at 4°C for 4 minutes two times. The last wash was repeated with dialysis buffer (25 mM Hepes pH 7.4, 100 mM KCl, 5mM $MgCl_2$, 0.5 mM EGTA). Glutathione beads were diluted to 50% slurry with dialysis buffer. Next, a 10-fold dialyzed protein volume of glutathione beads were added. Bead and WT K8-GST mixture was incubated at 4°C for overnight by

gentle agitation. The mixture was pelleted by centrifuging at 500 xg at 4°C for 4 minutes. Bound K8-GST protein was pelleted. Unbound protein was removed with a centrifuge step. Beads were washed with wash buffer including 25 mM Hepes, 150 mM KCl, 5mM $MgCl_2$, 0.5 mM EGTA, 1 mM DTT, 0.01% NP40 by gentle agitation for 10 minutes at 4°C. Wash was followed by a centrifuge step at 500 xg at 4°C for 4 minutes. The washing step was repeated twice. Then, beads were washed with harsh wash buffer including 25 mM Hepes, 600 mM KCl, 5mM $MgCl_2$, 0.5 mM EGTA, 1 mM DTT, 0.01% NP40. Last wash repeated with normal wash buffer to remove excess KCl. WT-GST-K8 was eluted in a buffer containing 100 mM TrisCl pH 8.0, fresh 10 mM Reduced Glutathione and 1mM DTT. Pellet was kept as recombinant WT K8-GST at -80°C for long storage and used in further experiments.

3.7. *In vitro* kinase assay and Mass Spectrometry

Isolated WT-K8-GST was incubated with purified Aurora B complex, Aurora B and INCENP fragments were co-expressed from bicistronic vector pGEX-2rbs with GST-tag at the N-terminus of Aurora B. Aurora B complex was purified with GST sepharose and eluted from beads by cleaving the GST-tag by PreScission protease in buffer including 50 mM Tris pH 7.5, 150 mM NaCl, 1 mM EDTA, 1 mM DTT, 10 µg/ml leupeptin and 10 µg/ml pepstatin. The purified Aurora B complex was gift from Dr. Masanori Mishima (University of Warwick). For in vitro kinase assay, 25 µg WT-K8-GST and ~ 0.75 µg Aurora B complex were incubated in 100 µl kinase reaction buffer including 20 mM PIPES pH 7, 2 mM $MgCl_2$, 2 mM EGTA, 100 mM NaCl and 0.2 mM ATP at 30°C for 40 minutes. Kinase reaction was dissolved in 50 µl 3X SDS Blue Loading Buffer supplemented with 100 mM Dithiothreitol (DTT) by boiling it at 85°C for 10 minutes. After alkylation with 100 mM IA (I6125, Sigma Aldrich), the samples were loaded into 12% Tris-Glycine Precast Gels (Pierce, 25247) and stained with Page Blue Protein Staining (Thermo Fisher Scientific, 24620). The band corresponding to Keratin 8:GST (66-81 kDa) was cut and after the washing steps, the gel plugs were digested by using 1:50 (Trypsin: Protein amount ratio) Sequencing Grade Modified Trypsin (Promega) at 37 °C overnight. Digests were desalted by Stage Tipping

using Empore C18 47mm disks and resuspended in 5% FA and 5% ACN for LC-MS/MS analysis

3.8. SDS-PAGE and Western Blotting

For SDS-PAGE, stacking and separated gels were poured sequentially. 10% separating gel included 5ml 30% acrylamide/ 0.8% bisacrylamide, 3.75ml 4X Tris.Cl/SDS pH 8.8, 6.25ml ddH2O, 0.05ml 10% (w/v) APS, 0.01ml TEMED. Stacking gel included 0.65ml 30% acrylamide/ 0.8% bisacrylamide, 1.25ml 4X Tris.Cl/SDS pH 8.8, 3.05 ml ddH2O, 0.025ml 10% (w/v) APS, 0.005ml TEMED. Equal amount of protein from each sample were loaded and run on 10% gel at 120V for 2 hours.

Separated proteins were transferred with the wet transfer into nitrocellulose membrane (Whatman Protran, BA85) at 40V and 4°C for overnight. Ponceau dye was used to confirm protein transfer. After ponceau was removed with distilled water, the membrane was blocked with 4% nonfat milk in TBS/0.1 % Tween20 (TBST) for 45 minutes at room temperature. Then, primary antibodies were diluted at the required amount in 2%BSA-TBS/0.1 % Tween20. The membrane was incubated with primary antibodies for 3 hours at room temperature or overnight at 4°C. At the end of primary antibody incubation, the membrane was washed with TBST for 10 minutes three times. Secondary antibodies were prepared in 4% nonfat milk in TBS/0.1 % Tween20 (TBST). The membrane was incubated with secondary antibodies for 1 hour and 30 minutes at room temperature. In the end of secondary antibody incubation, the membrane was washed with TBST for 10 minutes three times. The primary and secondary antibodies used for immunofluoresnce are listed on Table 3.1. and 3.3. To remove excess tween20, the final was done by TBS. Proteins were detected with ECL (Pierce ECL western blotting substrate 32106). Results were accumulated in ChemiDoc MP Imaging System (Bio-Rad, 12003154). Optionally, films were developed in the dark room.

3.9. Immunofluorescence, Microscopy and Quantification

For the immunofluorescence experiment, cells were seeded in 12-well plates on cover slips. Before fixation, the cells were washed with 1X PBS. To fix cells, two different methods were used according to visualization requirements: PFA or Methanol fixations. For PFA fixation,

cells were incubated in 3% PFA at 37°C for 15 minutes. For methanol fixation, cells were incubated in 100% methanol at -20°C for 5 minutes. Fixed coverslips were washed with 1X PBS three times. Then, the coverslips were incubated in PBS-0.1% Triton-X (PBS-Tx) for 5 minutes. For blocking, the coverslips were incubated in 2% BSA in PBS-Tx for 30 minutes at room temperature or for overnight at 4°C. Primary antibodies were diluted at the required amount in 2%BSA-TBS/0.1 % TritonX. The coverslips were incubated with primary antibodies for 3 hours at room temperature or overnight at 4°C. In the end of primary antibody incubation, the coverslip was washed with PBS-0.1% Triton-X for 5 minutes three times. Secondary antibodies were prepared in 2%BSA-TBS/0.1 % TritonX. The coverslips were incubated with secondary antibodies for 1 hour and 30 minutes at room temperature. In the end of secondary antibody incubation, the coverslip was washed with PBS-0.1% Triton-X for 5 minutes three times. DNA was stained with 1 µg/ml DAPI in 2% BSA in PBS-Tx for 5 minutes at room temperature. Then, coverslips were washed with PBS-0.1% Triton-X for 5 minutes three times. Lastly, a homemade mounting medium was used to mount the coverslips. Then, it was sealed with nail polish. The coverslips were stored at 20°C. The primary and secondary antibodies used for immunofluoresnce are listed on Table 3.2. and Table 3.3.

For microscopy imaging, Leica DMi8/SP8 TCS-DLS, Leica DMi8 wide-field microscope or Nikon 90i Confocal Microscope using LAS X Software and NIS-Element Imaging software and Nikon Eclipse APO λ 100X/1.40 Oil objectives lens were used. Image acquisition was done by HC PL APO 63x/1.40 Oil CS2 objective of Leica DMi8/SP8 TCS-DLS.

Immunofluorescence intensities were quantified using (ImageJ Wayne Rasband), NIH and FiJi software (Wayne Rasband, NIH). Briefly, RGB values of different spots at metaphase chromosome or on cleavage furrow were measured by keeping the area constant and an average of these values was taken. The same process was applied to random spots on the background of the cell and the fluorescence intensities were normalized according to the fluorescence intensity of the cell background. Graphs were plotted by GraphPad Prism 8.

3.10. Live Cell Imaging

Live-cell images were taken on inverted confocal or fluorescence microscopes, which are Leica DMi8/SP8 TCS-DLS and Leica DMi8 wide field respectively. Cells were seeded on µ-Slide 8 well (ibidi, 80826). Time-lapse images were collected at 37 °C and 5% CO2 in a humidified chamber during imaging.

3.11. Pulldown with GFP-Trap

GFP expressing cells were grown in 40% confluency and synchronized in interphase by double Thymidine Block and in mitosis by using S-trityl-L-cysteine (STC; Sigma-Aldrich). Cytokinesis synchronization was done by second thymidine block and nocodazole release Cell pellets were lysed in l ice-cold lysis buffer (20mM Tris-CL pH7.4, 150mM NaCl, 1mM MgCl2, 10%Glycerol, 0.5mM EDTA, 10mM NaF, 0.5%NP-40, 1mM beta-glycerolphosphate, 1mM sodium pyrophosphate, 1mM sodium orthovanadate, 1mM DTT, EDTA free protease inhibitor (Pierce, 88266,) by pipetting and passing through 25-gauge needle. Cell lysates were centrifuged at 14000 rpm for 15 min at +4°C. Dilution buffer (20mM Tris-CL pH7.4, 150mM NaCl, 1mM MgCl2, 10%Glycerol, 0.5mM EDTA, 10mM NaF) was added to the supernatant in 2:3 proportions. GFP-Trap®_A (Chromotek, gta-20) was used for pulling down Aurora B-GFP. The diluted lysate was mixed with the beads and rotated for 3 hours at 4°C. After washing the beads with dilution buffer, for elution, beads were re-suspended in 2X Laemmli Sample Buffer (4% (w/v) SDS, 20% Glycerol, 120mM Tris-Cl (pH 6.8), 0.02% (w/v) bromophenol blue, 100mM DTT) and boiled for 10 min at 95°C and SDS-PAGE and Western Blotting was performed.

Table 3.1. Primary Antibodies used in immunoblotting

Antibody	**Host**	**Company**	**Catalogue Number**	**Dilution**
Anti-Tubulin (DM1A)	Mouse	Cell Signaling	3873S	1:1000
Anti-GFP	Mouse	Roche	11814460001	1:1000
Anti-Keratin 8	Mouse	Santa Cruz	8020	1:1000
Anti-Aurora B	Mouse	Abcam	3609	1:300
Anti-INCENP	Rabbit	Abcam	12183	1:2500
Anti-p Histone H3 (Ser-10)	Rabbit	Santa Cruz	8656	1:300

Table 3.2. Primary Antibodies used in immunofluorescence

Antibody	**Host**	**Company**	**Catalogue Number**	**Dilution**
Anti-Tubulin (DM1A)	Mouse	Cell Signaling	3873S	1:1000
Anti-Keratin 8	Mouse	Santa Cruz	8020	1:1000
Anti-Aurora B	Mouse	Abcam	3609	1:100
Anti-INCENP	Rabbit	Bethyl Labs	IHC-00060	1:250
Anti-Tubulin	Rat	Abcam	6160	1:500
Anti-Polo Kinase 1	Rabbit	-	-	1:1000
Anti-BubR1	Mouse	-	-	1:100
Anti-phospho S34 Keratin 8	Rabbit	Davids Biotech	HAM-SB2 (Custom specific)	1:100
Phalloidin-iFlour	-	Abcam	Ab176756	1:5000

Table 3.3. Secondary antibodies used in immunoblotting and immunofluorescence

Antibody	**Host**	**Company**	**Catalogue Number**	**Dilution**
Anti-mous IgG HRP	Goat	Cell Signaling	7074S	1:2000
Anti rabbit IgG HRP	Horse	Cell Signaling	7076S	1:2000
Anti-mouse IRDye 680RD	Goat	Licor	926-68070	1:10000
Anti-rabbit IRDye 800CW	Goat	Licor	926-32211	1:10000
Anti-mouse IgG Alexa Flour (H+L) 488	Donkey	Life Technologies	A21202	1:1000
Anti-Rabbit IgG (H+L) Dylight 488	Goat	Thermo Scientific	35552	1:1000
Anti-mouse IgG Alexa Flour (R) 555 Fab2	Goat	Cell Signaling	4409S	1:1000
Anti-rabbit IgG Alexa Flour 555 Fab2	Goat	Cell Signaling	4413S	1:1000
Anti-Rat IgG (H+L) Alexa Flour 568	Goat	Life Technologies	A11077	1:1000

Anti-mouse IgG (H+L) Alexa Flour 633	Goat	Life Technologies	A21052	1:1000

Chapter 4

RESULTS

4.1. Subcellular Localization of Keratin 8 During Cell Cycle

In this thesis, we aimed to understand the role of Keratin 8 during the cell cycle and regulation by Aurora B kinase. First, we investigated the Keratin 8 dynamics during the cell division including interphase, mitosis and cytokinesis. For this purpose, we performed immunohistochemistry to understand Keratin 8 subcellular localization in different cell cycle stages. To understand the association with Aurora B, we stained endogenous K8 and INCENP protein, which is an interaction partner of Aurora B, with fluorescence labeled antibodies and DNA with DAPI. **Figure 4.1** shows Keratin 8 subcellular localization in HeLa cells in different cell cycle stages: interphase, prophase, metaphase, anaphase, telophase and late cytokinesis. At the beginning of the cell cycle, K8 localizes to the cytoplasm and forms an interlinking network in the interphase. When the cell progress to mitosis, K8 accumulates in the periphery of the rounded cell. In prophase and metaphase, K8 localizes from the surrounding of chromosome to the cell membrane and the K8 network becomes more soluble by diffusing to the cell periphery. At the beginning of cytokinesis, K8 displays unique localization. It concentrates on the opposite poles of daughter cells and disappears from cleavage furrow. Somehow, K8 localization is dismissed from the cleavage furrow. In late cytokinesis, it regains its even distribution throughout the cell when abscission takes place. It shows that Keratin 8 dynamicity changes during the cell cycle. It shows the unique distribution in cytokinesis and disappears on the cleavage furrow.

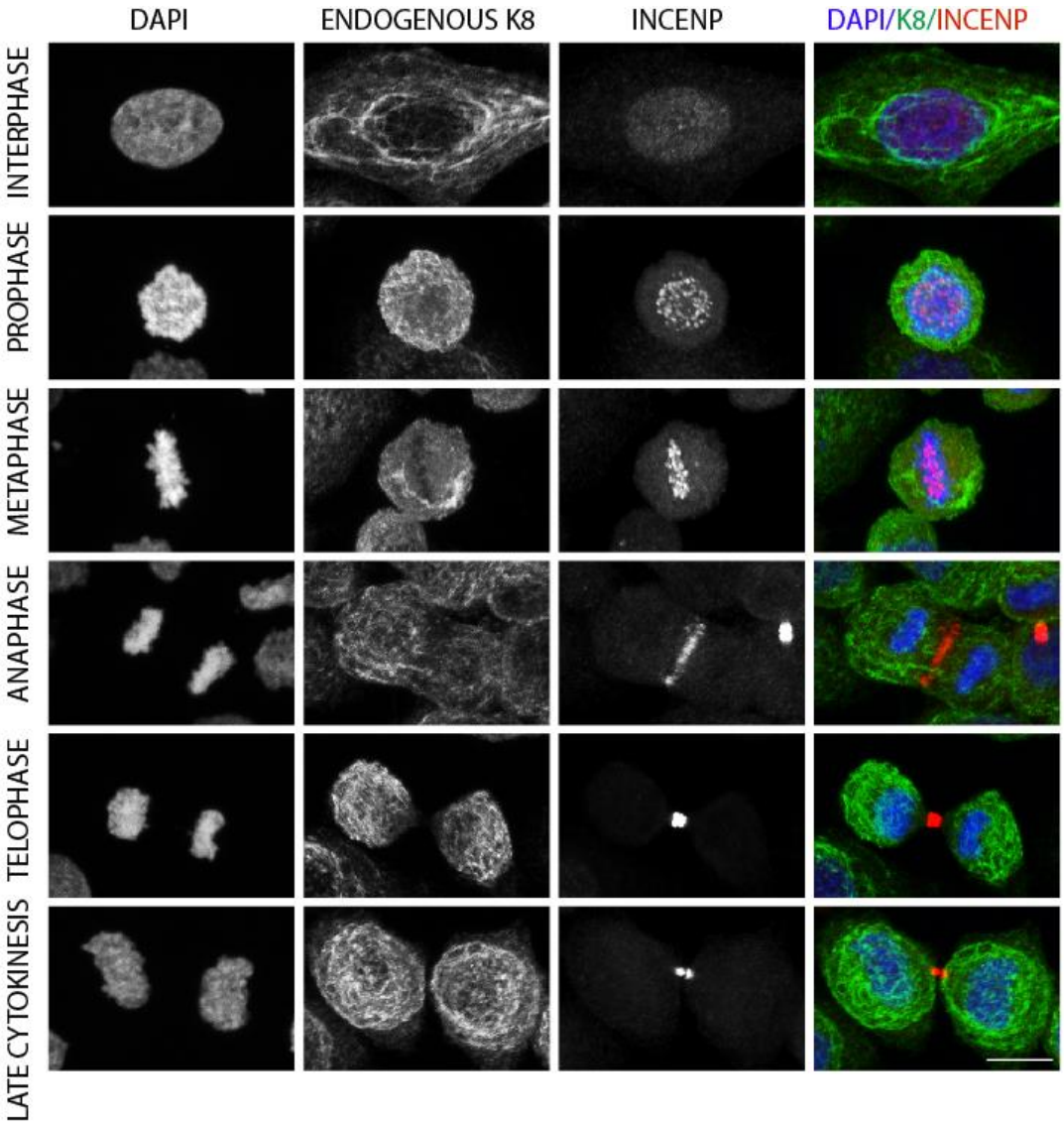

Figure 4.1. Subcellular Localization of Keratin 8 in Different Cell Cycle Stages. Immunofluorescence staining of HeLa cells during cell cycle with Keratin 8 (green), INCENP (red) antibodies and DNA (DAPI, blue). Scale bar, 10 µm.

4.2. Keratin 8 Knockout Causes Chromosome Segregation and Cytokinesis Defects

To better understand the role of Keratin 8 during cell division, we performed CRISPR/Cas9-mediated knockout of Keratin 8 in HeLa cell (K8 KO). First, we started with the generation of Keratin 8 knock-out cells in a cancer cell line. We confirmed a single Keratin 8 Knockout HeLa cell line with western blot analysis and immunofluorescence staining. **Figure 4.2**

shows efficient knockout of Keratin 8 in contrast to the control and non-targeting guide RNA expressing cells by western blot analysis. **Figure 4.3** shows the loss of Keratin 8 protein expression in K8 KO HeLa cells in contrast to the control (wild type) cells.

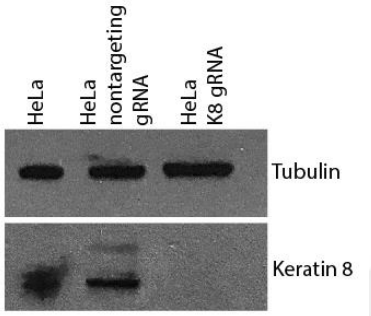

Figure 4.2. Western Blot analysis of Keratin 8 Knockout HeLa Cell.

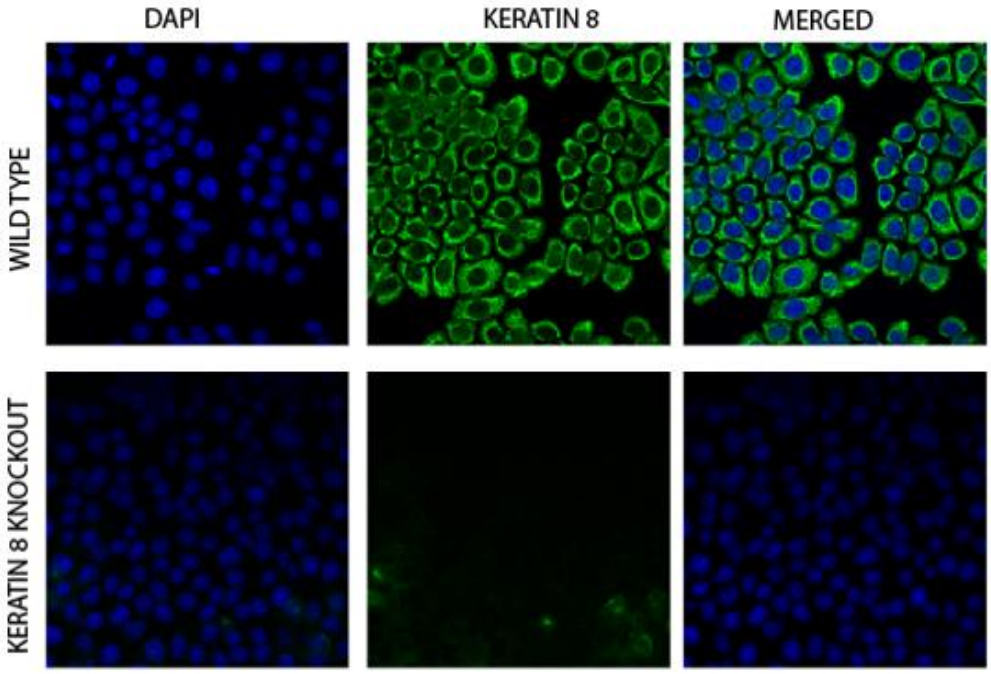

Figure 4.3. Immunofluorescence staining of Keratin 8 Knockout HeLa Cells. Control (wild type) and Keratin 8 knockout HeLa cells are stained with Keratin 8 (green) antibody and DNA (DAPI, blue).

After we managed to generate viable Keratin 8 Knockout HeLa cells, we performed live-cell imaging in wild type and K8 KO HeLa cells stably expressing Histone 2B-mCherry to understand the role of Keratin 8 in the cell cycle. Interestingly, K8 KO cells displayed defects in chromosome congression, which are misaligned and lagging chromosomes, and chromosome orientation, which is the failure of chromosome localization at the metaphase plate. K8 KO led to multinucleated cells because of failed abscission after cleavage furrow ingression. Then, we replenished Keratin 8 expression by exogenous K8-GFP expression in K8 KO HeLa S3 cells. We observed that the division proceeded without any detectable defects. **Figure 4.4** shows live-cell imaging of control, K8 KO and K8 KO expressing WT K8-GFP HeLa cells. Control cells perform successful cell division without any defects. The arrow shows chromosome orientation defect in K8 KO cells. During mitosis, chromosomes of K8 KO HeLa cells cannot localize to the metaphase plate. It ended up with multinucleation. K8 KO expressing WT K8-GFP HeLa cells shows successful cell division like control cells.

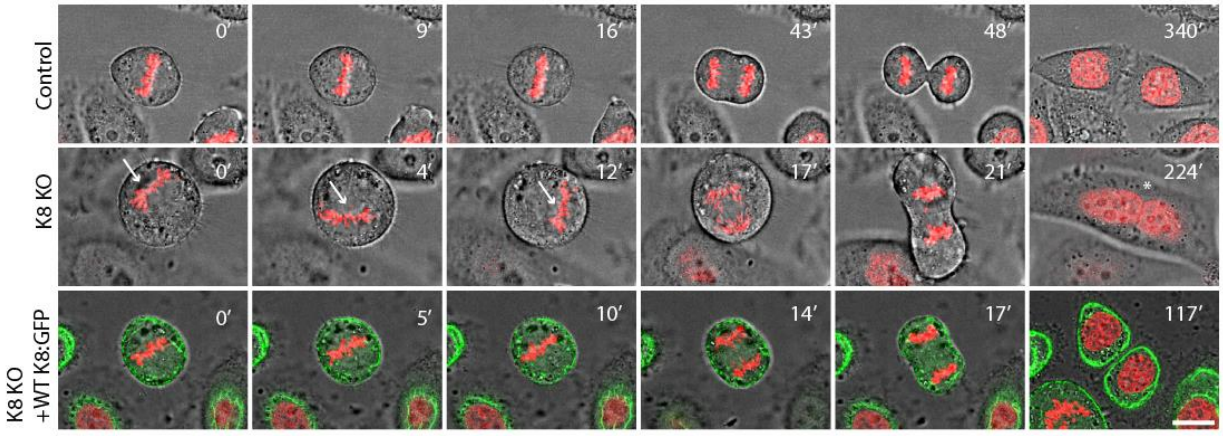

Figure 4.4. Keratin 8 Knockout causes chromosome segregation and cytokinesis defects. Representative image from live imaging of dividing HeLa cells (Video 1) expressing H2B-mcherry (red) in control, K8 Knockout (K8 KO) and K8-GFP (green) expressing rescued knockout (K8 KO+WT K8-GFP) cells.

We quantified chromosome orientation defects in live cells. To do that, we measured chromosome distance to one periphery of the cell during metaphase. **Figure 4.5** shows a schema for the quantification. As shown in **Figure 4.6,** Chromosomes of control HeLa cells are localized in the middle of the cell. Chromosome orientation was severely affected in K8 KO HeLa cells. WT K8-GFP expression in K8 KO HeLa cells rescued the phenotype.

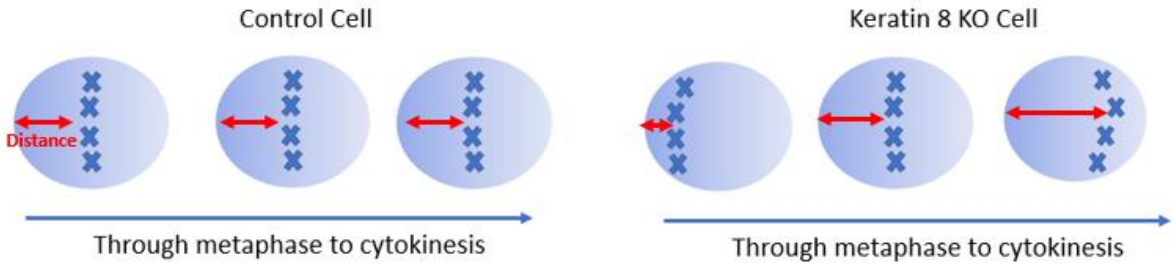

Figure 4.5. The representative schema for quantification of chromosome orientation in live cells.

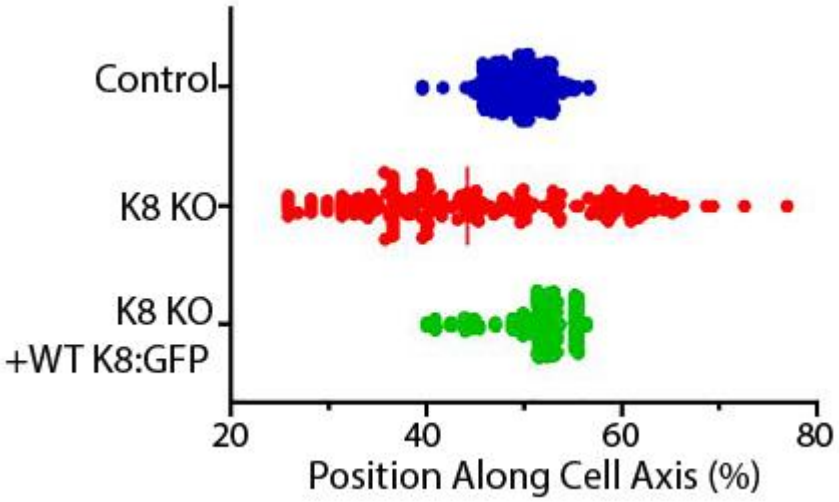

Figure 4.6. Quantification of Chromosome orientation in control, K8 KO and K8 KO expressing WT K8-GFP HeLa live cells.

We want to investigate the effect of K8 KO on cytokinesis. To do that, we quantified multinucleation in fixed cells which were stained with fluorescently labelled phalloidin antibody. **Figure 4.7** shows multinucleation defect in K8 KO HeLa cells. **Figure 4.8** represents the quantification results. K8 KO HeLa showed statistically significant ~2% increase in multinucleation compared to control.

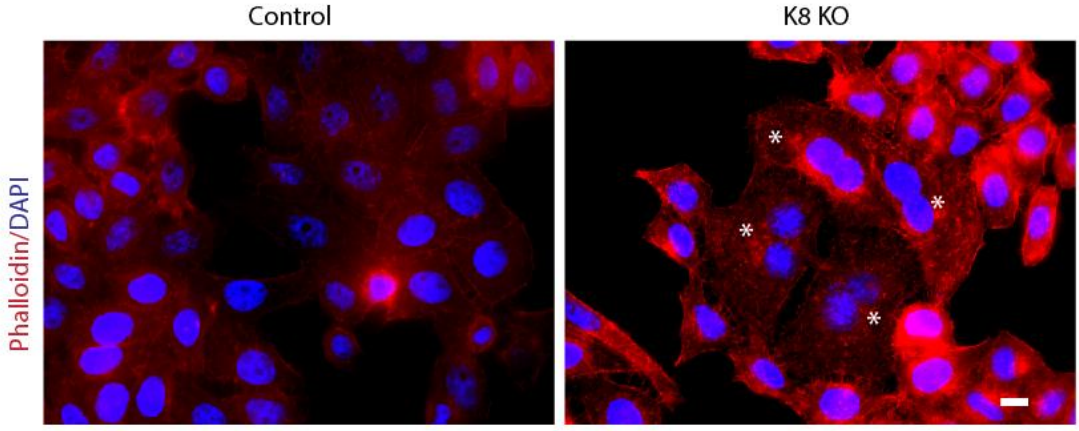

Figure 4.7. Representative image for multinucleated cells in control and K8 KO HeLa cells. Cells stained with phalloidin (red) antibody and DNA (DAPI, blue). Asterix, multinucleation. Scale bar, 10 µm.

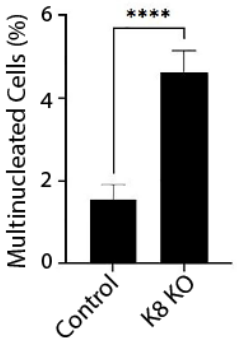

Figure 4.8. Quantification of Multinucleation in Fixed Control and K8 KO HeLa cells.

Quantification of multinucleated cells in control and K8 KO HeLa cells. Control, *n=1379;* K8 KO, *n=1425*. Data represents mean ± SEM (Standard Error Mean). **** $p<0.0001$, Kolmogorov-Smirnov test.

We further examined chromosome alignment defects during mitosis in fixed cells. We quantified misaligned chromosome percentages in the population. We stained cells with Polo Kinase 1 and α-tubulin antibodies. Polo Kinase 1 shows localization to spindle poles during metaphase. **Figure 4.9** shows chromosome congression defect in control, K8 KO and K8 KO expressing WT K8-GFP HeLa cells. DNA fragments halted around the metaphase chromosomes in K8 KO cells. In **Figure 4.10,** We observed a significant increase in the percentage of misaligned chromosomes in the population in K8 KO HeLa cells compared to control cells. The phenotype was rescued with an expression of WT K8-GFP in K8 KO HeLa cells. To get a better understanding of chromosome congression defects in K8 KO cells, we examined BUBR1 localization in control and K8 KO HeLa cells. **Figure 4.11** shows immunofluorescence staining of BUBR1 protein in control and K8 KO HeLa cells at metaphase. BUBR1 is a mitotic spindle checkpoint protein. It localizes to the kinetochore. If there is a problem with chromosome alignment, it inhibits the anaphase-promoting complex (APC) and activates the spindle assembly checkpoint (SAC). Suppose there is a missing kinetochore and microtubule attachment, BUBR1 recruits to unattached kinetochores. As shown in **Fig4.11**, BUBR1 localization increases in K8 KO cells at metaphase compared to

control cells. We quantified BUBR1 fluorescence intensity in fixed cells and observed a ~1.5-fold increase as shown in **Figure 4.12**.

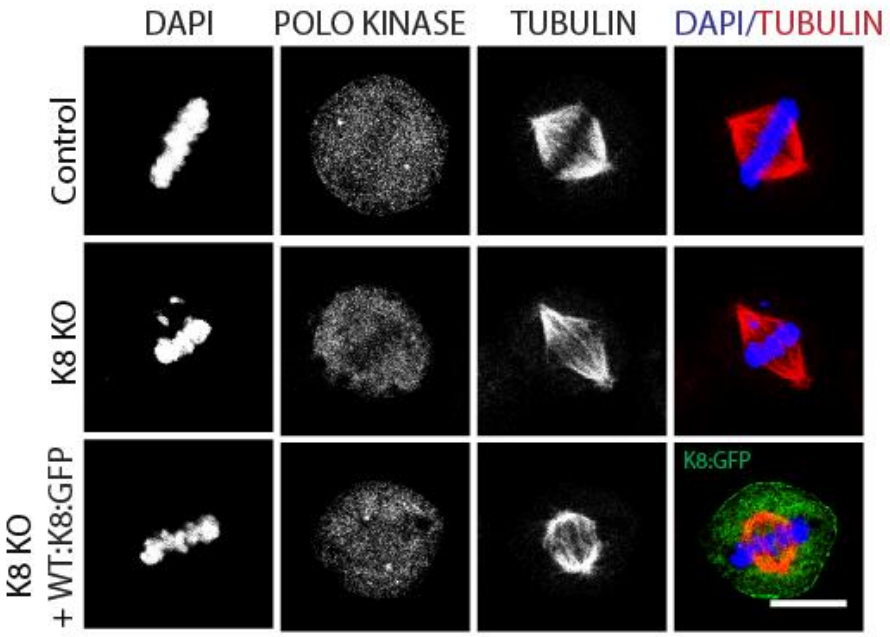

Figure 4.9. K8 KO causes misaligned chromosome at metaphase. Representative immunofluorescence images of metaphase cells in control, K8 KO and K8 KO+WT K8-GFP HeLa cells.

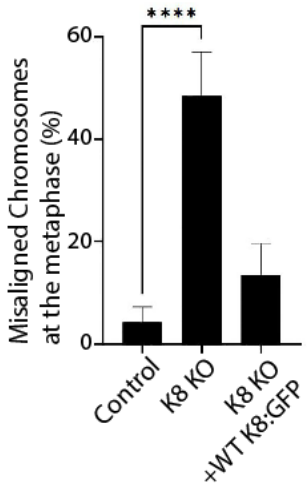

Figure 4.10. Quantification of the Percentage of Misaligned Chromosomes at Metaphase. Quantification of percentages of cells with at metaphase in control *(n=47)*, K8 KO *(n=33)* and K8 KO+WT K8-GFP *(n=30)*. Data represents mean ± SEM. **** p<0.0001, Mann-Whitney test.

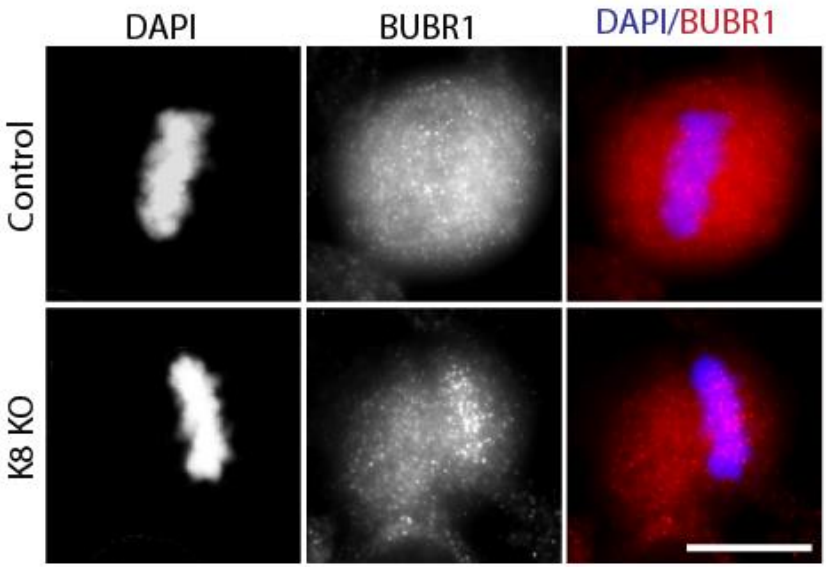

Figure 4.11. BUBR1 intensity increase at chromosomes in K8 KO cells at metaphase. Cells stained with BUBR1 (red) antibody and DNA (DAPI, blue). Scale bar, 10 µm.

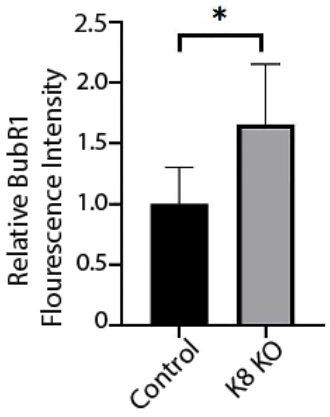

Figure 4.12. Quantification of BUBR1 fluorescence intensity at chromosome at metaphase in control and K8 KO HeLa cells.

We observed severe mitosis and cytokinesis defects when we knockout K8 in HeLa cells. As discussed in the literature review, intermediate filament proteins are major targets of Aurora B kinase. Since K8 KO causes chromosome alignment and cytokinesis abscission defect, we want to further understand the relationship between Keratin 8 and Aurora B. We stained fixed cells with Aurora B antibody in control and K8 KO HeLa cytokinesis cells. Foremost, K8 KO HeLa cells displayed lagging chromosomes and chromosome bridges during cytokinesis as shown in **Figure 4.13.** In **Figure 4.14,** Quantification of the percentage of abnormal chromosome segregation showed a statistically significant 3-fold increase in K8 KO HeLa cells compared to control cells. Interestingly, we also observed that Aurora B fluorescence intensity was decreased at cleavage furrow in K8 KO HeLa cells (**Figure 4.13**). These results suggested that Keratin 8 may have an important role in the activation of Aurora B kinase or its localization.

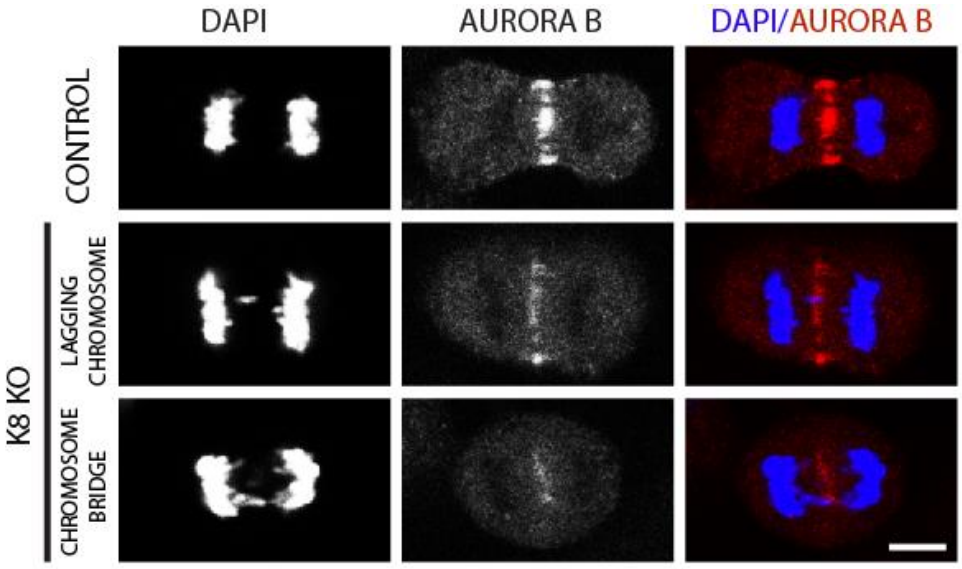

Figure 4.13. K8 KO causes chromosome segregation defects including chromosome bridge and lagging chromosome in cytokinesis. Representative immunofluorescence images of anaphase control and K8 KO HeLa cells. Abnormal chromosome segregation defects (lagging chromosome and chromosome bridge in cytokinesis) are shown in K8 KO cells.

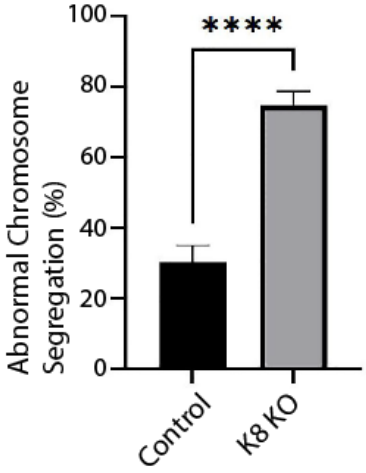

Figure 4.14. Quantification of the percentage of abnormal chromosome segregation defects in control and K8 KO HeLa cells. Quantification of percentages of cells with abnormal chromosome segregation in control *(n=52)*, K8 KO *(n=54)* HeLa cells.

After we observed decrease in Aurora B localization at the cleavage furrow, we performed live-cell imaging to better understand Aurora B dynamics in K8 KO HeLa cells. We exogenously co-expressed Aurora B GFP and Histone 2B-mcherry in control and K8 KO HeLa cells. **Figure 4.15** shows Aurora B localization in live control and K8 KO HeLa cells. In control cells, Aurora B is finely localized to chromosome at metaphase and cleavage furrow during cytokinesis. However, Aurora B localization was disrupted in K8 KO cells. We observed decreased localization of Aurora B at chromosomes and cleavage furrow. We quantified Aurora B intensity at metaphase. Quantification of Aurora B intensity at metaphase decreased 2-fold in K8 KO cells as shown in **Figure 4.16.** This data supports the idea that Aurora B cannot properly localize to the chromosomes and cleavage furrow in the absence of Keratin 8.

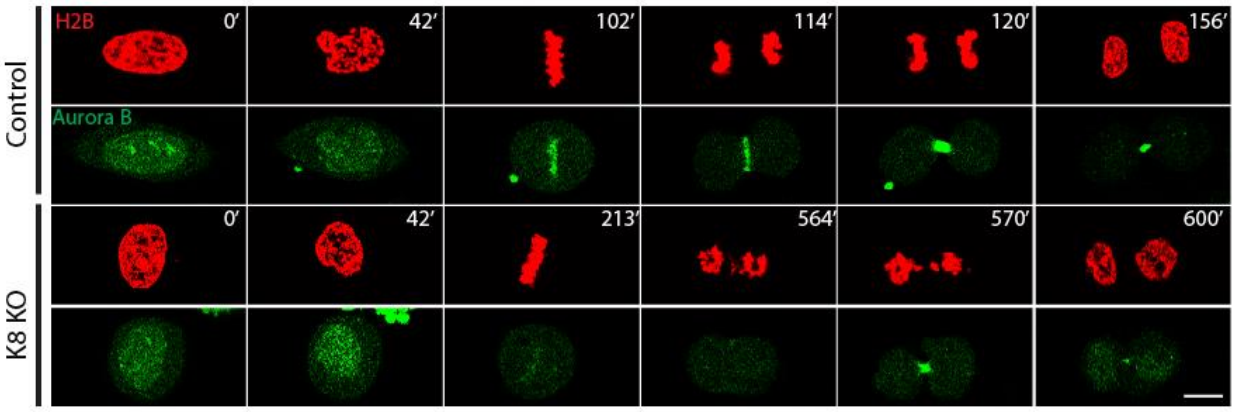

Figure 4.15. Live cell imaging of control and K8 KO HeLa cells expressing Aurora B-GFP and Histone 2B-mcherry. Representative image from live imaging of control or K8 KO HeLa cells expressing Aurora B-GFP (green) H2B-mcherry (red). Scale bars, 10 µm.

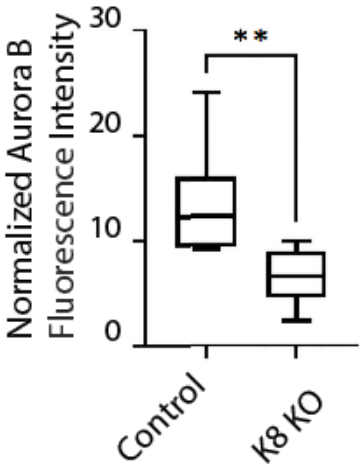

Figure 4.16. Quantification of Aurora B intensity at metaphase in live cell of control and K8 KO HeLa cells. Quantification of Aurora B fluorescence intensity at metaphase in control *(n=6)* and K8 KO *(n=8)* Hela cells. Data represents mean ± SEM. **p<0.01. Student's *t*-test.

4.3. Keratin 8 is a Substrate of the Aurora B

As explained in the literature, Keratin proteins are one of the targets of Aurora B during cell division [9]. We performed *in vitro* kinase assay to determine whether Keratin 8 is a real substrate of Aurora B or not. To do this, we generated Keratin 8-GST plasmid construct. Then, we expressed Keratin 8-GST fusion protein in bacteria because bacteria do not have a mechanism for post-translational modifications. We purified native Keratin 8 protein by using glutathione beads. We incubated Keratin 8-GST and active Aurora B complex with a fragment of INCENP in a kinase reaction buffer including ATP. As a negative control, we incubated Keratin 8 in the absence of active Aurora B. Then, both samples were analyzed by mass spectrometry. **Figure 4.17** shows a cartoon illustration of the experimental workflow of *in vitro* kinase assay. In this way, we were able to detect Aurora B-dependent Keratin 8 phosphorylation. Keratin 8 phosphopeptides and their non-phosphorylated counterparts are monitored by using HF-Exactive Mass Spectrometry in Parallel Reaction Monitoring (PRM)

mode. Phosphorylated and non-phosphorylated peptide intensities are quantified in both -/+ Aurora B kinase experiment set-up (**Figure 4.17).** Quantified intensities are analyzed with Skyline software. By this approach, we mapped the Aurora B kinase-dependent Keratin 8 phospho sites *in vitro*. S34, S37, S124, S330, S404 and S475 Keratin 8 residues were determined Aurora B dependent phosphorylation sides (**Figure 4.18.**).

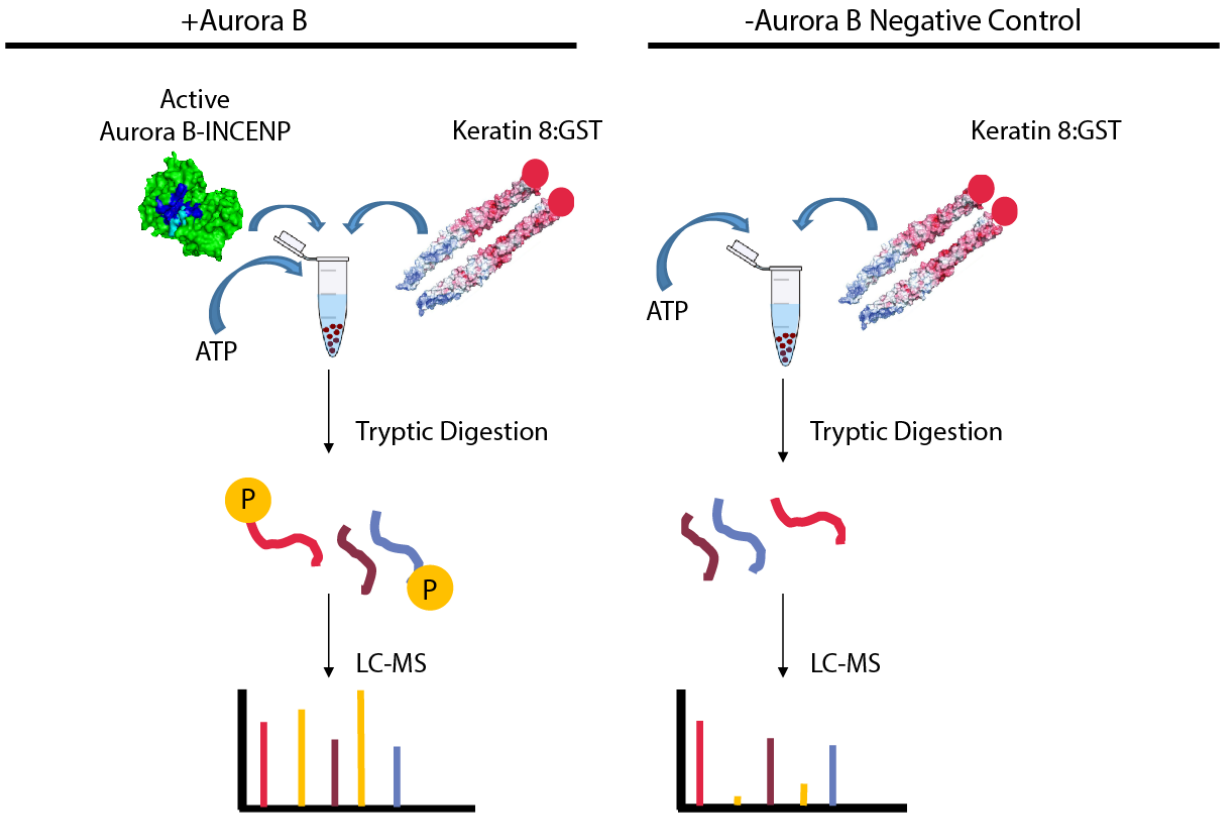

Figure 4.17. Cartoon Illustration of the Experimental Workflow of *In Vitro* Kinase Assay.

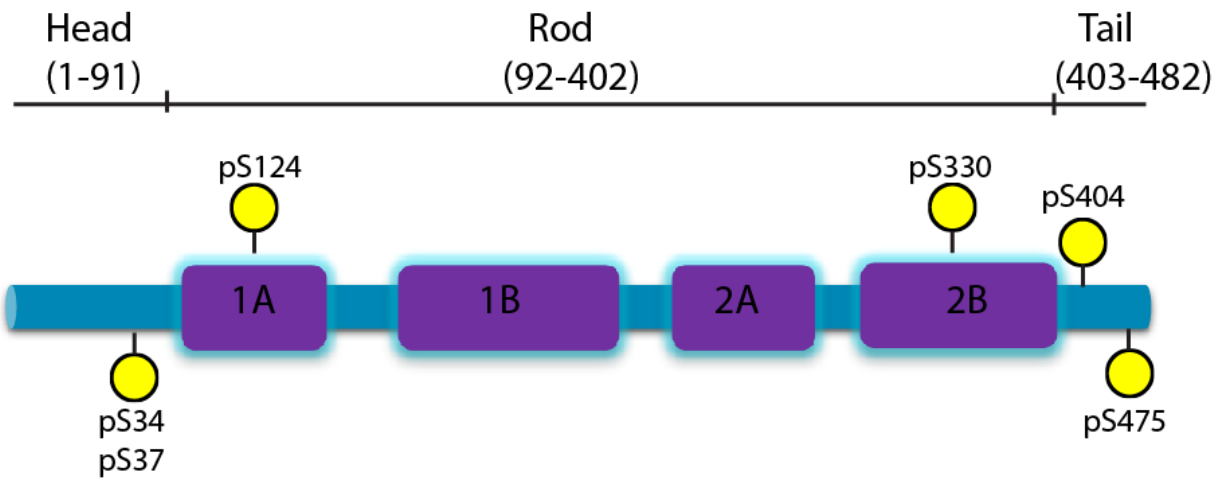

Figure 4.18. Mapping of Aurora B Dependent Phosphorylation Sides of Keratin 8 *In Vitro.*

Figure 4.19 shows Keratin 8 Ser34 phospho and nonphospho form peptide quantification with Skyline. **Figure 4.20** shows Keratin 8 Ser37 phospho and nonphospho form peptide quantification with Skyline. **Figure 4.21** shows Keratin 8 Ser124 phospho and nonphospho form peptide quantification with Skyline. **Figure 4.22** shows Keratin 8 Ser330 phospho and nonphospho form peptide quantification with Skyline. **Figure 4.23** shows Keratin 8 Ser404 phospho and nonphospho form peptide quantification with Skyline. **Figure 4.24** shows Keratin 8 Ser475 phospho and nonphospho form peptide quantification with Skyline. In a previous vivo study, S13, S34, S35, S36, S37, S39, S43, S44, S104 and S258 phospho sides of Keratin 8 are up-regulated in mitosis or cytokinesis [43].

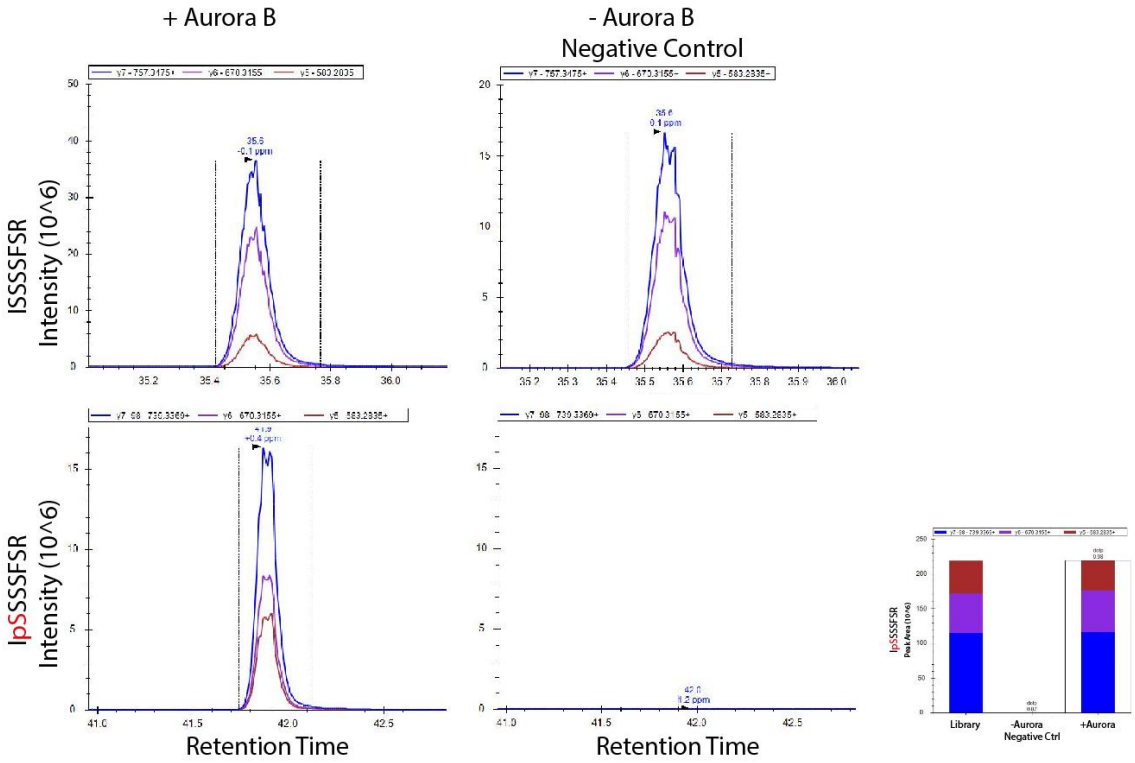

Figure 4.19. Keratin 8 Ser34 phospho and nonphospho form peptide quantification with Skyline

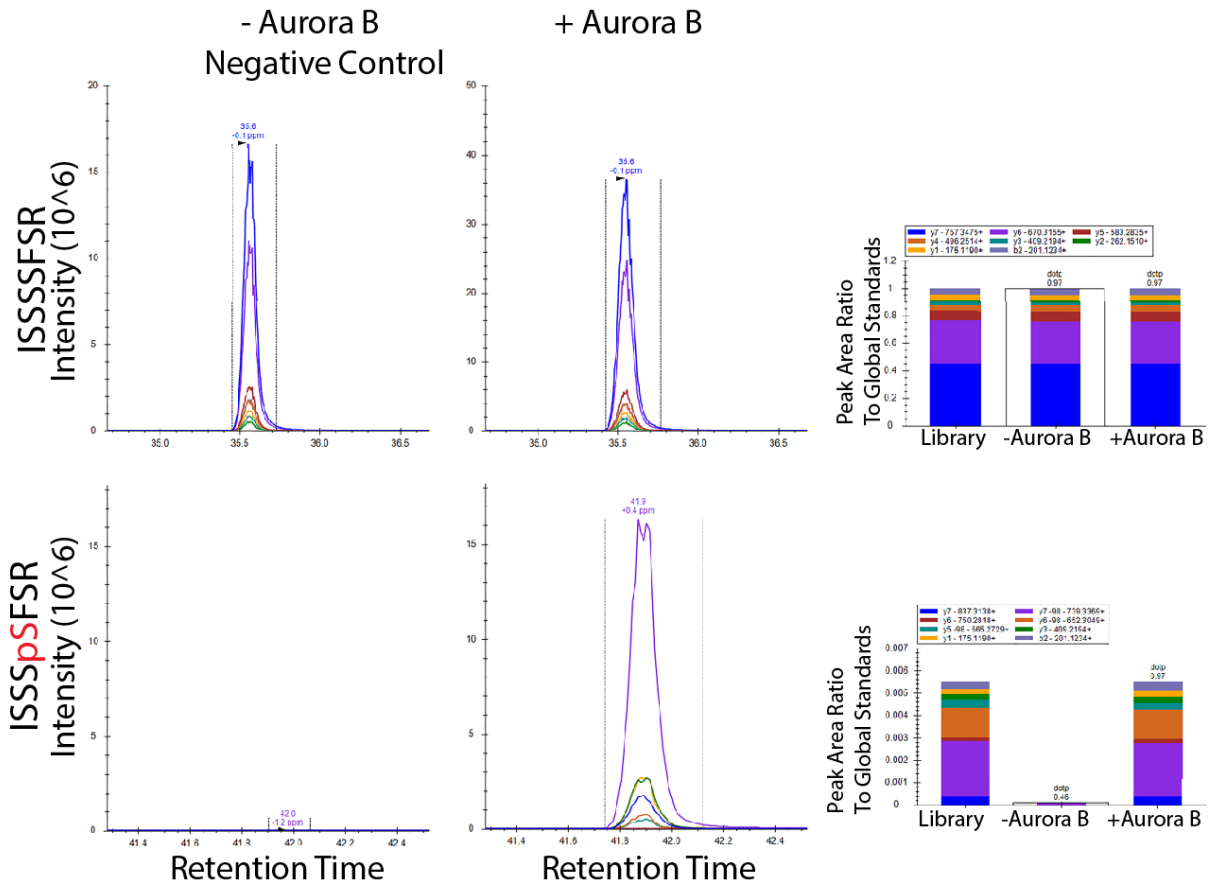

Figure 4.20. Keratin 8 Ser37 phospho and nonphospho form peptide quantification with Skyline.

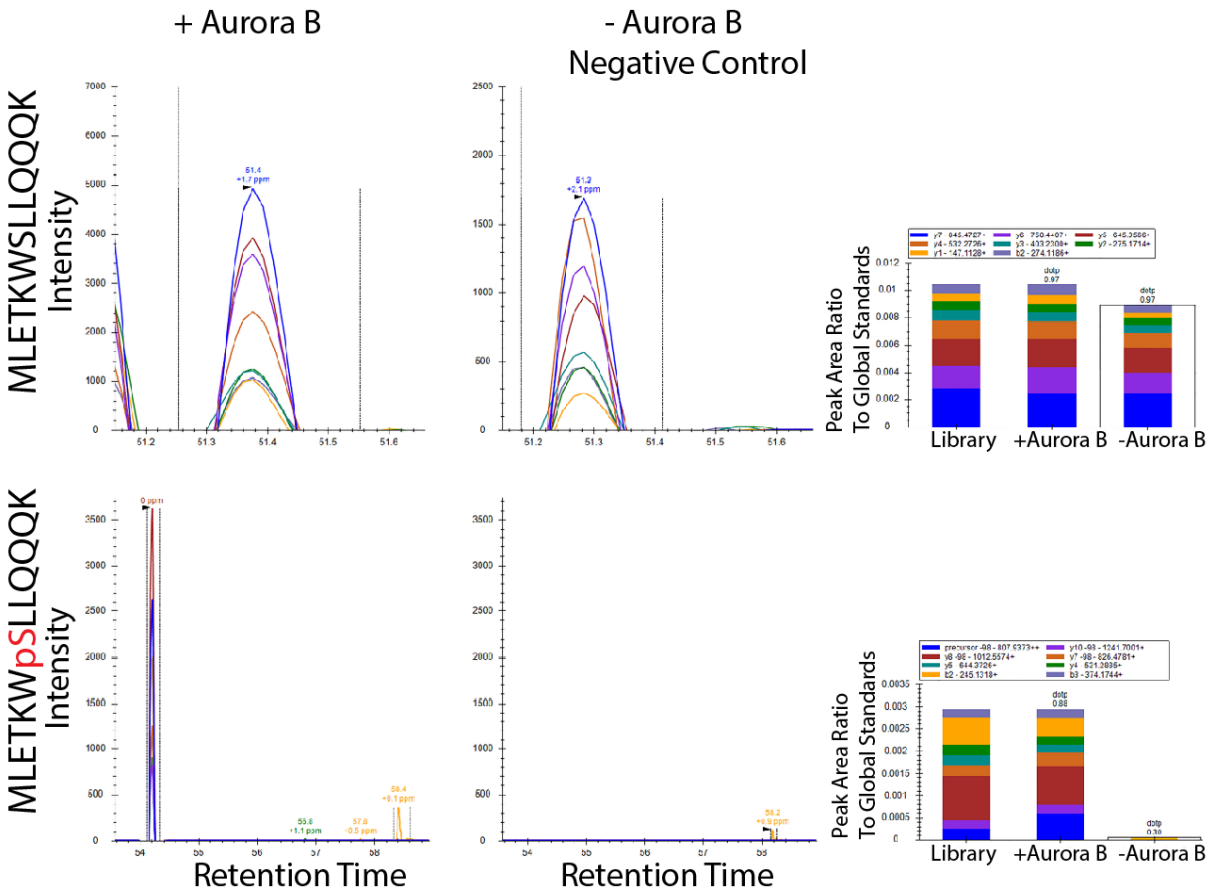

Figure 4.21. Keratin 8 Ser124 phospho and nonphospho form peptide quantification with Skyline.

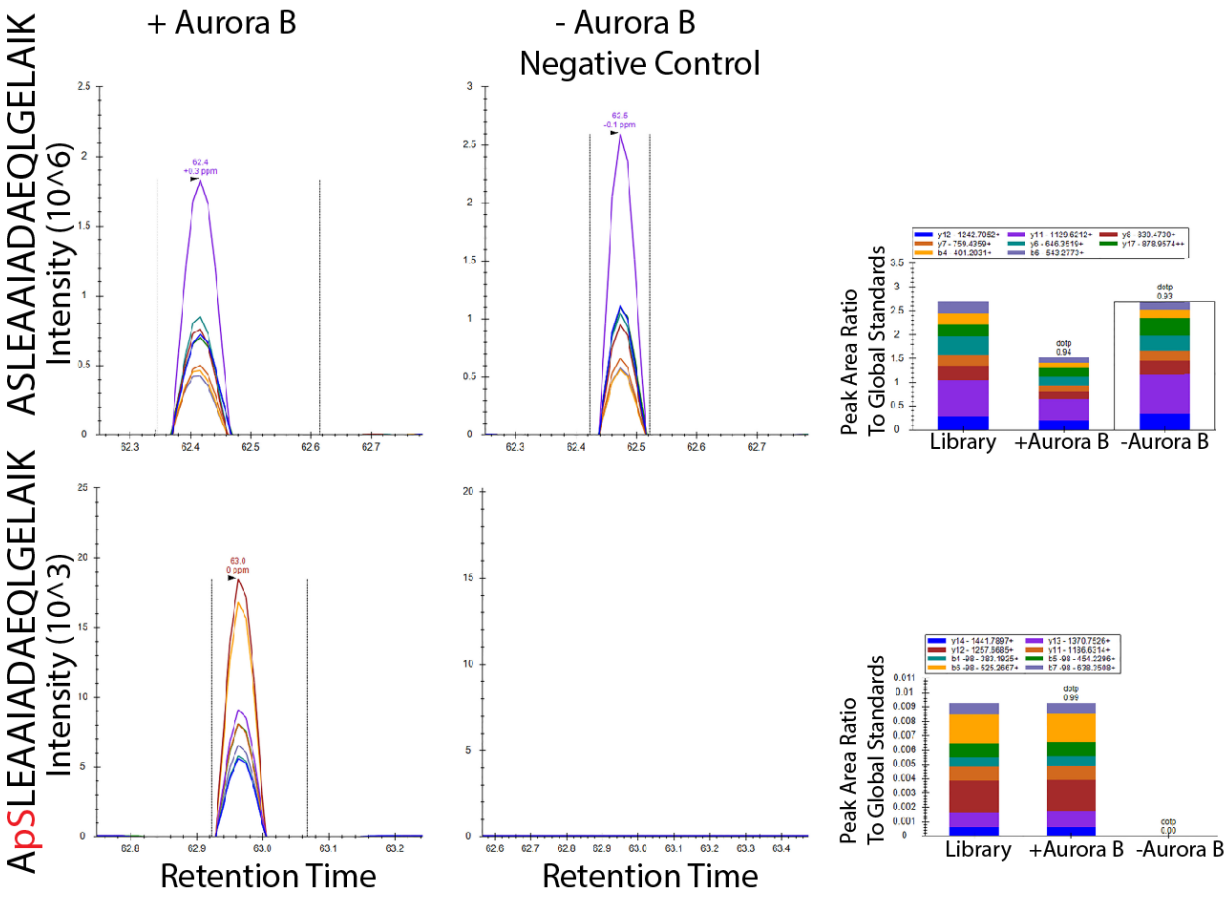

Figure 4.22. Keratin 8 Ser330 phospho and nonphospho form peptide quantification with Skyline.

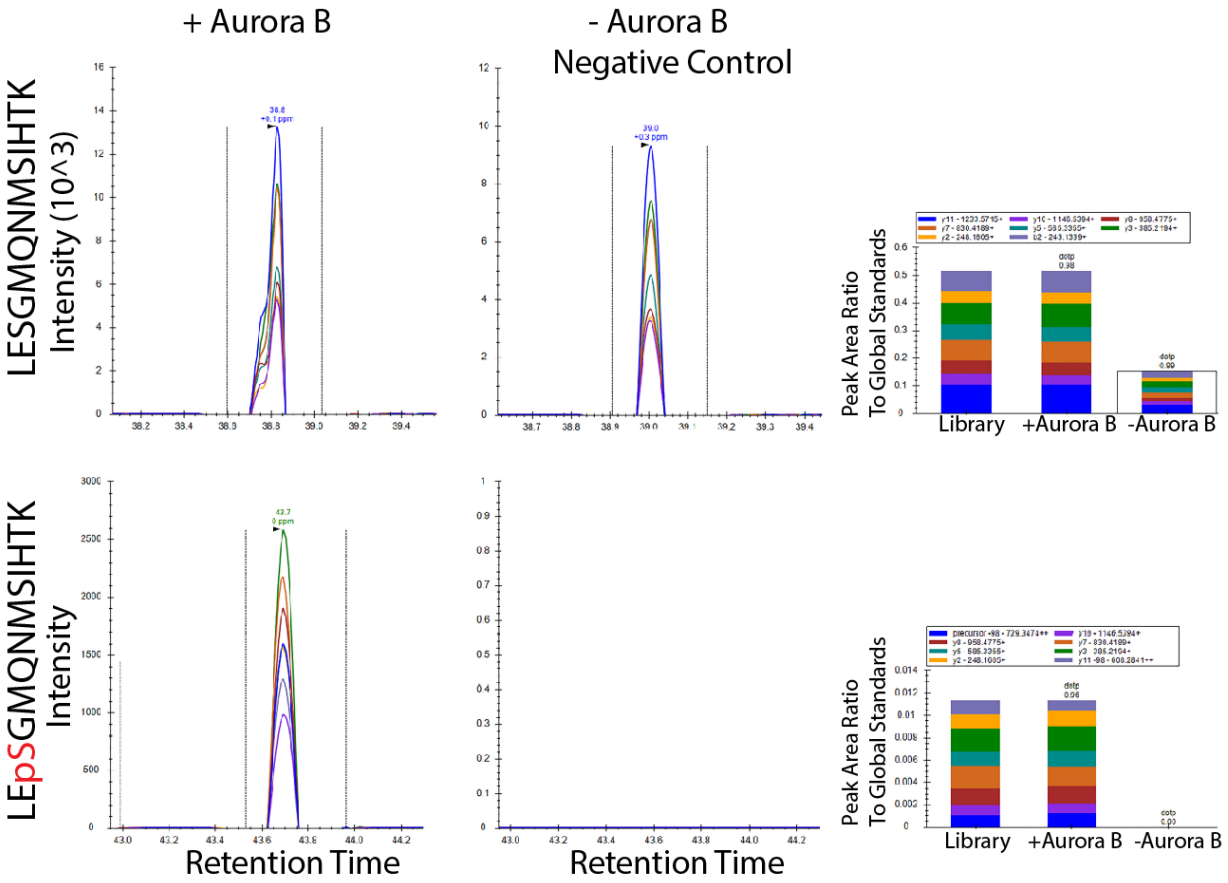

Figure 4.23. Keratin 8 Ser404 phospho and nonphospho form peptide quantification with Skyline.

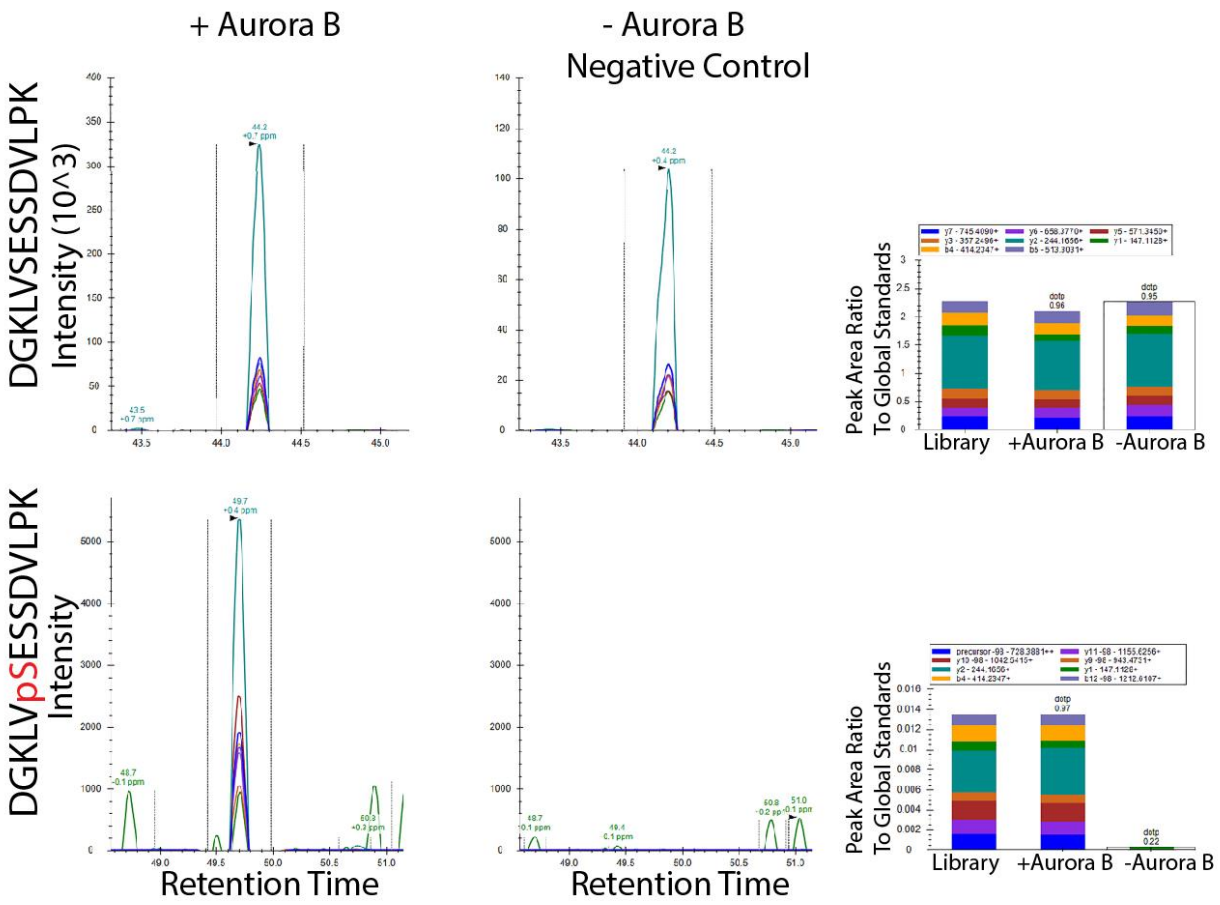

Figure 4.24. Keratin 8 Ser475 phospho and nonphospho form peptide quantification with Skyline.

4.4. Aurora B dependent Keratin 8 phosphorylation is required for successful cell division

In part 4.3, we observed that Aurora B phosphorylates Keratin 8 *in vitro* and *in vivo.* In a previous genome-wide phosphoproteome study, the effect of Aurora B kinase inhibition in global phosphoproteome was shown. In this study, abundant Aurora B specific phosphorylation sides of intermediate filaments were revealed. Keratin 8 and Keratin 18 were among these hits. Keratin 8 Ser13, Ser34, Ser37 sites were determined as potential Aurora B phosphorylation sides in cytokinesis because these phosphorylation intensities decreased upon VX680-mediated Aurora B inhibition in cytokinesis compared to untreated control [52].

To analyze the role of Aurora-B dependent phosphorylation of Keratin 8, we decided to focus on S13, 34, 35, 36 and 37 in a highly phosphorylated region at the head domain. **Figure 4.25** shows targeted Keratin 8 Serine residues to mutate to Alanine. We aimed to mutate each Serine residue to alanine by site-directed mutagenesis. Wild type Keratin 8-GFP constructs were sequentially mutated several times to obtain five serine mutations in one construct. We named the final construct as 5XA Keratin 8 mutant, where S13, S34, S35, S36 and S37 were mutated to alanine on K8-GFP.

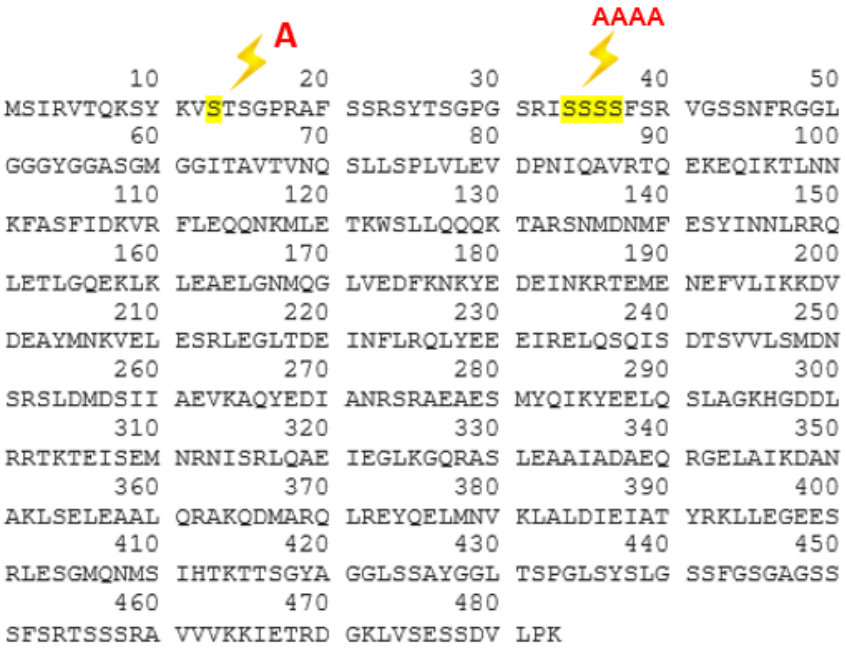

Figure 4.25. Aurora B Dependent Keratin 8 Sites Targeted to Mutate by Site-directed Mutagenesis.

Furthermore, we aimed to understand the role of these phosphorylation sites in cell division. To do this, we expressed WT K8-GFP and 5XA K8-GFP mutant in K8 KO HeLa cells. To understand the cell surface, we stained cells with fluorescence-labeled phalloidin antibody. Then, we quantified multinucleation which is a basic outcome of cell cycle failure. We observed a significant increase in the percentage of multinucleated cell population in 5XA K8-GFP mutant in K8 KO HeLa cells compared to control cells which are expressing or untreated HeLa cells. Additionally, we observed an increase in multinucleation in K8 KO cells and this phenotype is reversed by the expression of WT K8-GFP in K8 KO cells. **Figure 4.26** shows the representative images for multinucleation in control, K8 KO, WT K8-GFP expressing K8 KO and 5XA K8-GFP K8 KO HeLa cell populations. **Figure 4.27** represents the quantification of the percentage of the multinucleated cell. These results suggest that the 5XA K8 mutant disturbs cytokinesis and Aurora B dependent phosphorylation of Keratin 8 is required for successful cytokinesis.

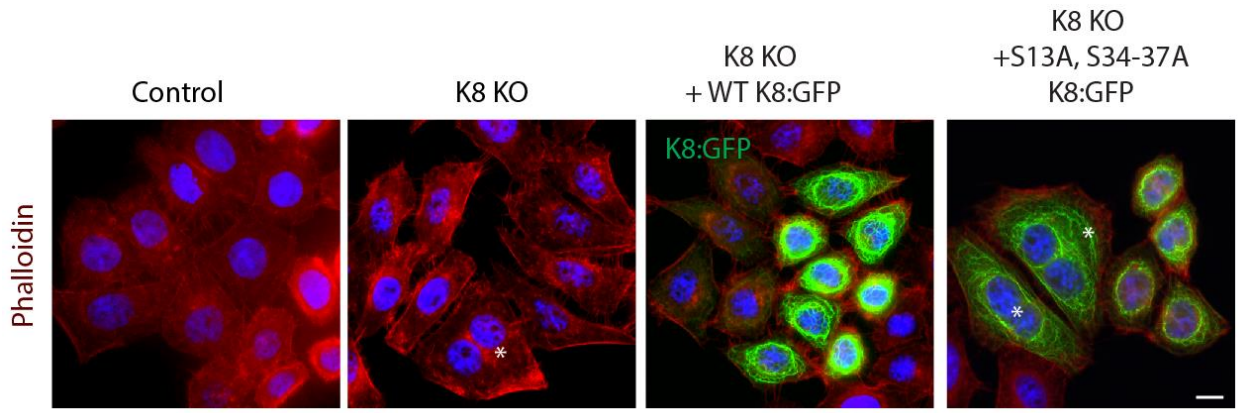

Figure 4.26. 5XA K8 mutation causes multinucleation. Imaging of fixed control, K8 KO, K8 KO HeLa cells expressing WT K8-GFP and S13,34-37A K8-GFP (green) using phalloidin (red) and DAPI (blue). Asterisks highlight multinucleated cells.

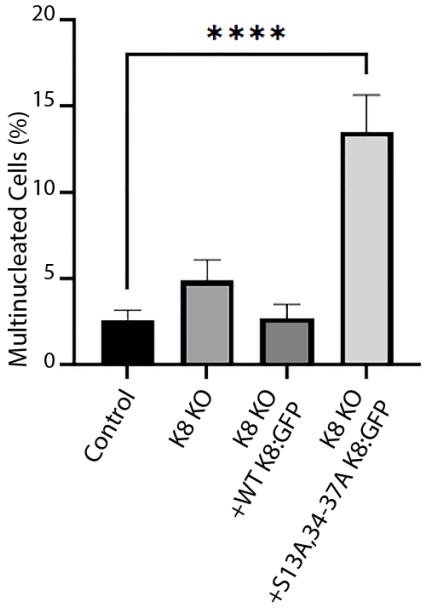

Figure 4.27. Quantification of the percentage of multinucleated cells in control, K8 KO, WT K8-GFP expressing K8 KO and 5XA K8-GFP expressing K8 KO HeLa cells. Quantification of percentage of multinucleated cells in control *(n=679)*, K8 KO *n=616)*,K8 KO + WT K8-GFP *(n=615)*, K8 KO + S13,34-37A K8-GFP *(n=208)*, HeLa cells. Data represents mean ± SEM. **** p<0.0001, Kolmogorov-Smirnov test.

4.5. Aurora B Dependent Keratin 8 Phosphorylation Plays Role in Chromosome Congression

Then, we questioned how Aurora B dependent phosphorylation of Keratin 8 plays a role in cell division. We aimed to understand its importance in chromosome congression during mitosis. For this reason, we stained cells with DAPI to visualize their chromosomes, polo kinase 1 and tubulin antibodies to determine cell cycle stages. We used the unique localization of Polo kinase 1 and tubulin proteins as a guide to analyze cells at the metaphase. **Figure 4. 28** shows representative images at metaphase for control, K8 KO, WT K8-GFP expressing K8 KO and 5XA K8-GFP K8 KO HeLa cells which are stained with Polo kinase 1, tubulin and DAPI. We quantified those cells for chromosome congression phenotype. **Figure 4.29** represents the quantification of the percentage of misaligned chromosomes at the metaphase in different cells. In control metaphase cells, we detected a minimum chromosome congression defect of around 10% in the population. In K8 KO cells, the chromosome congression percentage increased up to ~70%. Those cells showed higher misaligned chromosome defects at the metaphase. As shown in **Figure 4.28,** some satellite chromosomes remained around congressed chromosome at the metaphase. Expression of WT K8-GFP in K8 KO cells rescued the phenotype and those cells showed ~20% of misaligned chromosomes. When we expressed 5XA K8-GFP mutant in K8 KO cells, we observed a higher chromosome congression phenotype, ~40% in the population, compared to control and WT K8-GFP expressed K8 KO HeLa cells. In conclusion, we observed severe chromosome congression defects in K8 KO and 5XA K8-GFP expressing K8 KO cells. These data suggest that Keratin 8 and its phosphorylation are important for chromosome orientation during mitosis.

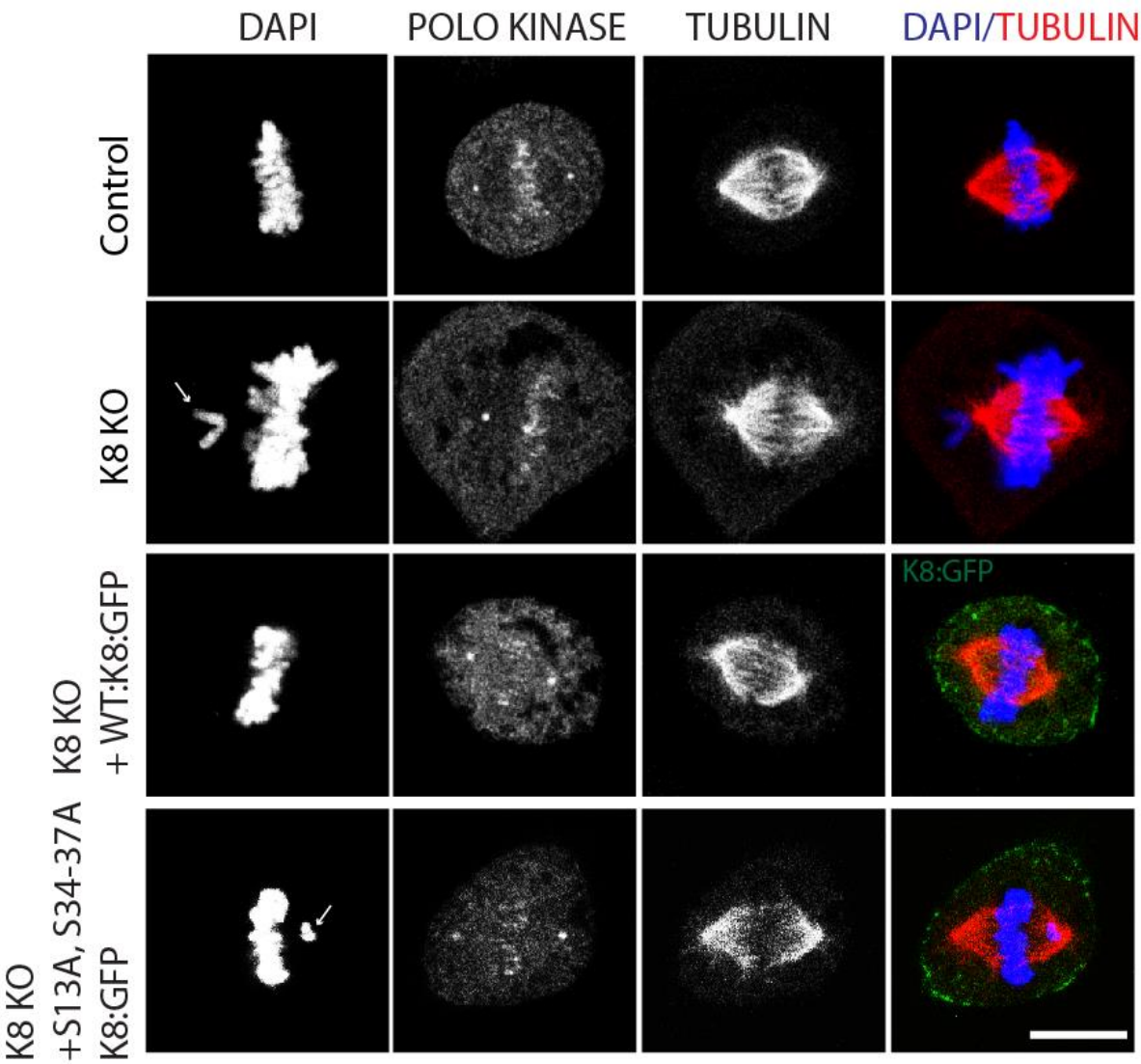

Figure 4.28. K8 KO and 5XA K8 mutation cause chromosome congression at the metaphase. Immunofluorescence staining against α-Tubulin (red), Polo Kinase antibodies and DAPI (blue) in control, K8 KO, K8 KO HeLa cells expressing WT K8-GFP and S13,34-37A K8-GFP. Misaligned chromosomes at the metaphase stages of K8 KO cell and K8 KO HeLa cells expressing S13,34-37A K8-GFP are highlighted with arrows.

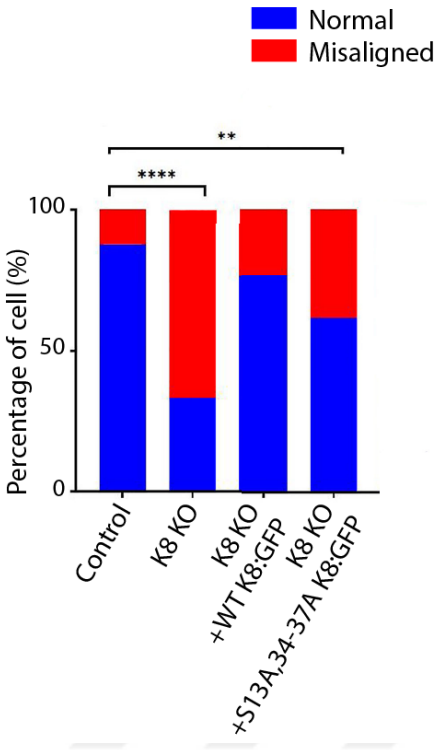

Figure 4.29. quantification of the percentage of misaligned chromosomes at the metaphase in control, K8 KO, WT K8-GFP expressing K8 KO and 5XA K8-GFP expressing K8 KO HeLa cells. Quantification of percentage of misaligned chromosomes in control *(n=33)*, K8 KO *(n=51)*, K8 KO+WT K8-GFP *(n=43)* and K8 KO + S13,34-37A K8-GFP *(n=42)* HeLa cells. **** $p<0.0001$, **$p<0.01$. Student's *t*-test.

4.6. 5XA K8 mutation causes persistent Keratin 8 bundles as the cleavage furrow ingress

After we understand the importance of Keratin 8 and its regulation during mitosis, we want to gain more insight into the role of Keratin 8 phosphorylation in cytokinesis. We started with the examination of the effect of mutated Keratin 8 on its localization during cytokinesis. To analyze that, we expressed WT K8-GFP and 5XA K8-GFP mutant in HeLa cells. We visualized those cells by staining them with INCENP antibody. **Figure 4.30** shows the WT K8-GFP and 5XA K8-GFP expressing HeLa cells in cytokinesis. Exogenous WT K8-GFP

disappeared at the cleavage furrow during cytokinesis. This result is consistent with the localization of endogenous K8 localization shown in **Figure 4.1.** As shown in **Figure 4.30,** 5XA K8-GFP persisted on the cleavage furrow and some residual Keratin 8 remained as bundle and bridges between two daughter cells. Exogenous WT K8 was successfully cleared from a narrow space in the ingression furrow. However, 5XA K8 mutation caused intact keratin fibers hanging between two daughter cells. We quantified K8-GFP fluorescence intensities at the cleavage furrow as shown in **Figure 4.31**. We observed increased Keratin 8 intensity in 5XA K8-GFP expressing HeLa cells compared to WT K8-GFP expressing HeLa cells.

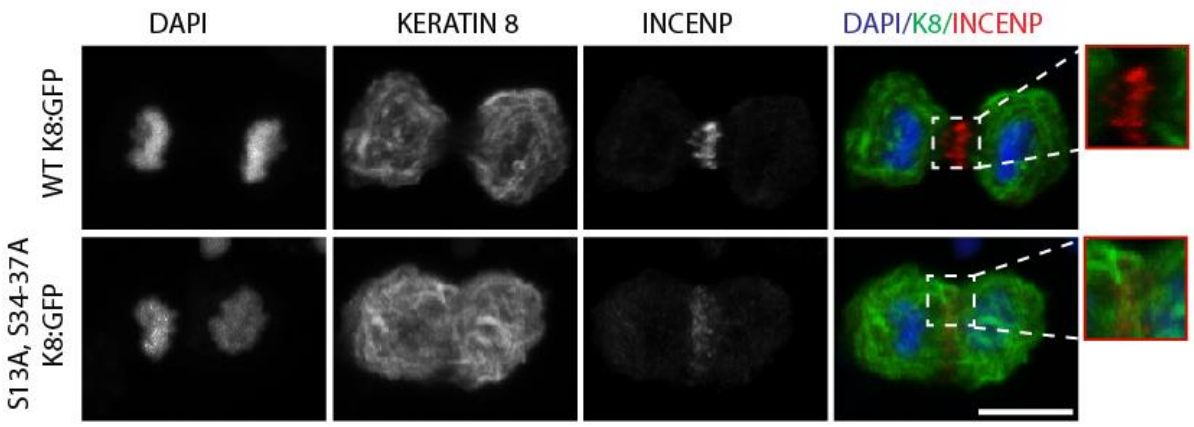

Figure 4.30. 5XA K8 mutation causes persistent Keratin 8 bundles at the cleavage furrow. Immunofluorescence staining of K8-GFP expressing cells against anti-INCENP (red) antibodies and DAPI (blue) in control (WT K8-GFP) and mutant (S13,34-37A K8-GFP) HeLa cells.

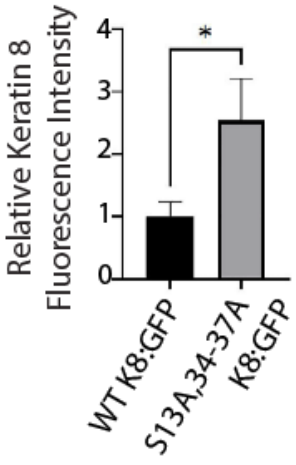

Figure 4.31. Quantification of Keratin 8 fluorescence intensities at the cleavage furrow in WT K8-GFP and 5XA K8-GFP expressing HeLa cells. Quantification of Keratin 8 fluorescence intensity at the cleavage furrow in WT K8-GFP *(n=14)* and S13,34-37A K8-GFP *(n=13)* expressing HeLa cells. Data represent mean ± SEM. * $p<0.05$. Student's *t*-test.

In the previous part, we used untreated Hela cells to understand the localization of mutant K8. Since it continued to express endogenous WT Keratin 8, mutant and wild-type keratin fibers come together for dimerization. To further validate our finding, we performed live imaging of WT and 5XA K8-GFP expressing K8 KO HeLa cells. In this way, we can eliminate the dimerization of endogenous WT and exogenous 5XA K8-GFP in control HeLa cells because K8 KO cells lack Keratin 8 protein. **Figure 4.32** shows capture from live imaging of WT and 5XA K8-GFP expressing K8 KO HeLa cells. Keratin 8 networks were quite similar in WT and mutant 5XA K8 in the interphase and mitosis stages of the cell cycle. However, in agreement with our previous observation, we observed that Keratin 8 bundles and bridges persisted at the cleavage furrow because of the non-phosphorylatable 5XA mutant. Eventually, 5XA K8-GFP expressing K8 KO cells ended up with multinucleation as a cytokinesis failure (**Figure 4.32**). In conclusion, these results suggest that Aurora B dependent phosphorylation of Keratin 8 is required for dissolving of Keratin 8 filaments at the cleavage furrow.

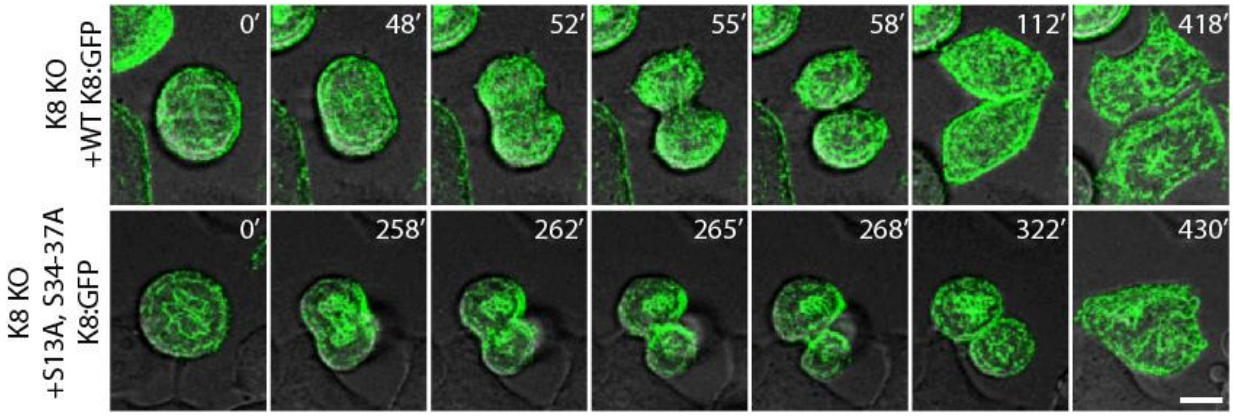

Figure 4.32 Live cell imaging of WT and 5XA K8-GFP expressing K8 KO HeLa cells. Representative images from live imaging of cell division in K8 KO HeLa cells expressing WT K8-GFP and S13,34-37A K8-GFP

4.7. Aurora B inhibition causes Keratin 8 bundles at the cleavage furrow

If a mutation in Aurora B dependent phosphorylation side of Keratin 8 causes keratin bundles and bridges at the cleavage furrow, Aurora B inhibition should affect the Keratin 8 distribution in a similar manner. To test this, we synchronized Hela cells at the mitosis with nocodazole and then released them to cytokinesis. Thirty minutes after the release, we treated the cells with small-molecule Aurora B inhibitors (AZD1152 and VX680) for a further thirty minutes. We stained control and AZD1152/VX680 treated cells by using anti-Keratin 8 and anti-INCENP antibodies. **Figure 4.33** represents control and Aurora B inhibitor treated HeLa cells in cytokinesis. Consistent with our previous results, Keratin 8 persisted as a large bundle at the cleavage furrow upon Aurora B inhibition with AZD1152/VX680, whereas K8 is diminished and cleared from the cleavage furrow. We quantified Keratin 8 fluorescence intensities at cleavage furrow in control and small molecule mediated Aurora B inhibited cells. As shown in **Figure 4.34,** We observed a ~2-fold increase in Keratin 8 intensity at cleavage furrow upon Aurora B inhibition in cytokinesis. To further confirm these results, we performed live-cell imaging of the same experimental set-up. **Figure 4.35** shows live-cell imaging of control and AZD1152/VX680 treated WT K8-GFP expressing K8 KO HeLa

cells. Strikingly we observed large bundles of Keratin filaments in Aurora B inhibitor treated cells. These results support that phosphorylation of Keratin 8 by Aurora B kinase is required for furrow ingression.

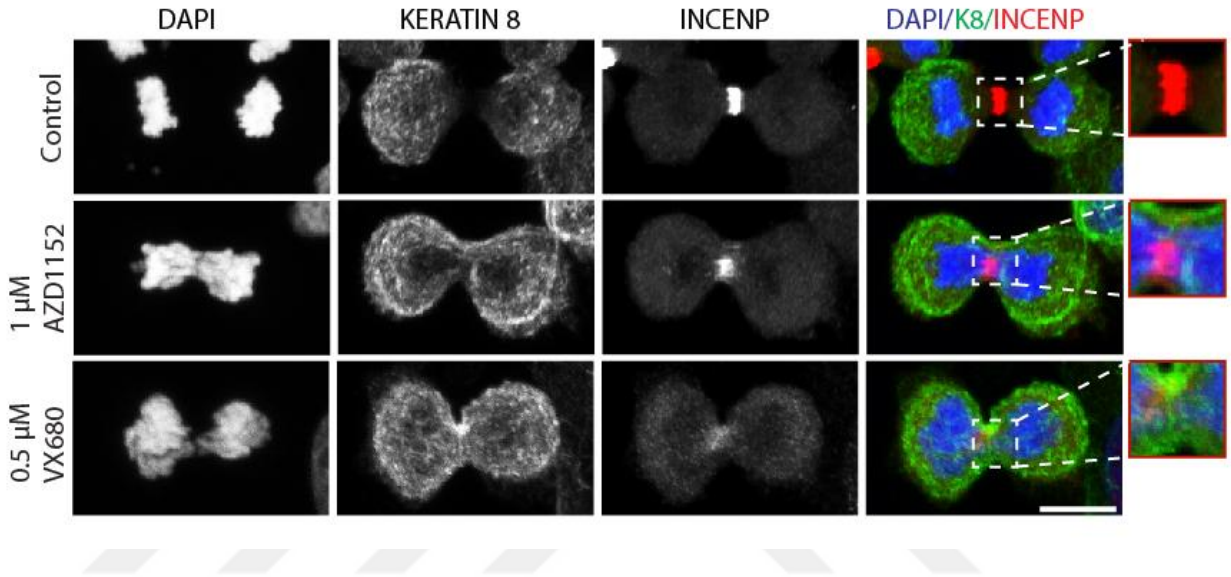

Figure 4.33. Aurora B inhibition causes persistent Keratin 8 bundles at the cleavage furrow. Immunofluorescence staining for Keratin 8 (green), INCENP (red) and DAPI (blue) in control and HeLa cells treated with 1 µM AZD1152 or 0.5 VX680 µM after thirty minutes of nocodazole release.

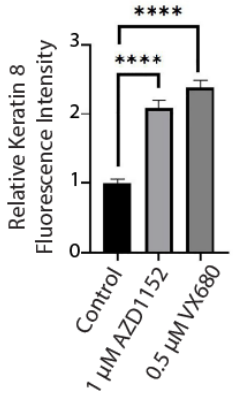

Figure 4.34. Quantification of Keratin 8 fluorescence intensity at the cleavage furrow in control and AZD1152/VX680 treated HeLa cells Quantification of Keratin 8 fluorescence intensity at the cleavage furrow in control *(n=65)*, 1 μM AZD1152 *(n=48)* or 0.5 VX680 μM *(n=57)* treated HeLa cells. Data represent mean ± SEM. ****p<0.0001. Student's *t*-test. Scale bars, 10 μm.

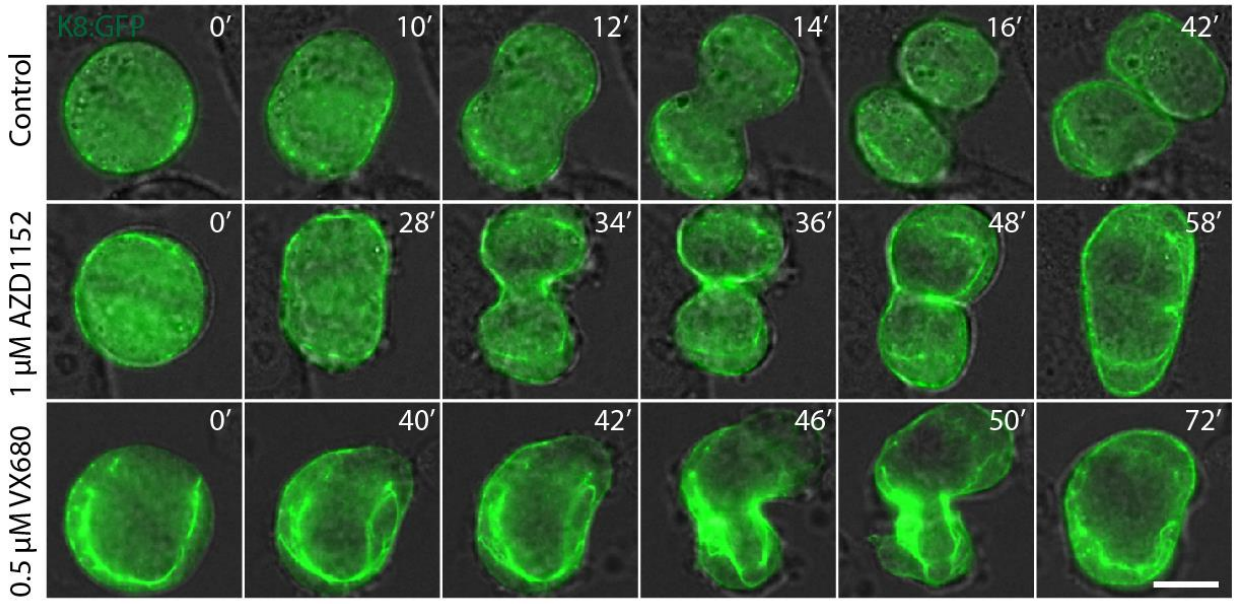

Figure 4.35. live-cell imaging of control and AZD1152/VX680 treated WT K8-GFP expressing K8 KO HeLa cells. Representative images from live imaging of K8 KO cells expressing WT K8-GFP that are treated with DMSO (control) or Aurora B inhibitors (1 μM AZD1152 or 0.5 VX680 μM). Scale bars, 10 μm.

4.8. Aurora B Dependent Phosphorylation of Keratin 8 Ser34 Localizes to Cleavage Furrow

We showed that Aurora B dependent phosphorylation is required for a successful cell division. However, there is an unknown mechanism of spatial-temporal regulation of Keratin 8 phosphorylation during cell division. To address this question, we developed a custom phosphospecific antibody against phospho Keratin 8 Ser-34. Antibody production has many difficult challenges during the process. The specificity of the raised antibody is a big issue. Poor specificity of an antibody makes it non-utilizable. To confirm our produced antibody, we tested phospho Keratin 8 Ser34 antibody in K8 KO HeLa cells. We immunostained unsynchronized K8 KO HeLa cells by using anti-phospho Keratin 8 Ser34 and anti-Keratin 8 antibodies. **Figure 36** shows immunostaining of K8 KO HeLa cells in different cell cycle stages by using anti-phospho Keratin 8 Ser34. As shown in **Figure 36,** K8 KO cells lack Keratin 8 and phosphor Keratin 8 Ser34 fluorescence signal. This result indicates that raised anti-phospho Keratin Ser34 antibody is not binding unspecific.

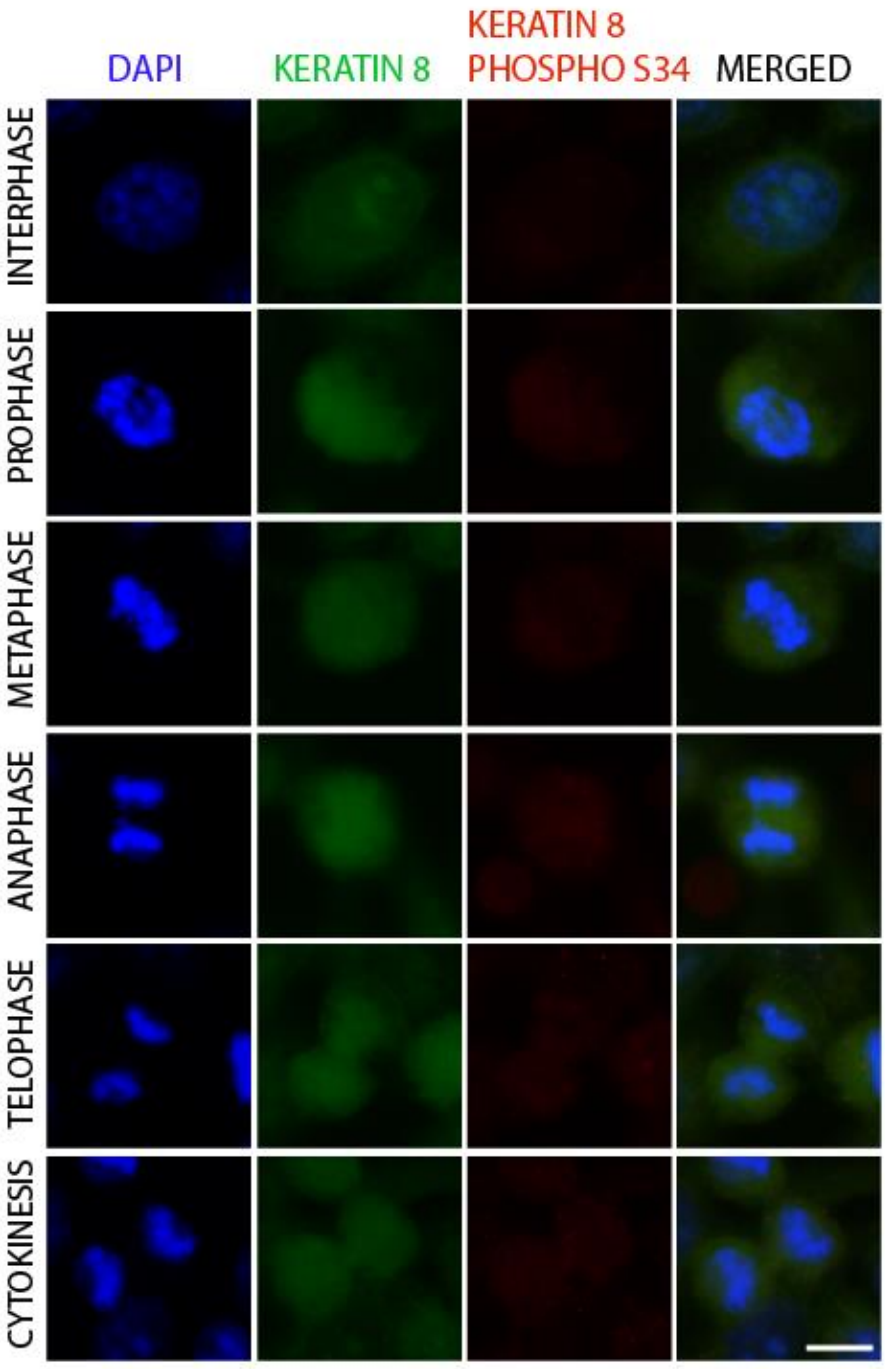

Figure 4.36. Phospho S34 Keratin 8 antibody is not detected in K8 KO HeLa cells. Immunofluorescence staining of Keratin 8 knockout HeLa cells at different cell cycle stages (interphase-cytokinesis) using Phospho S34 Keratin 8 (red) and Keratin 8 (green) antibodies and DAPI (blue). Scale bar, 10 µm.

To examine spatiotemporal regulation of Keratin 8 Ser34 phosphorylation, we aimed to determine the subcellular localization of phosphorylated Keratin 8 Ser34. To do that, we stained unsynchronized HeLa cells by using anti-Keratin 8 and anti-phospho Keratin 8 Ser 34 antibody. **Figure 4.37** shows phospho Keratin 8 Ser34 and Keratin 8 immunostaining of HeLa cells in different cell cycle stages. We observed that Keratin 8 formed a regular filament network the inside of the cell throughout the cell cycle whereas phosphorylated Keratin 8 Ser34 decorated cleavage furrow at the onset of anaphase until cleavage furrow ingress. It is distinctly localized at the contractile ring as the chromosome segregates and cleavage furrow ingress. Through the late cytokinesis, it decorated the neighboring cortical part of newly divided daughter cells during abscission. This result shows phosphorylation of Keratin 8 has a unique location during cell division.

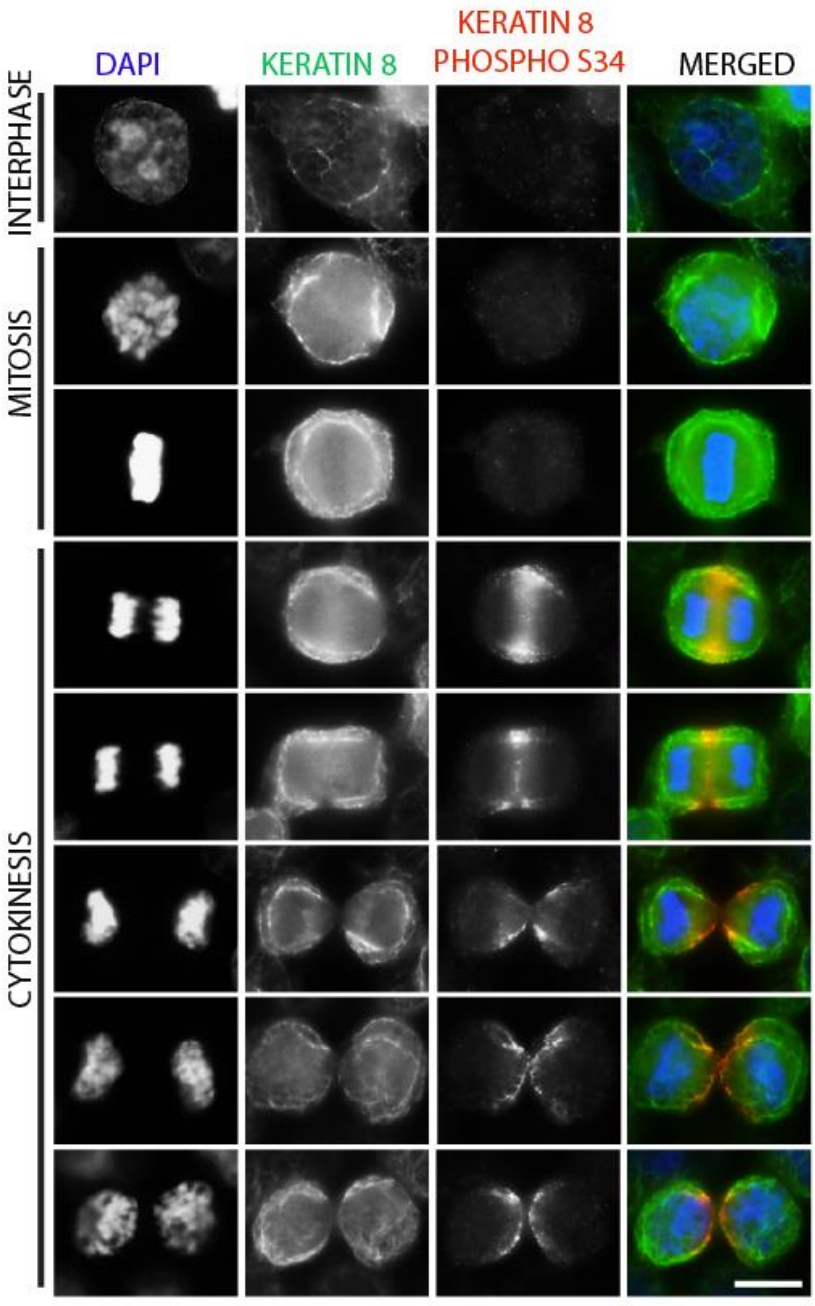

Figure 4.37. Phosphorylation of Keratin 8 Ser34 decorates cleavage furrow in HeLa cells. Representative images of Keratin 8 S34 phosphorylation at the cleavage furrow. Interphase, mitosis and cytokinesis Hela cells were immunostained against endogenous Keratin 8 (green), Keratin 8 phospho S34 (red) and DNA (DAPI, blue).

Although we showed Ser34 Keratin 8 is phosphorylated by Aurora B, we want to confirm the phosphorylation of Keratin Ser34 is dependent on Aurora B activity during cytokinesis. To show this in vivo, we treated cells with small-molecule Aurora B inhibitors, which are AZD1152 or VX680, to examine phospho Keratin 8 Ser34 level. Then, we stained control and AZD1152/VX680 treated HeLa cells by using anti-Aurora B and anti-phospho Keratin 8 Ser 34 antibodies. **Figure 4.38** represents immunostaining of control and Aurora B treated HeLa cells in cytokinesis. Remarkably, we observed that phospho Keratin 8 Ser34 wiped out at cleavage furrow upon Aurora B inhibition. We quantified phospho Keratin 8 Ser34 fluorescence intensities in control and Aurora B inhibitors treated HeLa cells as shown in **Figure 4.39**. Quantification shows that Phosphorylated S34 Keratin 8 completely abolished both at anaphase and telophase cells upon Aurora B inhibition.

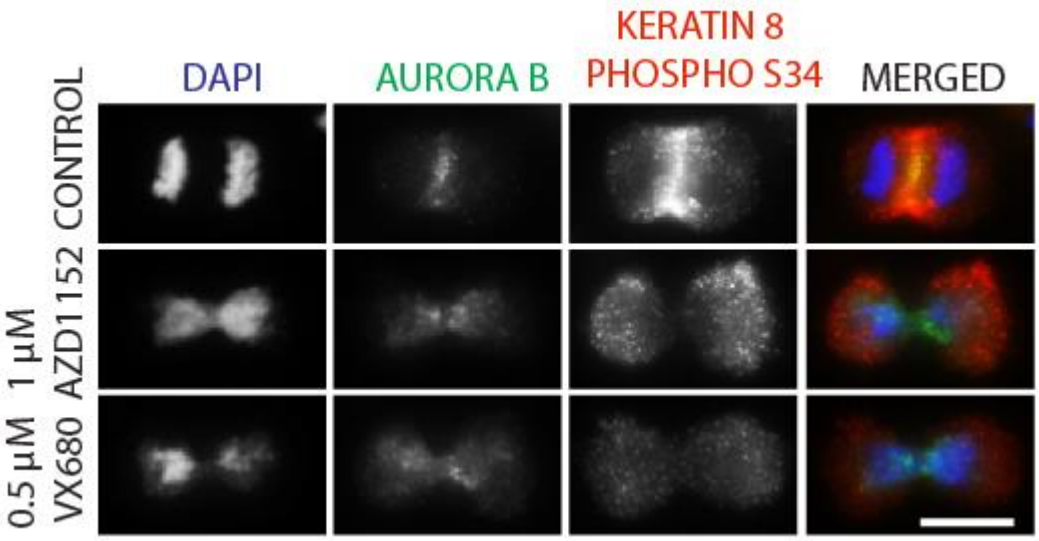

Figure 4.38. Phosphorylation of Keratin 8 Ser34 is Aurora B Dependent. Representative images of HeLa cells after Aurora B inhibition. Control, 1 µM AZD1152 or 0.5 VX680 µM treated cells were immunostained against Aurora B (green), Keratin 8 phospho S34 (red) and DNA (DAPI, blue). Scale bars, 10 µm.

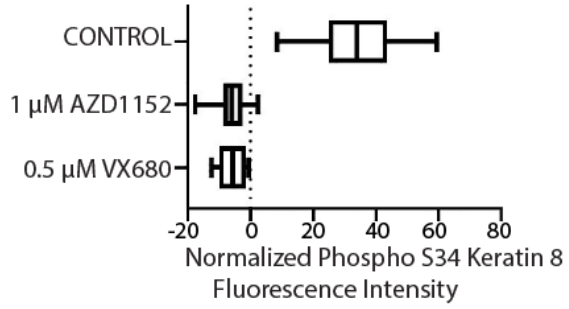

Figure 4.39. Quantification of phospho Keratin 8 Ser34 fluorescence intensity at the cleavage furrow in control and AZD1152/VX680 treated HeLa cells. Quantification of Keratin 8 phospho S34 fluorescence intensity at the cleavage furrow in control *(n=11)*, 1 µM AZD1152 *(n=9)* or 0.5 VX680 µM *(n=8)* treated HeLa cells. Data represent mean ± SEM. ****p<0.0001. Student's *t*-test.

4.9. Aurora B Dependent Phosphorylation of Keratin 8 Ser34 may be Conserved in Keratin Expressing Cells.

We want to understand whether the phosphorylation pattern of Keratin 8 Ser34 is conserved in keratin expressing cells. Additionally, we aimed to show spatiotemporal regulation of phosphorylation of Keratin 8 Ser34 in an epithelial cell line. For this reason, we tested the phospho-specific Keratin 8 Ser34 antibody in MCF7 epithelial cell line, which is obtained from breast adenocarcinoma. We stained unsynchronized HeLa cells by using anti-Keratin 8 and anti-phospho Keratin 8 Ser 34 antibody. **Figure 4.40** shows phospho Keratin 8 Ser34 and Keratin 8 immunostaining of MCF7cells in different cell cycle stages. As previously observed in HeLa cells, We detected unique decoration of phospho Keratin 8 Ser34 at the cleavage furrow from the onset of anaphase until the end of cytokinesis. We tested the localization of phospho Keratin 8 Ser34 upon Aurora B inhibition in MCF7 cells. We also observed a decrease in intensity of phospho Keratin 8 Ser34 in AZD1152/VX680 treated MCF7 cells compared to control cells as displayed in **Figure 4.41.** Altogether, these results suggest that Keratin proteins may have conserved phosphorylation sides, which are regulated

by a specific regulator at exact time. Aurora B dependent Keratin 8 Ser34 phosphorylation could be conserved in Keratin 8 expressing cells.

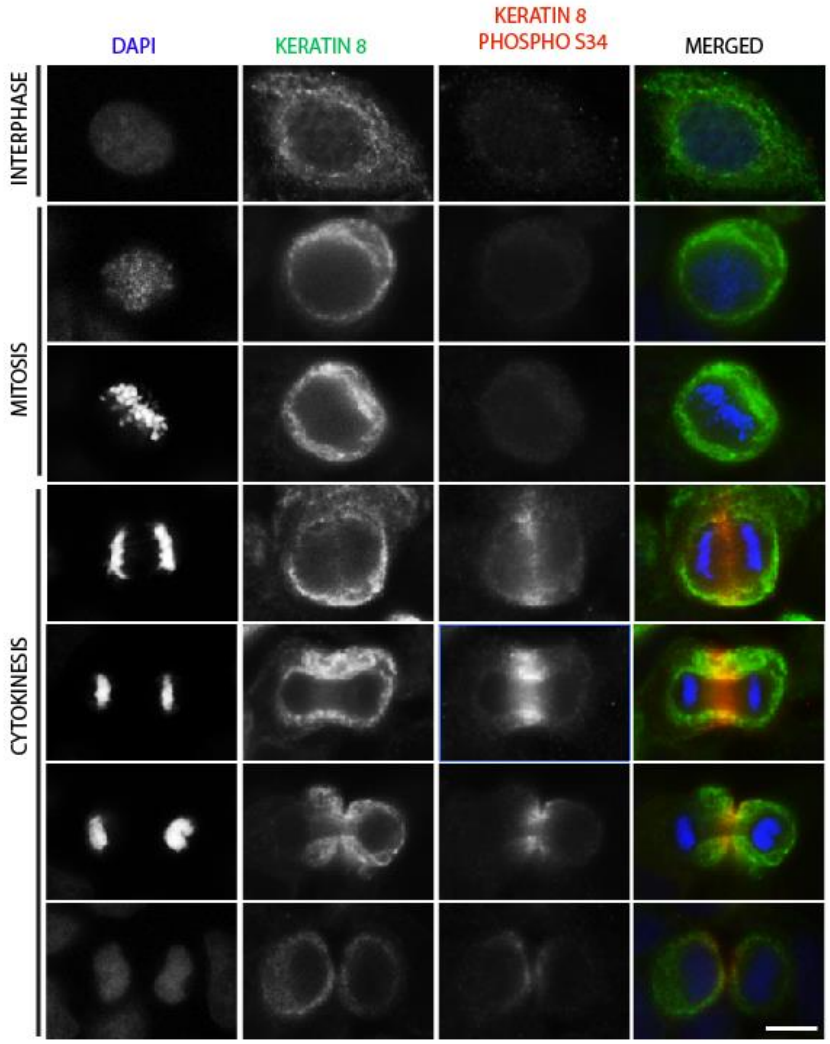

Figure 4.40. Localization of Phospho Keratin 8 Ser34 in MCF7 cells in different cell cycle stages. Immunofluorescence staining of MCF7 cells at different cell cycle stages (intephase, mitosis, cytokinesis) using Keratin 8 (green), Keratin 8 phospho S34 (red) antibodies and DAPI (blue).

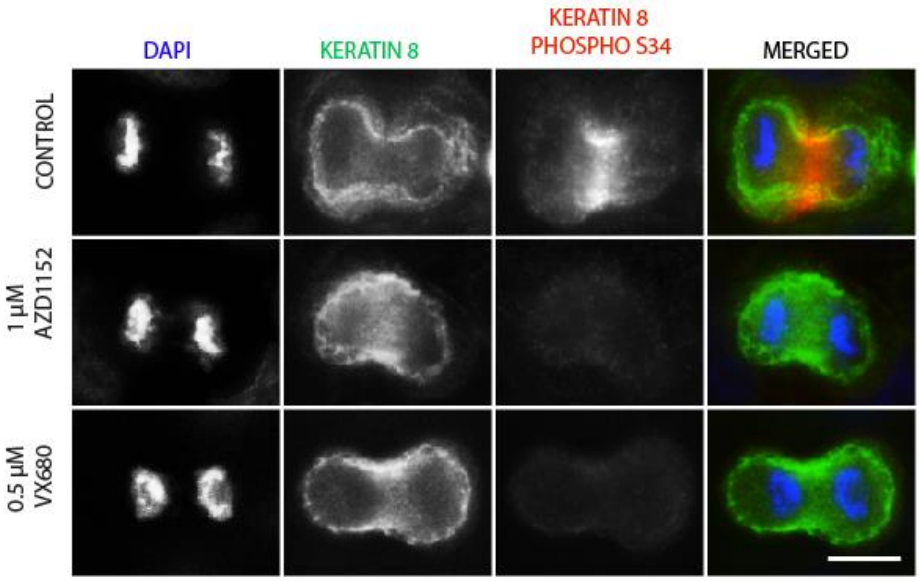

Figure 4.41. Phosphorylation of Keratin 8 Ser34 is Aurora B Dependent in MCF7 epithelial cells. Immunofluorescence staining of control (DMSO) and Aurora B kinase inhibitor (1 µM AZD1152 or 0.5 VX680 µM) treated MCF7 cells using Keratin 8 (green), Keratin 8 phospho S34 (red) antibodies and DAPI (blue). Scale bars, 10 µm.

4.10. Keratin 8 interacts with Aurora B in a cell cycle-dependent manner.

In previous parts, we addressed the regulation of Keratin 8 depending on Aurora B activity during cell division. Our findings strongly suggest that Keratin 8 and Aurora B is interacting directly and the interaction is cell cycle-dependent. We aimed to examine whether Aurora B physically associates with Keratin-8 during cell division. To do that, we used Aurora B-GFP expressing cells where GFP tagged Aurora B is expressed under its own promoter using bacterial artificial chromosome (BAC) trans genomics. As a control, we employed empty GFP expressing HeLa cells. We pull downed GFP tagged Aurora B from the cell extracts arrested in interphase and mitosis. In parallel, we pulled downed only GFP in control cells. As shown in **Figure 4.42**, Aurora B interacted with Keratin 8 in mitosis but not in the interphase, suggesting that Aurora B-Keratin 8 interaction is cell cycle-dependent.

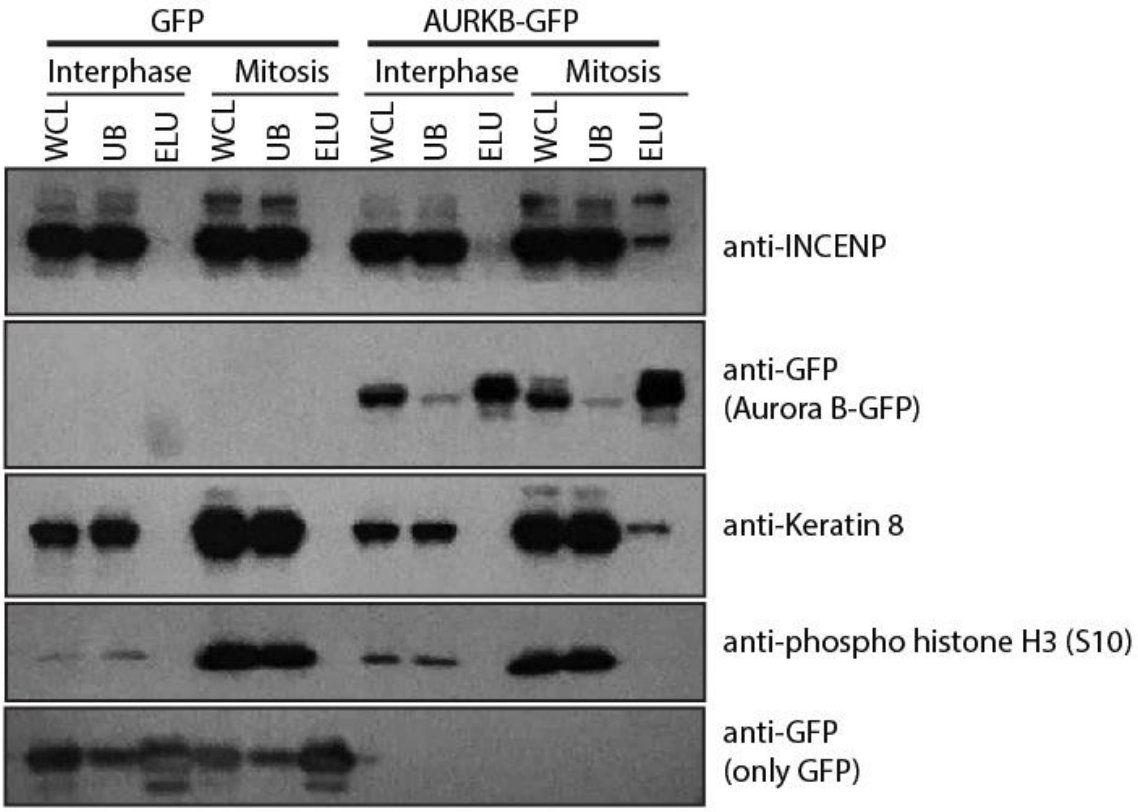

Figure 4.42. GFP Pull Down in Empty GFP and Aurora B-GFP expressing HeLa Kyto cells arrested in mitosis and cytokinesis. GFP pulldown of HeLa cells stably expressing Aurora B-GFP in bacterial artificial chromosomes (BAC). Immunoblotting of whole-cell lysates (WCL), unbound (UB) and elutes (ELU) from control (Empty GFP) and Aurora B-GFP expressing interphase and mitosis cells using anti-INCENP, anti-Keratin 8, anti phospho histone H3 (S10)

On the parallel, to validate the physical interaction between Keratin 8 and Aurora B, we employed a pull-down experiment with K8 GFP. To perform the experiment, we expressed empty GFP, WT K8-GFP and mutant 5XA K8 in K8 KO HeLa cells. Then, we synchronized cells to interphase, mitosis and cytokinesis. Empty GFP expressing K8 KO cells were used as a control. We pull downed GFP-tagged proteins. In **Figure 4.43,** we observed that small

quantities of Aurora B interacted with wild-type Keratin 8 in mitosis and cytokinesis. We did not observe Keratin8 and Aurora B interaction in interphase. Interestingly, we observed mutant 5XA K8 GFP did not interact with Aurora B during the cell cycle. These results suggest that Aurora B interacts with Keratin 8 cell cycle-dependent manner.

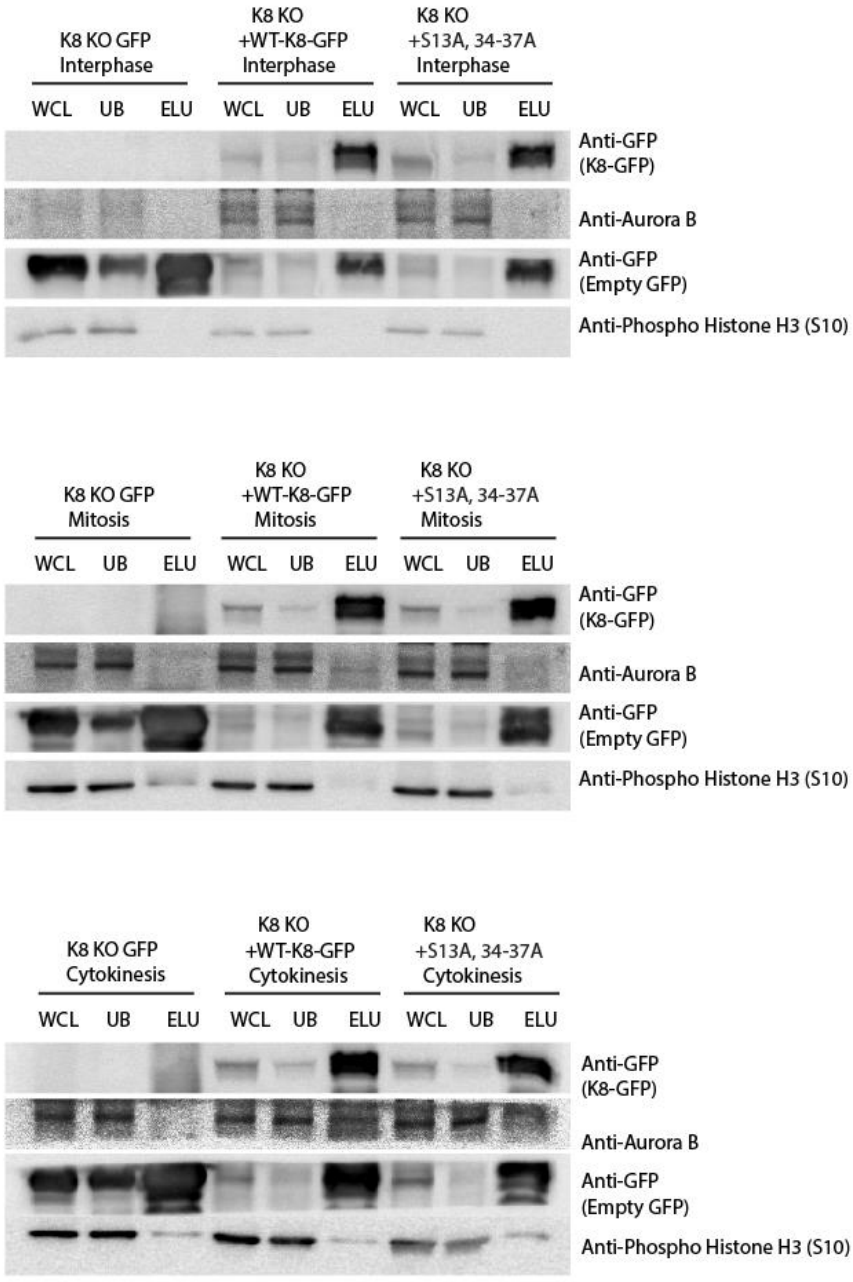

Figure 4.43. WT but not non-phosphorylatable Keratin 8 associates with Aurora B in mitosis and cytokinesis. GFP pulldown of K8 KO HeLa cells expressing empty GFP, WT K8-GFP and S13,34-37A K8-GFP. Western Blot analysis of whole cell lysates (WCL), unbound (UB) and elutes (ELU) from interphase, mitosis and cytokinesis cells were subjected to the immunoblotting using anti-GFP, anti-Aurora B, anti phospho histone H3 (S10) antibodies.

4.11. Keratin 8 targets Aurora B kinase to the chromosomes and midzone

Previously as shown in **Figure 4.13,** we observed a decrease in Aurora B level at cleavage furrow in K8 KO HeLa cells. We want to address whether Keratin 8 itself or the phosphorylated form of Keratin 8 takes a role in conducting Aurora B localization. To examine that, we stained control, K8 KO, WT K8-GFP and 5XA K8-GFP expressing K8 KO HeLa cells by using anti-Aurora B antibody. **Figure 4.44** displays Aurora B localization in control, K8 KO, WT K8-GFP and 5XA K8-GFP expressing K8 KO HeLa mitosis cells. We observed that Aurora B level decreased in K8 KO and 5XA K8-GFP expressing K8 KO HeLa cells compared to control and WT K8-GFP expressing K8 KO HeLa cells. Quantification of Aurora B intensity at the chromosomes confirms these observations (**Figure 4.45**). On the parallel, we performed the same process for cytokinesis cells. Reiteratedly, we observed Aurora B intensity decreased at cleavage furrow in K8 KO and 5XA K8-GFP expressing K8 KO HeLa cells compared to control and WT K8-GFP expressing K8 KO HeLa cells. **Figure 4.46** shows Aurora B localization in control, K8 KO, WT K8-GFP and 5XA K8-GFP expressing K8 KO HeLa cytokinesis cells. When we quantified Aurora B fluorescence level at the cleavage furrow, as shown in **Figure 4.47**, we found consistent results with our observation.

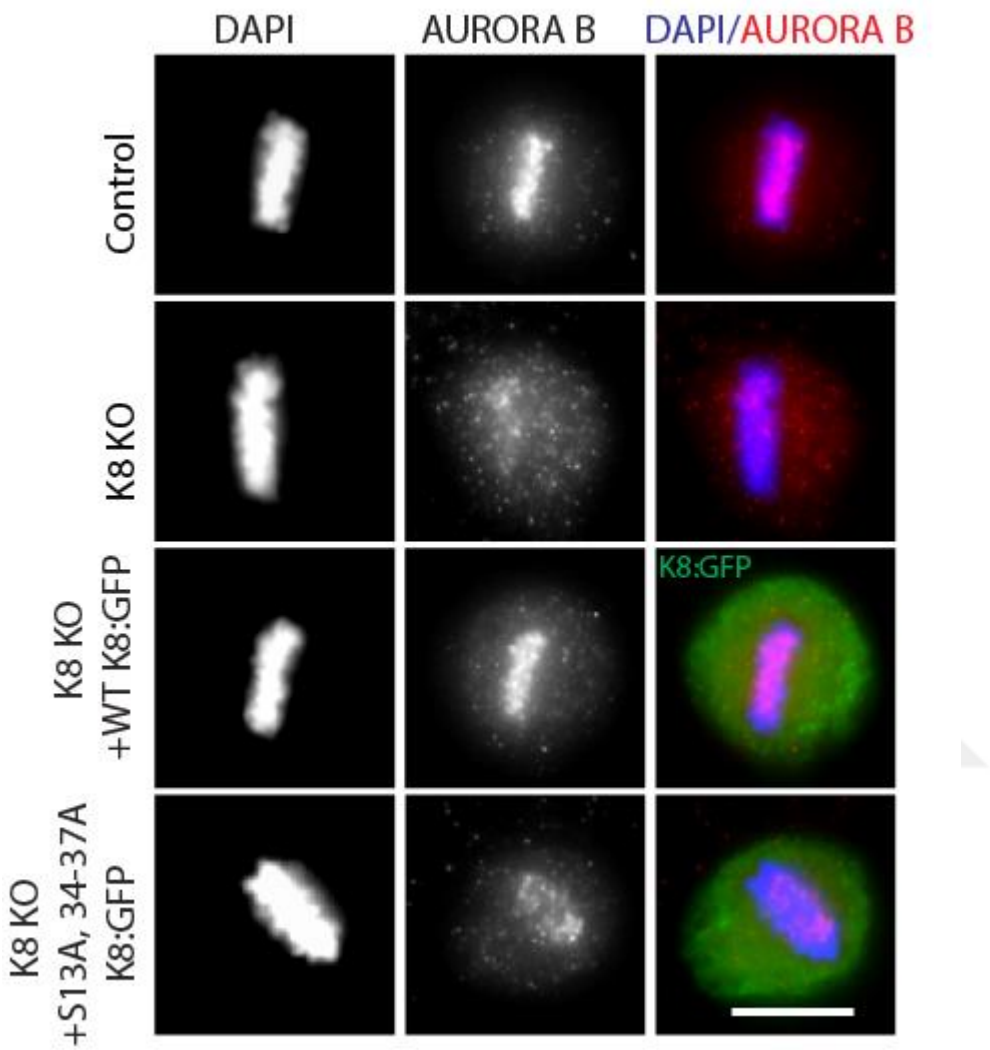

Figure 4.44. Aurora B localization in control, K8 KO, WT K8-GFP and 5XA K8-GFP expressing K8 KO HeLa mitosis cells. Representative images of Aurora B kinase localization in control, K8 KO, K8 KO HeLa cells expressing WT K8-GFP and S13,34-37A K8-GFP. Metaphase cells are immunostained against Aurora B (red) and DNA (DAPI, blue)

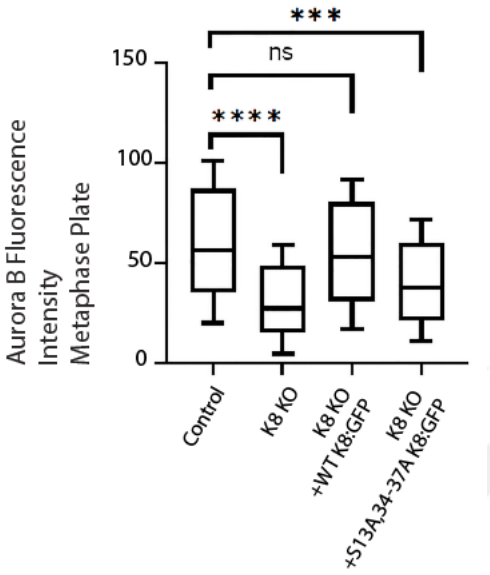

Figure 4.45. Quantification of Aurora B fluorescence intensity at the chromosomes in control, K8 KO, WT K8-GFP and 5XA K8-GFP expressing K8 KO HeLa mitosis cells. Quantification of Aurora B fluorescence intensity at the metaphase chromosomes in control *(n=43)*, K8 KO *(n=49)*, K8 KO + WT K8-GFP *(n=45)* and K8 KO + S13,34-37A K8-GFP *(n=49)* HeLa cells. Data represent mean ± SEM. ****p<0.0001, ***p<0.001, n.s., no significant difference. Student's *t*-test.

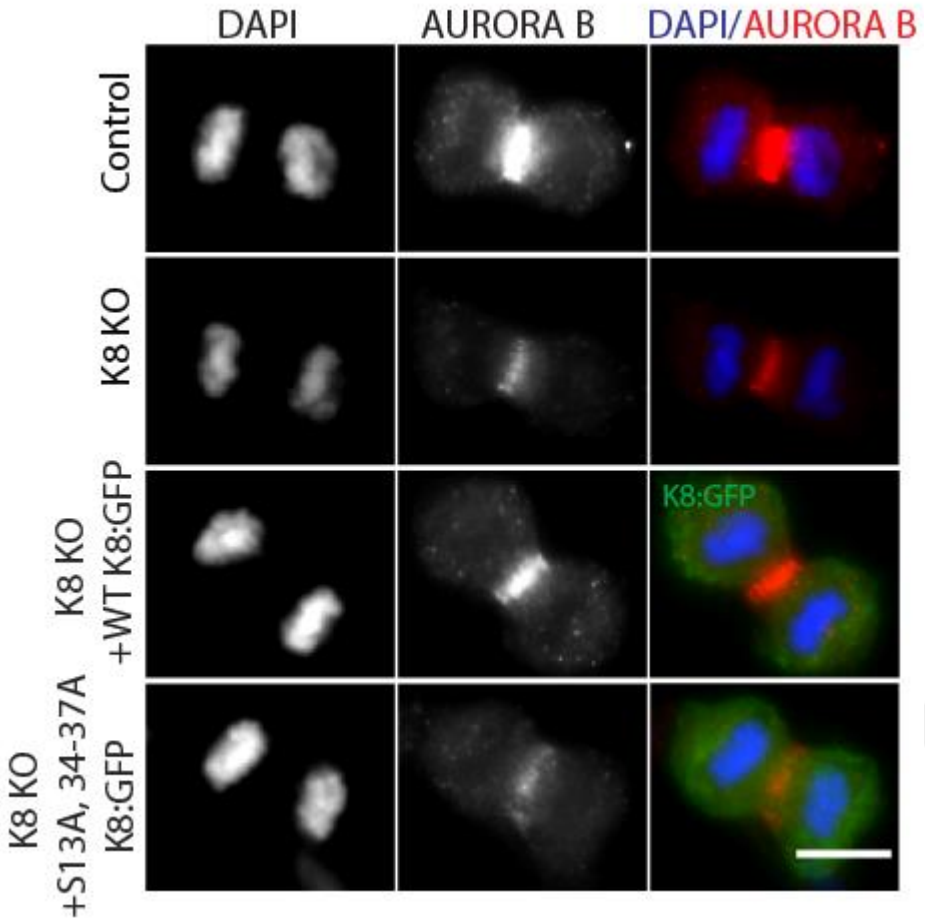

Figure 4.46. Aurora B localization in control, K8 KO, WT K8-GFP and 5XA K8-GFP expressing K8 KO HeLa cytokinesis cells. Representative images of Aurora B kinase localization in control, K8 KO, K8 KO HeLa cells expressing WT K8-GFP and S13,34-37A K8-GFP. Anaphase cells are immunostained against Aurora B (red) and DNA (DAPI, blue). Scale bars, 10 µm.

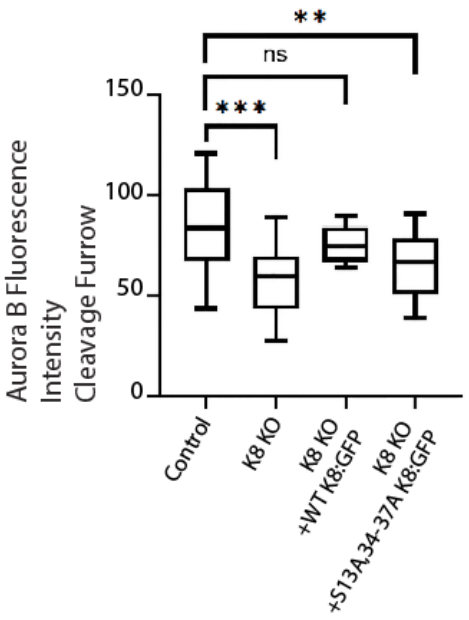

Figure 4.47. Quantification of Aurora B fluorescence intensity at cleavage furrow in in control, K8 KO, WT K8-GFP and 5XA K8-GFP expressing K8 KO HeLa cytokinesis cells. Quantification of Aurora B fluorescence intensity at the midzone in control *(n=20)*, K8 KO *(n=20)*, K8 KO + WT K8-GFP *(n=13)* and K8 KO + S13,34-37A K8-GFP *(n=13)* HeLa cells. Data represent mean ± SEM. ***p<0.001, **p<0.01, n.s., no significant difference. Student's *t*-test.

Chapter 5

DISCUSSION

Keratin proteins form a solid network and provide cell mechanical strength. Although it is known that their primary function is providing firmness to the cell, they have been heavily investigated in differentiation, migration and apoptosis. The role of keratins in cell division has not been an exciting area to explore until now. In this thesis, we aimed to study the role of Keratin 8 in cell division and its regulation. The robust nature of keratins makes them challenging to study, but also attractive. It is interesting to understand how this robust protein is regulated and organized in cell division, which is a dynamic process. We aimed to enlighten how Keratin 8 takes a role in cell division and its possible regulation mechanism by master kinases.

In this study, we focused on the substrate-kinase relationship between Keratin 8 and Aurora B kinase. Latest studies have shown that cytoskeleton proteins are one of the major targets of Aurora B during cell division, especially in cytokinesis. Vimentin, the member of intermediate filaments, is phosphorylated at Ser55 and Ser56 residues by Aurora B kinase during cytokinesis [9]. It is well known that intermediate filaments are heavily regulated through post-translational modification such as phosphorylation, acetylation, sumoylation or ubiquitination. The modifications change the solubility of intermediate filaments and reorganize the protein network. It is significant to contribute additional cellular functions to protein other than stiffness. Some minor modifications cause drastic changes in protein morphology and biochemistry. For example, nuclear lamina disassemblies by CDK1 phosphorylation during mitosis. Additionally, it has been revealed that K8 and K18 phosphorylation are affected by Aurora B inhibition during cytokinesis [9]. Consequently, there is a lot to discover in this field. Here, we showed that Keratin 8 takes an important role in chromosome congression and cytokinesis and Aurora B dependent phosphorylation of Keratin 8 Ser34 provides reorganization of Keratin 8.

We started with an investigation of the role of Keratin 8 during cell division. In this work, we presented that the cell failed to achieve successful chromosome orientation, segregation and abscission in the absence of Keratin 8 **(Figure 5.1A)**. Since we observed multiple defects related with both mitosis and cytokinesis, we focused on understanding its regulation by Aurora B kinase, which is highly functional starting from mitosis to end of cytokinesis. Firstly, we questioned whether Keratin 8 is the real substrate of Aurora B or not. We successfully mapped six Aurora B dependent phosphorylation sites (**Figure 4.18**). These sites were determined as Ser34, Ser37, Ser124, Ser330, Ser404 and S475 residues. Some of these serine residues perfectly fit to consensus Aurora B motif. In the literature, it is well established that keratin filaments are highly regulated through phosphorylation, mostly on their head and tail domains. Therefore, we focused on sequential serine residues (Ser34-37) located on the head domain of Keratin 8. Non-phosphorylatable Ser34-37 Keratin 8 (mutant 5XA) persisted on the cleavage furrow and eventually resulted in multinucleated cells (**Figure 4.30, 4.32**). In a previous study, it has been shown that keratin filaments are cleared up between sister asters in *Xenopus egg* extract and this process is retained depending on Aurora B activity [49]. However, there were several missing mechanisms not addressed in this study. It was not answered how Aurora B reorganized Keratin 8 during the process. In our study, we try to address answering these questions. First, similarly to Field's study, we observed that Aurora B inhibition results in Keratin 8 bundles in cleavage furrow in human cells. Then, we raised a phospho-specific antibody against phosphorylated Keratin 8 Ser34. The advantage of antibody was to understand the spatiotemporal regulation of Keratin 8 during the cell division. Strikingly, we observed distinct localization of phosphorylated Keratin 8 Ser34 to cleavage furrow starting from early anaphase until the end of the cytokinesis. We revealed Aurora B dependent phosphorylation of Keratin 8 Ser34 decorates cleavage furrow and provides its disassembly at the cleavage furrow (**Figure 4.37, Figure 4.38, Figure 5.1B**). The phospho-S34 Keratin antibody generated in this study provides a readout of the spatial extent of Aurora B kinase activity as well as a biomarker for cytokinesis. Spatial regulation of Aurora B kinase was previously demonstrated using a live cell FRET biosensor [53,54], which has the advantage of temporal readout, but our antibody is technically simpler to implement and useful for fixed samples. Multiple anti-mitotic

phospho-antibodies are used to detect mitotic cells including phospho-Histone H3 antibodies [55], however it is not feasible to distinguish between mitosis and cytokinesis cells with those [56]. Phospho-S34 Keratin would serve as a great biochemical biomarker to examine cytokinesis cells in the population. Given the fact that Keratin-8 is a widely used tumor diagnostic biomarker in epithelial malignancies [57], anti-phospho-S34 Keratin antibodies would have great value in assessing cell cycle progression in cancer cells and monitoring response of anti-mitotic cancer chemotherapy.

Further, we showed that Aurora B dependent phosphorylation of Keratin 8 Ser34 could be a conserved mechanism in Keratin 8 expressing epithelial cells. We observed phosphorylated Ser34 specifically localized cleavage furrow in breast adenocarcinoma-derived MCF7 cells (**Figure 4.40, Figure 4.41**). The distinct localization of phosphorylated Keratin 8 Ser34 makes it a good potential marker for cytokinesis. There are valid mitotic markers, such as phospho Histone 2B S10, frequently used in cell cycle research, but there is a necessity for valid cytokinesis markers in the field. Furthermore, phospho Keratin 8 Ser34 may be used in epithelial malignancies.

Interestingly, we detected Keratin 8 interacts with Aurora B in cell cycle-dependent manner (**Figure 4.42, 4.43**). Additionally, we observed that Aurora B localization is disrupted in the absence of Keratin 8 in the cell. When Keratin 8 is not phosphorylated at Ser34 residue, Aurora B also failed to localize at chromosome and cleavage furrow (**Figure 4.44, Figure 4.46, Figure 5.1C-D**). These findings suggest somehow, Keratin 8 is facilitating Aurora B localization during the cell cycle. It is conceivable that Keratin 8 may create a niche for recruitment of Aurora B and phosphorylated Keratin 8 Ser34 provides positive feedback for Aurora B localization. The necessity of Aurora B dependent Keratin phosphorylation for the constriction of cleavage furrow and Keratin 8's role in targeting Aurora B to the chromosomes and midzone suggest their functional interaction. Keratin 8 knockout cells exhibit a higher percentage of cells with chromosome congression, segregation and cytokinesis defects most likely due to impaired localization of Aurora B. Unlike Aurora B kinase, Keratin 8 is only express in epithelial cells, therefore their functional dependency

should be cell type and differentiation dependent. Keratin-8 may target Aurora B to the chromosome and midzone to facilitate its extra function of Keratin segregation in epithelial lineages. More work is required to decipher the molecular details of Keratin dependent function of Aurora B. Overall, our study demonstrates a functional interaction between Aurora B and Keratin 8 for a successful cytokinesis in Keratin expressing cells which provides an insight into mechanism of cell type specific pathways during cytokinesis. Overall, the thesis depicts that Aurora B dependent re-organization is important for successful cell division.

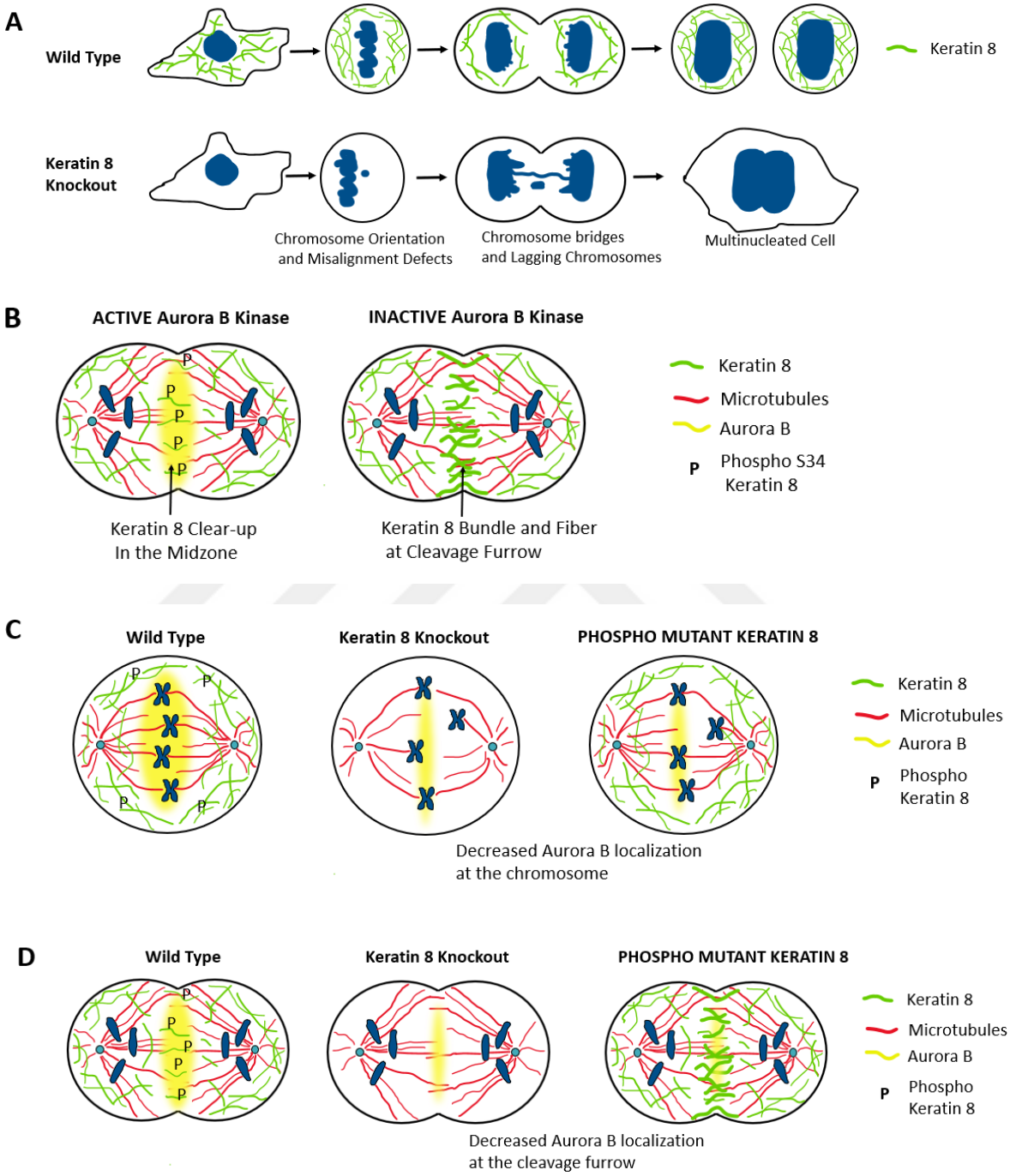

Figure 5.1. A proposed model for role and regulation of Keratin 8 during cell division. **A.** Summarizes defects of Keratin 8 knockout. **B.** Illustrates the regulation of Keratin 8 in cytokinesis through Aurora B. **C.** Illustrates possible function of keratin 8 and phosphorylated Keratin 8 on Aurora B localization at metaphase. **D.** Illustrates possible function of keratin 8 and phosphorylated Keratin 8 on Aurora B localization in cytokinesis.

BIBLIOGRAPHY

1. Bischoff, J. R. et al. A homologue of Drosophila aurora kinase is oncogenic and amplified in human colorectal cancers. EMBO J. 17, 3052–3065 (1998).

2. Walter, a O., Seghezzi, W., Korver, W., Sheung, J. & Lees, E. The mitotic serine/threonine kinase Aurora2/AIK is regulated by phosphorylation and degradation. Oncogene 19, 4906–4916 (2000).

3. Goto, H. et al. Aurora-B regulates the cleavage furrow-specific vimentin phosphorylation in the cytokinetic process. J. Biol. Chem. 278, 8526–8530 (2003).

4. Wheatley, S. P., Carvalho, A., Vagnarelli, P. & Earnshaw, W. C. INCENP is required for proper targeting of Survivin to the centromeres and the anaphase spindle during mitosis. Curr. Biol. 11, 886–890 (2001).

5. D'Avino, P. P., & Capalbo, L. (2015). New auroras on the roles of the chromosomal passenger complex in cytokinesis: implications for cancer therapies. Frontiers in oncology, 5, 221.

6. Eyers, P. A., Churchill, M. E., & Maller, J. L. (2005). The Aurora A and Aurora B protein kinases: a single amino acid difference controls intrinsic activity and activation by TPX2. Cell cycle, 4(6), 784-789.

7. Takeshita, M. et al. Aurora-B overexpression is correlated with aneuploidy and poor prognosis in non-small cell lung cancer. Lung Cancer 80, 85–90 (2013).

8. Lampson, M. a. & Cheeseman, I. M. Sensing centromere tension: Aurora B and the regulation of kinetochore function. Trends Cell Biol. 21, 133–140 (2011).

9. Polat, Ayse Nur, et al. "Phosphoproteomic analysis of Aurora kinase inhibition in monopolar cytokinesis." Journal of proteome research 14.9 (2015): 4087-4098.

10. Alberts, Bruce. Molecular biology of the cell. Garland science, 2017.

11. Collas, Philippe, Katherine Le Guellec, and Kjetil Taskén. "The A-kinase–anchoring protein AKAP95 is a multivalent protein with a key role in chromatin condensation at mitosis." The Journal of cell biology 147.6 (1999): 1167-1180.

12. Burke, Brian, and Jan Ellenberg. "Remodelling the walls of the nucleus." Nature reviews. Molecular cell biology 3.7 (2002): 487.

13. Gong, Delquin, et al. "Cyclin A2 regulates nuclear-envelope breakdown and the nuclear accumulation of cyclin B1." Current biology 17.1 (2007): 85-91.

14. King, R.W., et al., How proteolysis drives the cell cycle. Science, 1996. 274(5293): p. 1652-1659.

15. Chen, Chun-Ting, Heidi Hehnly, and Stephen J. Doxsey. "Orchestrating vesicle transport, ESCRTs and kinase surveillance during abscission." Nature reviews. Molecular cell biology 13.8 (2012): 483-488.

16. Eggert, U.S., T.J. Mitchison, and C.M. Field, Animal cytokinesis: from parts list to mechanisms. Annu. Rev. Biochem., 2006. 75: p. 543-566.

17. Piekny, Alisa J., and Michael Glotzer. "Anillin is a scaffold protein that links RhoA, actin, and myosin during cytokinesis." Current biology 18.1 (2008): 30-36.

18. Matsumura, Fumio. "Regulation of myosin II during cytokinesis in higher eukaryotes." Trends in cell biology 15.7 (2005): 371-377.

19. Bischoff, James R., et al. "A homologue of Drosophila aurora kinase is oncogenic and amplified in human colorectal cancers." The EMBO journal17.11 (1998): 3052-3065.

20. Carvajal, Richard D., Archie Tse, and Gary K. Schwartz. "Aurora kinases: new targets for cancer therapy." Clinical Cancer Research 12.23 (2006): 6869-6875.

21. Michaelis, M. et al. Aurora kinases as targets in drug-resistant neuroblastoma cells. PLoS One 9, e108758 (2014).

22. Fernández-Miranda, G. et al. Genetic disruption of aurora B uncovers an essential role for aurora C during early mammalian development. Development 138, 2661–2672 (2011).

23. Khan, J., Ezan, F., Crémet, J. Y., Fautrel, A., Gilot, D., Lambert, M., ... & Prigent, C. (2011). Overexpression of active Aurora-C kinase results in cell transformation and tumour formation. PloS one, 6(10), e26512.

24. Parra, María Teresa, et al. "Dynamic relocalization of the chromosomal passenger complex proteins inner centromere protein (INCENP) and aurora-B kinase during male mouse meiosis." Journal of Cell Science 116.6 (2003): 961-974.

25. Kitagawa, M., & Lee, S. H. (2015). The chromosomal passenger complex (CPC) as a key orchestrator of orderly mitotic exit and cytokinesis. Frontiers in cell and developmental biology, 3, 14.

26. Carmena, M., Wheelock, M., Funabiki, H., & Earnshaw, W. C. (2012). The chromosomal passenger complex (CPC): from easy rider to the godfather of mitosis. Nature reviews Molecular cell biology, 13(12), 789-803.

27. Gassmann, R., Carvalho, A., Henzing, A. J., Ruchaud, S., Hudson, D. F., Honda, R., ... & Earnshaw, W. C. (2004). Borealin: a novel chromosomal passenger required for stability of the bipolar mitotic spindle. The Journal of cell biology, 166(2), 179-191.

28. Hauf, S., Cole, R. W., LaTerra, S., Zimmer, C., Schnapp, G., Walter, R., ... & Peters, J. M. (2003). The small molecule Hesperadin reveals a role for Aurora B in correcting kinetochore–microtubule attachment and in maintaining the spindle assembly checkpoint. The Journal of cell biology, 161(2), 281-294.

29. Knowlton, A. L., Lan, W., & Stukenberg, P. T. (2006). Aurora B is enriched at merotelic attachment sites, where it regulates MCAK. Current Biology, 16(17), 1705-1710.

30. Giet, R. & Glover, D. M. Drosophila aurora B kinase is required for histone H3 phosphorylation and condensin recruitment during chromosome condensation and to organize the central spindle during cytokinesis. J. Cell Biol. 152, 669–681 (2001).

31. Guse, A., M. Mishima, and M. Glotzer, Phosphorylation of ZEN-4/MKLP1 by aurora B regulates completion of cytokinesis. Current biology, 2005. 15(8): p. 778-786.

32. Goto, H., et al., Aurora-B regulates the cleavage furrow-specific vimentin phosphorylation in the cytokinetic process. Journal of Biological Chemistry, 2003. 278(10): p. 8526-8530.

33. Alberts, Bruce, et al. "Biology of the Cell." New York: Garland Science, Taylor and Francis Group (2002): 21.

34. Vuoriluoto, K., et al. "Vimentin regulates EMT induction by Slug and oncogenic H-Ras and migration by governing Axl expression in breast cancer." Oncogene 30.12 (2011): 1436.

35. Leader, M., et al. "Vimentin: an evaluation of its role as a tumour marker." Histopathology 11.1 (1987): 63-72.

36. Lodish, Harvey. Molecular cell biology. Macmillan, 2008.

37. Moll, Roland, Markus Divo, and Lutz Langbein. "The human keratins: biology and pathology." Histochemistry and cell biology 129.6 (2008): 705.

38. Karantza, V. "Keratins in health and cancer: more than mere epithelial cell markers." Oncogene 30.2 (2011): 127.

39. Bonifas, J. M., A. L. Rothman, and E. H. Epstein Jr. "Epidermolysis bullosa simplex: evidence in two families for keratin gene abnormalities." Science 254.5035 (1991): 1202.

40. Lane, E. B., and E. L. Rugg. "A mutation in the conserved helix termination peptide of keratin 5 in hereditary skin blistering." Nature 356.6366 (1992): 244.

41. Chen, Y., Cui, T., Yang, L., Mireskandari, M., Knoesel, T., Zhang, Q., ... & Petersen, I. (2011). The diagnostic value of cytokeratin 5/6, 14, 17, and 18 expression in human non-small cell lung cancer. Oncology, 80(5-6), 333-340.

42. Cheung, K. J., Gabrielson, E., Werb, Z., & Ewald, A. J. (2013). Collective invasion in breast cancer requires a conserved basal epithelial program. Cell, 155(7), 1639-1651.

43. Alam, Hunain, et al. "Loss of keratin 8 phosphorylation leads to increased tumor progression and correlates with clinico-pathological parameters of OSCC patients." PLoS One 6.11 (2011): e27767.

44. Toivola, D. M., Ku, N. O., Resurreccion, E. Z., Nelson, D. R., Wright, T. L., & Omary, M. B. (2004). Keratin 8 and 18 hyperphosphorylation is a marker of progression of human liver disease. Hepatology, 40(2), 459-466.

45. Zatloukal, K., Stumptner, C., Fuchsbichler, A., Fickert, P., Lackner, C., Trauner, M., & Denk, H. (2004). The keratin cytoskeleton in liver diseases. The Journal of pathology, 204(4), 367-376.

46. Snider, Natasha T., and M. Bishr Omary. "Post-translational modifications of intermediate filament proteins: mechanisms and functions." Nature reviews. Molecular cell biology 15.3 (2014): 163.

47. Lane, E. B., S. L. Goodman, and Lo K. Trejdosiewicz. "Disruption of the keratin filament network during epithelial cell division." The EMBO Journal1.11 (1982): 1365.

48. Inaba, H., Yamakawa, D., Tomono, Y., Enomoto, A., Mii, S., Kasahara, K., ... & Inagaki, M. (2018). Regulation of keratin 5/14 intermediate filaments by CDK1, Aurora-B, and Rho-kinase. Biochemical and biophysical research communications, 498(3), 544-550.

49. Field, C. M., Pelletier, J. F., & Mitchison, T. J. (2019). Disassembly of actin and keratin networks by Aurora B kinase at the midplane of cleaving Xenopus laevis eggs. Current Biology, 29(12), 1999-2008.

50. Carmena, M., Wheelock, M., Funabiki, H., and Earnshaw, W.C. (2012). The chromosomal passenger complex (CPC): from easy rider to the godfather of mitosis. Nat Rev Mol Cell Biol 13, 789-803.

51. Orr, B., De Sousa, F., Gomes, A.M., Afonso, O., Ferreira, L.T., Figueiredo, A.C., and Maiato, H. (2021). An anaphase surveillance mechanism prevents micronuclei formation from frequent chromosome segregation errors. Cell Rep 37, 109783.

52. Özlü N, Monigatti F, Renard BY, Field CM, Steen H, Mitchison TJ, Steen JJ. Binding partner switching on microtubules and aurora-B in the mitosis to cytokinesis transition. Mol Cell Proteomics. 2010 Feb;9(2):336-50.

53. Fuller, B.G., Lampson, M.A., Foley, E.A., Rosasco-Nitcher, S., Le, K.V., Tobelmann, P., Brautigan, D.L., Stukenberg, P.T., and Kapoor, T.M. (2008). Midzone activation of aurora B in anaphase produces an intracellular phosphorylation gradient. Nature 453, 1132-1136.

54. Liu, D., Vader, G., Vromans, M.J., Lampson, M.A., and Lens, S.M. (2009). Sensing chromosome bi-orientation by spatial separation of aurora B kinase from kinetochore substrates. Science 323, 1350-1353.

55. Hendzel, M.J., Wei, Y., Mancini, M.A., Van Hooser, A., Ranalli, T., Brinkley, B.R., Bazett-Jones, D.P., and Allis, C.D. (1997). Mitosis-specific phosphorylation of histone H3 initiates primarily within pericentromeric heterochromatin during G2 and spreads in an

ordered fashion coincident with mitotic chromosome condensation. Chromosoma 106, 348-360.

56. Karayel, O., Sanal, E., Giese, S.H., Uretmen Kagiali, Z.C., Polat, A.N., Hu, C.K., Renard, B.Y., Tuncbag, N., and Ozlu, N. (2018). Comparative phosphoproteomic analysis reveals signaling networks regulating monopolar and bipolar cytokinesis. Sci Rep 8, 2269.

57. Karantza, V. (2011). Keratins in health and cancer: more than mere epithelial cell markers. Oncogene 30, 127-138.